




MISSOURI
S&T

CENTER FOR TRANSPORTATION INFRASTRUCTURE AND SAFETY



Roller Compacted Concrete: Field Evaluation and Mixture Optimization

by



Kamal H. Khayat, (Ph.D., P.E.) P.I.
Nicolas Ali Libre, (Ph.D.) co-P.I.



August 2014



**NUTC
R363**

**A National University Transportation Center
at Missouri University of Science and Technology**

Disclaimer

The contents of this report reflect the views of the author(s), who are responsible for the facts and the accuracy of information presented herein. This document is disseminated under the sponsorship of the Department of Transportation, University Transportation Centers Program and the Center for Transportation Infrastructure and Safety NUTC program at the Missouri University of Science and Technology, in the interest of information exchange. The U.S. Government and Center for Transportation Infrastructure and Safety assumes no liability for the contents or use thereof.

Technical Report Documentation Page

1. Report No. NUTC R363	2. Government Accession No.	3. Recipient's Catalog No.
4. Title and Subtitle Roller Compacted Concrete: Field Evaluation and Mixture Optimization	5. Report Date August 2014	6. Performing Organization Code
	8. Performing Organization Report No. Project #00043605	
7. Author/s Kamal H. Khayat, P.I., Nicolas Ali Libre, co-P.I.	10. Work Unit No. (TRAIS)	
9. Performing Organization Name and Address Center for Transportation Infrastructure and Safety/NUTC program Missouri University of Science and Technology 220 Engineering Research Lab Rolla, MO 65409	11. Contract or Grant No. DTRT06-G-0014	
	13. Type of Report and Period Covered Final	
12. Sponsoring Organization Name and Address U.S. Department of Transportation Research and Innovative Technology Administration 1200 New Jersey Avenue, SE Washington, DC 20590	14. Sponsoring Agency Code	
	15. Supplementary Notes	
<p>16. Abstract</p> <p>Roller Compacted Concrete (RCC) as an economical, fast construction and sustainable materials has attracted increasing attention for pavement construction. The growth of roller-compacted concrete pavement used in different regions is impeded by concerns regarding its compatibility with domestic materials, environmental conditions and local restrictions. This report addresses the short-term and long-term performance of RCC made with materials locally available in the state of Missouri. The report also provides a comprehensive review on the current practices and recent developments in material selection and aggregate gradation and mixture design methods.</p> <p>The research project involved an extensive sampling and testing carried out to evaluate fresh and mechanical properties as well as shrinkage and key durability characteristics of the RCC used for widening Route 160 near Doniphan. The results of compressive strength, modulus of elasticity, splitting tensile strength, and flexural strength of the concrete mixtures used for the pavement of route 160 are presented and discussed. In-situ compressive strength and relative bond strength were also determined on the cores taken from the pavement. The compressive strengths of the core samples were very close to those of specimens cast at the job site. Both in-situ and laboratory testing confirm that the tested RCC satisfies the mechanical requirements given by Missouri Standard Specifications for Highway Construction.</p> <p>Short-term and long-term performance of the RCC is also evaluated using embedded vibrating wire gage sensors to monitor variations in temperature and deformation in the pavement over time. The measured shrinkage of concrete pavement was found to be significantly lower than the corresponding deformation in RCC specimens tested in standard laboratory condition.</p> <p>RCC mixture is then optimized to enhance its mechanical properties and durability characteristics. Various aggregate types, water to cement ratios, and cementitious materials were investigated in the optimization procedure. The basic concept of mixture proportions was to optimize the solid skeleton of RCC through minimizing the void ratio of the solid particles. The workability and strength criteria were considered in the selection of final optimum RCC mixture. Mechanical properties of RCC were found to be better than or equal to the conventional pavement concrete as the reference material. Obtained data confirms the feasibility of producing RCC with local materials that complies with MoDOT requirements.</p> <p>Air entrained RCC is also investigated in the research program. Air-entrained RCC is also investigated in this research program. The experiments show that the air-entrainment is difficult in dry mixtures such as RCC and that the air bubbles are not stable during mixing and compaction of RCC; however, the preliminary study presented and discussed in this report showed that air entrainment can be achieved in the RCC. Adjusting the amount of air content, the stability of air bubbles during the transport and compaction and uniformity of air-void distribution across the pavement, are among the important issues that should be addressed before using air-entrained RCC in the field applications. The durability results reveals that a little amount of spherical air bubbles entrained in the RCC mixture can have a beneficial influence on the frost resistance durability of concrete. The frost durability tests show that air-entrained RCC performs superior compared to non-air entrained RCC in frost resistance tests. However, the result indicates that the non-air entrainment RCC can be quite resistant to frost action if the concrete ingredients are well adjusted.</p>		

17. Key Words Recycled concrete aggregate, field performance, durability, sustainability, pavement construction	18. Distribution Statement No restrictions. This document is available to the public through the National Technical Information Service, Springfield, Virginia 22161.		
19. Security Classification (of this report) unclassified	20. Security Classification (of this page) unclassified	21. No. Of Pages 118	22. Price

Form DOT F 1700.7 (8-72)



Final Report

Roller Compacted Concrete Field Evaluation and Mixture Optimization

Kamal H. Khayat, (Ph.D., P.E.) P.I.

Nicolas Ali Libre, (Ph.D.) co P.I.

August 13, 2014

Center for Infrastructure Engineering Studies

MISSOURI UNIVERSITY OF SCIENCE AND TECHNOLOGY

Table of Content

TABLE OF CONTENT	1
SUMMARY	7
1 INTRODUCTION	9
1.1 BACKGROUND, PROBLEM AND JUSTIFICATION	9
1.2 OBJECTIVES AND SCOPE OF WORK	11
1.3 OUTLINE	12
2 LITERATURE REVIEW	12
2.1 MATERIALS	12
2.1.1 <i>Aggregates</i>	13
2.1.2 <i>Cementitious materials</i>	15
2.1.3 <i>Water</i>	16
2.1.4 <i>Chemical Admixtures</i>	16
2.2 MIX DESIGN PROCEDURE	17
2.2.1 <i>Consistency approach</i>	18
2.2.2 <i>Soil-compaction approach</i>	19
2.2.3 <i>Examples of RCC mixture proportions</i>	20
2.3 WORKABILITY OF RCC	21
2.3.1 <i>Vebe test</i>	22
2.3.2 <i>Sampling procedure of RCC</i>	24
2.4 MECHANICAL CHARACTERISTICS OF RCC	25
2.4.1 <i>Compressive strength</i>	25
2.4.2 <i>Flexural strength</i>	26
2.4.3 <i>Splitting Tensile strength</i>	27
2.4.4 <i>Modulus of elasticity</i>	27
2.4.5 <i>Coefficient of Thermal expansion</i>	28
2.4.6 <i>Drying Shrinkage</i>	28
2.5 DURABILITY CHARACTERISTICS	29
2.5.1 <i>Freeze and thaw resistance</i>	30
2.5.2 <i>Deicing Salt-Scaling Resistance</i>	30
2.5.3 <i>Porosity and the permeability</i>	30
2.5.4 <i>Electrical resistivity</i>	31
3 TESTING PROTOCOLS	32
3.1 COMPRESSIVE STRENGTH	32
3.2 FLEXURAL STRENGTH	32
3.3 SPLITTING TENSILE STRENGTH	33
3.4 MODULUS OF ELASTICITY	34
3.5 COEFFICIENT OF THERMAL EXPANSION	35
3.6 DRYING SHRINKAGE	35
3.7 FREEZE AND THAW RESISTANCE	36
3.8 DEICING SALT-SCALING RESISTANCE	38

3.9	PERMEABLE VOIDS	38
3.10	ELECTRICAL RESISTIVITY	39
4	FIELD EVALUATION OF CONCRETE USED FOR RCC PAVEMENT	41
4.1	CONCRETE SAMPLING	44
4.2	FRESH CONCRETE PROPERTIES DETERMINED IN-SITU	46
4.3	MECHANICAL PROPERTIES OF SAMPLES SPECIMENS	47
4.3.1	<i>Compressive strength</i>	47
4.3.2	<i>Flexural strength</i>	49
4.3.3	<i>Splitting tensile strength</i>	49
4.3.4	<i>Modulus of elasticity</i>	49
4.4	IN-SITU MECHANICAL PROPERTIES	50
4.4.1	<i>Compressive strength</i>	52
4.4.2	<i>Relative bond strength</i>	52
4.4.3	<i>Coefficient of thermal expansion (CTE)</i>	54
4.5	DRYING SHRINKAGE	54
4.6	DURABILITY CHARACTERISTICS	55
4.6.1	<i>Freeze-thaw resistance</i>	55
4.6.2	<i>Deicing salt scaling resistance</i>	57
4.6.3	<i>Permeable air voids</i>	57
4.6.4	<i>Surface electrical resistivity</i>	58
4.7	SUMMARY OF RCC CHARACTERISTICS	59
5	INSTRUMENTATION OF RCC PAVEMENT	59
5.1	INSTALLATION OF THE MONITORING SYSTEM	59
5.2	LONG-TERM DEFORMATION MONITORING	62
5.2.1	<i>Shrinkage deformation in pavement</i>	63
5.2.2	<i>Total deformation in RCC pavement</i>	67
6	DEVELOPMENT OF RCC MIX DESIGN	68
6.1	RCC MATERIALS SELECTION	68
6.1.1	<i>Aggregate</i>	68
6.1.2	<i>Cementitious materials</i>	72
6.1.3	<i>Chemical admixtures</i>	73
6.2	OPTIMIZATION OF PARTICLES SIZE DISTRIBUTION	73
6.2.1	<i>Empirical PSD optimization</i>	74
6.2.2	<i>Theoretical models for PSD optimization</i>	78
6.2.3	<i>PSD optimization software</i>	79
6.2.4	<i>Selection of optimum aggregate type and proportions</i>	81
6.3	OPTIMIZATION OF PASTE VOLUME AND COMPOSITION	82
6.3.1	<i>Experimental matrix</i>	83
6.3.2	<i>Optimum water-to-solid ratio</i>	85
6.3.3	<i>Strength properties</i>	86
6.3.4	<i>Workability evaluation</i>	89
6.4	SELECTION OF OPTIMIZED RCC MIXTURE PROPORTION	91

7	PERFORMANCE OF OPTIMIZED RCC MIXTURE	92
7.1	PHYSICAL AND MECHANICAL PROPERTIES OF OPTIMIZED RCC	92
7.1.1	<i>Compressive strength</i>	93
7.1.2	<i>Flexural strength</i>	94
7.1.3	<i>Splitting tensile strength</i>	95
7.1.4	<i>Modulus of elasticity</i>	95
7.1.5	<i>Drying shrinkage</i>	95
7.1.6	<i>Coefficient of thermal expansion (CTE)</i>	96
7.2	DURABILITY CHARACTERISTICS OF OPTIMIZED RCC	97
7.2.1	<i>Electrical resistivity</i>	97
7.2.2	<i>Permeable voids</i>	98
7.2.3	<i>Deicing salt scaling resistance</i>	99
8	COMPARISON AND CONCLUSION	104
8.1.1	<i>Mechanical properties</i>	105
8.1.2	<i>Long-term deformation</i>	107
8.1.3	<i>Permeable voids and electrical resistivity</i>	108
8.1.4	<i>Frost resistance</i>	109
8.1.5	<i>Concluding remarks</i>	110
8.1.6	<i>Future work</i>	110
	ACKNOWLEDGMENT	111
	REFERENCES	112

List of Figures

Figure 1- Increased use of RCC pavements in North America [Harrington, 2010]	10
Figure 2- Suggested Limits for RCC pavement aggregate gradation	14
Figure 3- Typical moisture content-Density relationship established in soil-compaction approach	20
Figure 4- Vebe test Apparatus for evaluating consistency of fresh RCC.....	23
Figure 5- Concrete surface after Vebe test, (left) dry RCC with Vebe >90 sec, (right) RCC with adequate consistency with Vebe=45 sec	24
Figure 6- Hammer, rectangular head and circular heads used for sampling RCC	25
Figure 7- Compressive Strength test.....	32
Figure 8- Setup of flexural strength test (ASTM C78)	33
Figure 9- The splitting tensile test setup used in this program	34
Figure 10- The test setup used for measuring modulus of elasticity.....	35
Figure 11- Measurement of drying shrinkage.....	36
Figure 12- Dynamic modulus of elasticity testing apparatus for freeze-thaw test	37
Figure 13- Freeze-thaw chamber according to ASTM C666, procedure A	37
Figure 14- Chamber used for Deicing salt-scaling resistance test	38
Figure 15- The apparatus used for measuring permeable voids in concrete	39
Figure 16- Testing apparatus of surface and bulk resistivity of concrete.....	40
Figure 17: Overview of the highway 1600 Job J9P2186 near Doniphan, MO.....	41
Figure 18- RCC production facilities used for widening Route 160	42
Figure 19- RCC pavement construction in Route 160.....	43
Figure 20- Sampling of concrete specimens	45
Figure 21- Storage of concrete specimens at the job site	46
Figure 22- RCC workability test.....	47
Figure 23- Development of Compressive strength in field RCC.....	48
Figure 24- Location of core drilling	50
Figure 25: Joint between two casting layers showing increased porosity as observed for core C2	51
Figure 26- Apparatus used for testing the relative bond strength	52
Figure 27- Failure surface in the bond strength test, (left) joint between two lifts, (right) inside the lift .	53
Figure 28- Shrinkage of concrete specimens in the lab	55
Figure 29- Cast in field RCC specimens after 30 cycles of freezing and thawing.....	56
Figure 30: Tower with two installed vibrating wire gages	60
Figure 31: Installed DAQ system powered by solar panel	60
Figure 32: Location of installed monitoring system.....	60
Figure 33: Schematic representation of sensors locations (plan view)	61
Figure 34: Compaction of RCC above installed sensors.....	61
Figure 35- Temperature of concrete pavement (top) and ambient temperature (bottom)	63
Figure 36- Total strain and iso-thermal strain recorded by the C-top gage	64
Figure 37- Frequency analysis of the total strain recorded by the C-top gage.....	65
Figure 38- Iso-thermal strains measured by installed gages in the concrete pavement.....	66

Figure 39- Mean shrinkage strain and total strain in RCC pavement	67
Figure 40- Aggregate quarries.....	69
Figure 41- Aggregate samples investigated in the research program	69
Figure 42- Particle size distribution of sand, intermediate and coarse aggregates, and grading limits given by the Missouri Standard Specifications For Highway Construction	71
Figure 43- Percent of aggregate retained on each sieve	72
Figure 44- Particle size distribution of cementitious materials	73
Figure 45- Gyrotory intensive compaction tester (ICT).....	75
Figure 46- Ternary Packing Diagram (TPD) of blended aggregates (red points show the packing density measurements).....	77
Figure 47- 3D representation of measured packing density in aggregate blends.....	77
Figure 48- Screen shot of PSD optimization software	80
Figure 49- ACI 325 aggregate gradation limits for RCC and the corresponding Andreasen packing models	81
Figure 50- PSD of selected aggregate combination vs. PSD of Andreasen model with $q=0.35$	82
Figure 51- Percent retained on each sieve in selected aggregate combination.....	82
Figure 52- Identification code or RCC trial mixtures.....	83
Figure 53- Dry density vs. w/s of RCC mixtures	87
Figure 54- Compressive strength vs. w/s.....	88
Figure 55- Vebe time vs. w/s.....	90
Figure 56- Compressive strength of optimized RCC mixtures	94
Figure 57- Shrinkage of optimized RCC mixtures.....	96
Figure 58- Electrical surface resistivity of optimized RCC mixtures.....	98
Figure 59- Surface of RCC specimens after subjecting to freeze-thaw cycles, Mix #1 (CM)	100
Figure 60- Surface of RCC specimens after subjecting to freeze-thaw cycles, Mix #2 (CH-AEA).....	102
Figure 61- Cumulative scaled-off materials during salt scaling test in the optimized RCC mixtures	104
Figure 62- Comparison of compressive strength.....	106
Figure 63- Comparison of flexural and tensile strengths.....	106
Figure 64- Comparison of shrinkage of investigated mixtures	108
Figure 65- Comparison of Surface resistivity and permeable voids	109
Figure 66- Comparison of water absorption.....	109

List of Tables

Table 1- Combined Aggregate gradation limit according to Missouri Standard Specifications For	14
Table 2- Maximum allowable SCM replacement in RCC mixtures to Missouri Standard Specifications For Highway Construction.....	16
Table 3- Factors affecting the mixture proportions.....	18
Table 4- Examples of RCC mixture proportions [Harrington et al., 2010]	21
Table 5- Relation between surface resistivity and risk of corrosion in concrete.....	32
Table 6- Nomenclature of test specimens.....	44
Table 7- Sampling and testing program.....	46
Table 8- Results consistency measurements by means of Vebe consistency measurements	47
Table 9- Compressive strength of the specimens cast in the field	48
Table 10- Flexural strength of concrete specimens cast in the field	49
Table 11- Tensile strength of concrete specimens cast in the field.....	49
Table 12 – Modulus of elasticity of concrete specimens cast in the field	50
Table 13- Compressive strength of the core specimens.....	52
Table 14- Results of relative bond strength tests on core specimens.....	53
Table 15 – Coefficient of thermal expansion of cast-in-place specimens and drilled cores.....	54
Table 16 – Frost durability of sampled RCC (ASTM C666, procedure A)	56
Table 17 – Deicing salt scaling test results of cast-in-place RCC.....	57
Table 18 – Permeable air voids of cast-in-place RCC.....	58
Table 19 – Surface resistivity of cast-in-place RCC	58
Table 20- Proposed materials test methods and protocols.....	70
Table 21- Physical properties of investigated aggregates	72
Table 22- Physical and chemical characteristics of cementitious materials.....	73
Table 23- IC-testing parameters	75
Table 24- Aggregate combinations investigated in empirical PSD optimization	76
Table 25- Details of experimental program used to optimize the binder content and composition.....	84
Table 26- Optimized RCC mixture proportions.....	92
Table 27- Compressive strength of optimized RCC mixtures.....	93
Table 28- Flexural strength of optimized RCC mixtures	94
Table 29- Splitting tensile strength of optimized RCC mixtures	95
Table 30 – Modulus of elasticity of optimized RCC mixtures	95
Table 31 – Coefficient of thermal expansion of optimized RCC mixtures	96
Table 32 – Surface resistivity of cast-in-place RCC	97
Table 33 – Water absorption, density and permeable voids of optimized RCC.....	98
Table 34 – Deicing salt scaling test results of cast-in-place RCC.....	99
Table 35- Summary of Mixture proportions	105

Summary

Roller Compacted Concrete (RCC) as an economical, fast construction and sustainable materials has attracted increasing attention for pavement construction. The growth of roller-compacted concrete pavement used in different regions is impeded by concerns regarding its compatibility with domestic materials, environmental conditions and local restrictions. This report addresses the short-term and long-term performance of RCC made with materials locally available in the state of Missouri. The report also provides a comprehensive review on the current practices and recent developments in material selection and aggregate gradation and mixture design methods.

The research project involved an extensive sampling and testing carried out to evaluate fresh and mechanical properties as well as shrinkage and key durability characteristics of the RCC used for widening Route 160 near Doniphan. The results of compressive strength, modulus of elasticity, splitting tensile strength, and flexural strength of the concrete mixtures used for the pavement of route 160 are presented and discussed. In-situ compressive strength and relative bond strength were also determined on the cores taken from the pavement. The compressive strengths of the core samples were very close to those of specimens cast at the job site. Both in-situ and laboratory testing confirm that the tested RCC satisfies the mechanical requirements given by Missouri Standard Specifications for Highway Construction.

Short-term and long-term performance of the RCC is also evaluated using embedded vibrating wire gage sensors to monitor variations in temperature and deformation in the pavement over time. The measured shrinkage of concrete pavement was found to be significantly lower than the corresponding deformation in RCC specimens tested in standard laboratory condition.

RCC mixture is then optimized to enhance its mechanical properties and durability characteristics. Various aggregate types, water to cement ratios, and cementitious materials were investigated in the optimization procedure. The basic concept of mixture proportions was

to optimize the solid skeleton of RCC through minimizing the void ratio of the solid particles. The workability and strength criteria were considered in the selection of final optimum RCC mixture. Mechanical properties of RCC were found to be better than or equal to the conventional pavement concrete as the reference material. Obtained data confirms the feasibility of producing RCC with local materials that complies with MoDOT requirements.

Air entrained RCC is also investigated in the research program. Air-entrained RCC is also investigated in this research program. The experiments show that the air-entrainment is difficult in dry mixtures such as RCC and that the air bubbles are not stable during mixing and compaction of RCC; however, the preliminary study presented and discussed in this report showed that air entrainment can be achieved in the RCC. Adjusting the amount of air content, the stability of air bubbles during the transport and compaction and uniformity of air-void distribution across the pavement, are among the important issues that should be addressed before using air-entrained RCC in the field applications. The durability results reveals that a little amount of spherical air bubbles entrained in the RCC mixture can have a beneficial influence on the frost resistance durability of concrete. The frost durability tests show that air-entrained RCC performs superior compared to non-air entrained RCC in frost resistance tests. However, the result indicates that the non-air entrainment RCC can be quite resistant to frost action if the concrete ingredients are well adjusted.

1 Introduction

1.1 Background, Problem and Justification

Roller-compacted concrete (RCC) is a relatively stiff mixture of aggregate, cementitious materials, and water, that is compacted by vibratory rollers and hardened into concrete [ACI 325.10]. RCC gets its name from the heavy vibratory steel drum and rubber-tired rollers used to compact it into its final form. RCC consists of the same basic ingredients as conventional concrete (i.e. well-graded aggregate, cementitious materials, and chemical admixtures, if required) but has different mixture proportions. With well-graded aggregates, proper cement, and water content, and dense compaction, RCC pavements can achieve strength properties equal to or higher than those of conventional concrete, with low permeability. Fresh RCC is stiffer than typical concrete used in pavement construction. Its consistency is stiff enough to remain stable under vibratory rollers, yet wet enough to permit adequate mixing and distribution of paste without segregation.

Since early 1980s when the U.S. Army Corps of Engineers began researching and use of RCC pavements at military facilities in the United States, significant efforts have been made to promote and standardize the use of RCC in pavement and mass concrete construction. In North America, the use of RCC for pavement applications has expanded significantly over the past decades (Figure 1), particularly in the construction of low-volume roads and parking lots [Pittman 2009]. Generally viewed as more economical and relatively easier to produce, RCC has gradually been considered an attractive alternative to conventional road construction. Presently, a significant number of off-highway pavement projects in the United States and Canada have been completed using RCC technology.

RCC has several features that make it attractive for pavement applications. Pavement construction is a concrete intensive job. One mile of 2-lane road typically requires 3,000-4,000 cubic yard of concrete. With this mass production of concrete comes the negative side effect of large amounts of carbon dioxide emissions. These emissions are created mainly from the production of Portland cement, a major component of concrete. RCC usually requires lower

paste compared to conventional concrete used in pavement construction. This saves cement and reduces the carbon footprint associated with pavement construction. This feature makes RCC as an attractive material for sustainable pavement construction. In addition, when RCC is used in pavement, there is no need for the use of forms during placement and no need to finishing. These features make the RCC a good choice for increasing the speed of paving.

Despite the various constructability advantages offered by the RCC technique, further studies of the hardened and durability properties of this material are needed. One of the concerns, expressed by several potential users in cold climate, is the ability of RCC to resist frost attack. Even though the heavy compaction applied on RCC usually results in a denser structure comparing to conventionally vibrated concrete but it is difficult to obtain a proper air-void system in such dry mixtures when they are produced under field conditions. That raises question on the performance of RCC subjected to freeze-thaw cycles. There is relatively little systematic information available on this topic. In addition, RCC characteristic is mainly affected by the properties of materials available for concrete production. Mixture proportions should be adapted to the materials locally available and RCC characteristic should be adjusted to conforms with domestic requirements. These issues require further investigation of RCC to achieve desired characteristic and adapt the current state of practice in pavement construction to the RCC production.

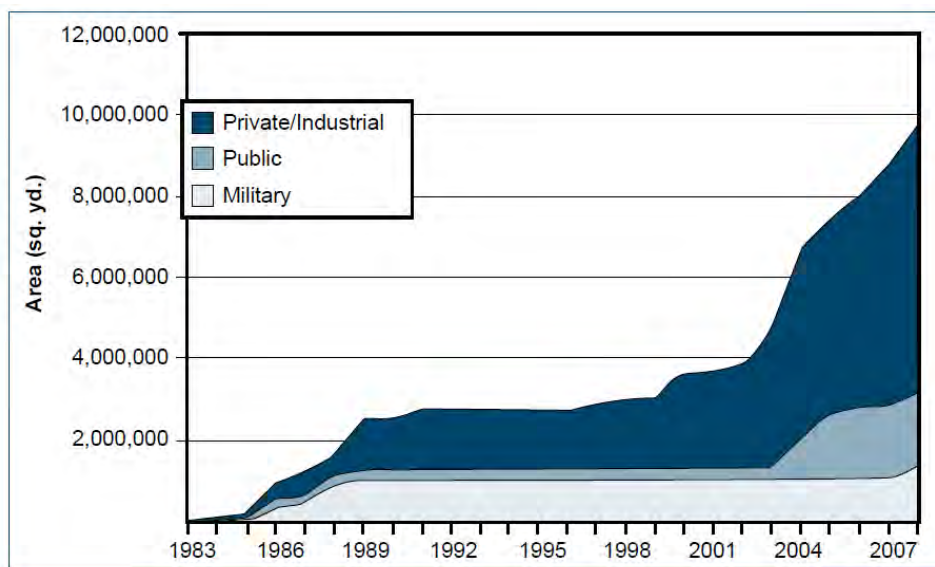


Figure 1- Increased use of RCC pavements in North America [Harrington, 2010]

This study provides feedback to future field implementation of RCC technology in transportation-related infrastructure. This report is intended for those interested in designing and producing RCC pavements for industrial, agricultural, and/or urban applications. It provides both MoDOT and design engineers with a resource to design, test, and implement RCC in transportation-related infrastructure. The report does not deal with the application of RCC in construction of mass concrete which differs with respect to materials selection, mix proportioning and properties.

1.2 Objectives and scope of work

The objective of this research project is to elaborate the performance of RCC as a new concrete material alternative for pavement construction. To this aim, literature review, laboratory optimization, field-testing, and evaluation of performance in the actual pavement is performed. The study presented in this report includes:

- Implementation of RCC in route 160 near Doniphan, MO, and evaluation of the workability, mechanical properties, and durability of the concrete.
- Instrumentation of the RCC pavement with vibrating wire gages (VWGs) to study strain deformation
- Optimize the RCC mixture proportions to enhance performance of RCC pavement for future applications
- adapt with the Missouri DOT requirements.
- Sampling and testing field-cast concrete and laboratory optimized concrete and comparing its performance to conventional concrete used in pavement construction.
- Analyze the information gathered throughout the testing to develop findings, conclusions, and recommendations for future applications of RCC technology in pavement construction

This investigation synthesizes the current technical knowledge related to the implementation of RCC with the current pavement construction practices. It deals with the state of practices recognized by Missouri Department of Transportation (MoDOT). The extensive testing program

conducted in this investigation provides insight on short-term and long-term characteristics of RCC made with local materials available in the state of Missouri.

1.3 Outline

This report consists of seven chapters and one appendix. Chapter 1 briefly explains the history and benefits of using RCC in pavement constructions. Chapter 1 presents the objectives of this study, scope of work, and research plan. Literature review of RCC characteristics is presented in Chapter 2. Workability of fresh RCC as well as its mechanical and durability properties are discussed. Chapter 2 reviews the various testing procedures used for evaluating RCC characteristics. Field evaluation of RCC pavements and corresponding experimental results are presented in Chapter 3. Chapter 4 describes the instrumentation in the pavement of route 160. The results collected up to one year after construction are presented in this Chapter. Chapter 5 presents results of mixture optimization of RCC using materials locally available in Missouri. Chapter 6 outlines summary of the properties obtained for the optimized RCC mixtures. The properties of optimized RCC is compared with the RCC used in the road 160 as well as the conventional pavement concrete as the reference. Chapter 7 presents the conclusion of the investigation and recommendations based on the findings of this investigation.

2 Literature review

2.1 Materials

The basic materials generally used for conventional concrete including water, cementitious materials, and fine and coarse aggregates are applicable in producing RCC. However, the RCC ingredients are used in different proportions. Pavement design strength, durability requirements, and intended application all influence the selection of materials for use in RCC pavement mixtures. The correct selection of materials is important to the production of quality RCC mixes. Knowledge of mixture ingredients, along with construction requirements and specifications for the intended project, is important in order to ensure an RCC mixture meets the design and performance objectives.

2.1.1 Aggregates

RCC usually contains more aggregate (75 to 85 percent by volume) and less paste comparing to conventional concrete therefore aggregate properties significantly affect both the fresh and hardened characteristics of RCC. In freshly mixed RCC, aggregate properties affect the workability of a mixture and its potential to segregate and the ease with which it will properly consolidate under a vibratory roller. The strength, modulus of elasticity, thermal properties, and durability of the hardened concrete are also affected by the aggregate properties.

Aggregates should generally meet the quality requirements of ASTM C33 as well as Missouri Standard Specifications for Highway Construction, Section 1005 "AGGREGATE FOR CONCRETE". Even though aggregates used in conventional concrete with a good proven record should also perform well in RCC, proper selection of suitable aggregates will result in greater economy in construction and longer serviceability of RCC pavements.

Aggregate used in RCC differs from conventional concrete in its gradation requirements. Less paste in the mixture reduces the workability of RCC and may increase the risk of segregation. Particle size distribution of aggregate is critically important in RCC to ensure proper consolidation of fresh concrete under roller vibration and preventing aggregate segregation during transportation of placement of concrete. Well-graded aggregates should be used in RCC to optimize paste content, minimize void space, reduce segregation, and provide a dense, smooth and tight surface. RCC mixtures often require a higher proportion of fine aggregate to coarse aggregate than conventional concrete. This will result in a more homogenous mixture and reduces the risk of segregation. Typical gradation specifications call for 50% to 65% passing the No. 4 (4.75 mm) sieve. In order to further minimize segregation during handling and placing and to provide a smooth pavement surface texture, the nominal maximum size aggregate is typically limited to 3/4 in (19.0 mm). Suggested grading limits of combined coarse and fine aggregate that have been used to produce satisfactory RCC pavement mixtures are shown in Figure 2. The different gradation requirement comes from the need of the RCC aggregate skeleton to be effectively consolidated under compaction efforts from the paver and to ensure segregation resistance.

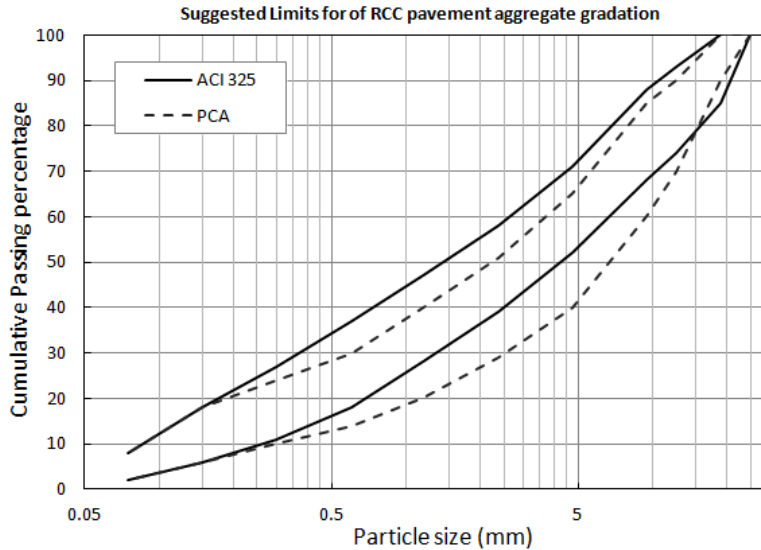


Figure 2- Suggested Limits for RCC pavement aggregate gradation

According to “General Provisions and Supplemental Specifications to 2011 Missouri Standard Specifications for Highway Construction”, the aggregate used in RCC shall be well-graded without gradation gaps and the particle size distribution of combined aggregate shall conform to the limits given in Table 1. This limit is equal to the limit given by PCA, as shown in Figure 2.

Table 1- Combined Aggregate gradation limit according to Missouri Standard Specifications For Highway Construction

Sieve Size	Percent Passing by Weight
1 in.	100
½ in.	70-90
3/8 in.	60-85
No. 4	40-60
No. 200	0-8

In addition to nominal maximum size aggregate and percent passing the No. 4 (4.75 mm) sieve, the dust fraction (material passing the No. 200 (75 µm) sieve) is also critical in RCC pavement mixes. The use of aggregate fractions finer than the 75 µm (No. 200) sieve, if non-plastic, may be a beneficial means to reduce fine aggregate voids. However, their effect on the fresh and hardened RCC properties should be evaluated in the mixture proportioning study. In addition to the general requirements for aggregate given in Section 1005, the Missouri Standard

Specifications for Highway Construction requires that the plasticity index of the aggregates used in RCC shall not exceed 5.

2.1.2 Cementitious materials

Selection of volume and composition of cementitious materials depends, in part, on the required workability, ultimate mechanical strength, the rate of development of mechanical properties, and durability criteria. RCC mixtures used in pavement construction are usually produced with a lower binder content comparing to the conventional concrete used in pavement applications. The cementitious materials in Roller Compacted Concrete Pavement (RCCP) is usually ranging from 420 to 600 lb/yd³ (250 to 350 kg/m³), which represents 12% to 16% of the total weight of dry materials. The cementitious materials in RCC mixture proportions are usually expressed as a percent of total dry materials, computed using the following formula:

$$\begin{aligned} & \text{Cementitious materials (\%)} \\ &= \frac{\text{Weight of cementitious materials}}{\text{Weight of cementitious materials} + \text{Oven dried aggregate}} \end{aligned}$$

A good starting point for the cement content in trial batch may be between 11% and 13% of dry weight. Excessive volume of cementitious materials can induce greater shrinkage cracking and significantly increase production costs without necessarily enhancing mechanical strength or extending pavement's service-life. In contrast, in a low cement content mixture, there might be not sufficient paste to fill all the voids and the concrete may be subjected to segregation due to the low consistency. Missouri Standard Specifications for Highway Construction requires that the total amount of cementitious materials shall not be below 400 lb/yd³ (240 kg/m³).

In addition to the binder volume, applicable limits on binder composition required for exposure conditions and alkali reactivity should follow standard concrete practice. A detailed discussion on the selection and use of hydraulic cements may be found in ACI 225R. Many of the RCC pavements constructed to date have been constructed using Type I or II Portland cement [ACI-325]. Supplementary Cementitious materials such as Class F or Class C fly ash and slag are

normally used as partial replacement for cement material in RCC mixtures. Fly ash contents generally range from 15% to 20% of the total volume of cementitious material.

According to Missouri Standard Specifications for Highway Construction, the maximum fly-ash replacement ratio should be limited to 25% of total binder content in order to prevent scaling of the concrete pavement surface. Missouri Standard Specifications for Highway Construction allows using ternary binders in RCC. Ternary binders are those binders that contain a combination of portland cement and two supplementary cementitious materials. Missouri Standard Specifications for Highway Construction applies certain restrictions on the maximum replacement level of SCMs in RCC mixtures (See Table 2).

Table 2- Maximum allowable SCM replacement in RCC mixtures to Missouri Standard Specifications For Highway Construction

Supplementary Cementitious Material (SCM)	
SCM	Maximum Percent of Total Cementitious Material
Fly Ash (Class C or Class F)	25%
Ground Granulated Blast Furnace Slag (GGBFS)	30%
Silica Fume	8%
Ternary Combinations	40%

All cementitious materials including cement, blended cement, and Supplementary Cementitious Materials (SCMs) shall be in accordance with Missouri Standard Specifications for Highway Construction, Division 1000.

2.1.3 Water

Water quality for RCC pavement is governed by the same requirements as for conventional concrete.

2.1.4 Chemical Admixtures

Chemical admixtures have had only limited use in RCC pavement mixtures. Water reducers or superplasticizers are rarely used in RCC production [ACI 325.10]. Retarding admixtures may be beneficial in delaying the setting time of the RCC so that it may be adequately compacted or so

that the bond between adjacent lanes or succeeding layers is improved. Because RCC mixtures are very dry, admixtures must be added in higher quantities than are used in conventional concrete to be effective. Higher amount of water reducers or retarders may have undesirable side-effects like delay or slow down RCC hydration. Therefore, any admixture considered should be tested prior to use to determine its effects on fresh and hardened RCC properties.

Concrete pavement are usually subjected to freeze-thaw cycles and deicing salts. Air Entraining Agents (AEA) are known to be useful in intentional creation of tiny air bubbles and improving freeze-thaw resistance of concrete. AEA's are more active in the presence of additional water. Experimental investigation indicated that very dry mixtures require AEA 5 to 10 times greater than conventional concrete. The practicality of producing air-entrained RCC in the field has not yet been demonstrated. To date, minimizing frost damage in RCC has been achieved by proportioning mixtures with sufficiently low water-cementitious materials ratio (w/c) so that the permeability of the paste is low. However, proper air-entrainment of RCC is the best way to assure adequate frost resistance [PCA-2004]. Further research is still required in producing air-entrained RCC with properly distributed air bubbles.

2.2 Mix Design Procedure

Regardless of mixture proportioning method or type of concrete, all concrete mixtures should comply with certain requirements. Constructability, mechanical and durability characteristics, and economical aspects are the major influencing factors in mixture proportioning of concrete. The RCC mixture proportion should be adjusted properly to ensure long-term performance of RCC. The major influencing factors that are usually considered in the mixture proportioning of RCC are shown in Table 3. Generally, the primary differences in proportions of RCC pavement mixtures and conventional concrete pavement mixtures are:

- RCC has a lower paste volume and water content, therefore it is much drier than conventional concrete and has lower workability

- RCC is generally not air-entrained because proper formation and distribution of air-bubbles in a very dry mix as RCC is challenging.
- RCC requires a larger fine aggregate content in order to produce a combined aggregate that is well-graded and stable under the action of a vibratory roller
- Nominal maximum size of aggregates in the RCC used in pavements is usually limited to 3/4 in. (19 mm) in order to minimize segregation and produce a relatively smooth surface texture.

Table 3- Factors affecting the mixture proportions

Constructability	Mechanical strength	Economics	Durability and performance
Concrete should achieve required density with optimal compaction effort. Mixture should be workable enough. Segregation should be prevented.	Compressive strength and flexural strength should met the design criteria	Use of locally available materials, lower cement consumption, use of SCM	Controlled shrinkage, low cracking, low water permeability, good abrasion resistance, no ASR

Due to several differences in fresh properties of conventional concrete and the RCC, most of the mixture proportioning techniques available for conventional concrete cannot be directly applied to mix design of RCC. Thus, various mixture proportioning methods have been specifically developed for designing RCC mixtures with adequate characteristics. Among those, the most common mixture proportioning methods are based on two empirical approaches: 1) Consistency or workability approach and 2) Maximum Density Approach. These two mixture proportioning approaches are briefly discussed here. More details about these mixture proportioning can be found in ACI 325.10R and ACI 211.3R.

2.2.1 Consistency approach

This approach focuses on workability of RCC in fresh state. For RCC to be effectively consolidated, it must be dry enough to support the weight mass of a vibratory roller yet wet enough to permit adequate compaction of the paste throughout the mass during the mixing and compaction operations. Although the slump test is the most familiar

means of measuring concrete workability, it is not suitable to measure RCC consistency. The modified Vebe test, as described in Section 2.3.1, is usually recommended to evaluate RCC consistency. The consistency approach usually requires fixing specific mixture parameters such as water content, cementitious materials content, or aggregate content, and then varying one parameter to obtain the desired level of consistency. In this way, each mixture parameter can be optimized to achieve the desired fresh and hardened RCC properties. The optimum modified Vebe time is influenced by the water content, particle size distribution of solid particles. Aggregate properties including nominal maximum size of aggregate, fine aggregate content, and the amount of aggregate finer than the 75 μm (No. 200) sieve affect workability of RCC in fresh state. After preliminary mixture proportioning, the Vebe time of given RCC mixture should be compared with the results of on-site compaction tests conducted on RCC compacted by vibratory rollers to determine if adjustments in the mixture proportions are necessary. The desired time is determined based on the results of density tests and evaluation of cores.

2.2.2 Soil-compaction approach

Methods that use this approach involve establishing a relationship between dry or wet unit weight and moisture content of the RCC by compacting specimens over a range of moisture contents. Such a typical relationship is shown in Figure 3. It is similar to the method used to determine the relationship between the moisture content and the unit weight of soils and soil-aggregate mixtures. The relatively high cementitious material contents and high quality aggregates used in RCC distinguish it from soil cement and cement-treated base course. The basic concept in this method is to maximize the packing density of solid materials by adjusting the moisture content. The volume of cementitious materials is determined based on the target compressive and flexural strength as well as the durability requirements. Well-graded aggregates play crucial roles in achieving a mixture with the highest packing and lowest void ratio. This method is more appropriate when small-size aggregates are used along with a relatively high

content of cementitious materials. Thus, pavement RCC mixtures are usually designed using the soil-compaction approach.

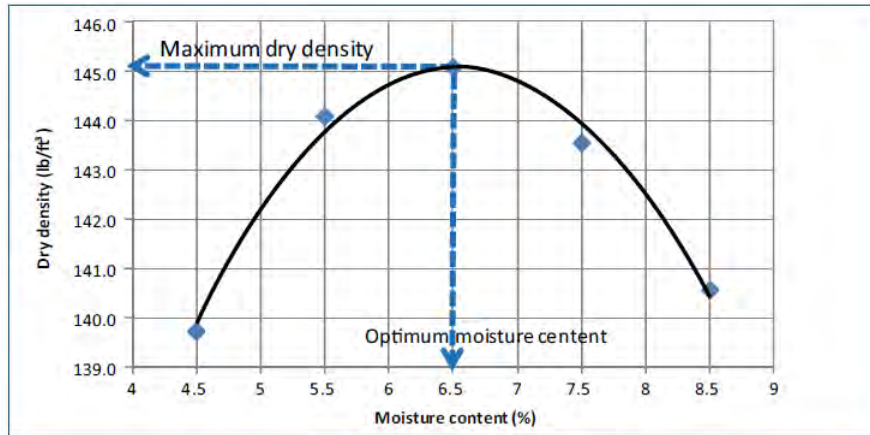


Figure 3- Typical moisture content-Density relationship established in soil-compaction approach

A hybrid consistency-compaction mix design approach was employed in this research program to develop the optimized mixture proportions of RCC. In other words both proper workability and maximum density criteria are considered in the mixture proportioning procedure. Details are presented in Chapter 6.

Regardless of what approach is used, a proper mixture proportions must produce the densest RCC mix possible with maximum workability. The goal is to produce an RCC mixture that has sufficient paste volume to coat the aggregates and fill the voids. The water content should be carefully adjusted to result in a mixture, which is workable enough that make it easy to achieve required density. The binder volume and composition should be properly selected to ensure the required mechanical characteristics are achieved in the mixture. The concrete should also be durable in the environmental condition to which the concrete will be exposed.

2.2.3 Examples of RCC mixture proportions

RCC mixture proportions may vary substantially in different regions and applications. Properties of local materials, availability of supplementary materials, the required strength level and exposure condition are among those parameters that affect the optimum mixture proportions for each application in a specific region. Some RCC mixture examples are presented in Table 4 to give a general overview of typical mixture proportions of RCC.

Table 4- Examples of RCC mixture proportions [Harrington et al., 2010]

Reference/Construction site			Port of Tacoma, WA Intermodal Yard	CTL Mix	Chattanooga, TN	Brownsville, TX	South Carolina	Atlanta, GA I285 Shoulder	Canada PCA RD135
Binders	Cement	(pcy)	450	504	300	504	444	500	500 ₁
	Fly ash	(pcy)	100	0	150	0	0	0	0
Aggregates	Maximum aggregate size (in.)	(in.)	5/8	3/4	3/4	3/4	1	1/2	3/4
	Coarse aggregate	(pcy)	1,700	1,378	2,110	1,287	1,759	1,650	2,117
	Fine aggregate	(pcy)	1,700	2,106	1,657	1,762	1,658	1,650	1,349
	Fines (passing No. 200)	(%)	3-7	2	3.6	2	--	--	--
Water ₂		(pcy)	257	211	190	236	216	266	160
Admixtures	Water reducer or retarder	(oz)	--	--	18	--	--	0	41
	Air entraining admixture	(oz)	--	--	0	--	--	0	41
Compaction parameters	Maximum wet density	(pcf)	154.3	152	--	147.2	--	150.3	156.9
	w/cm	--	0.47	0.42	0.42	0.47	0.49	0.53	0.32
	Aggregate/cementitious (weight)	--	6.18	6.91	8.37	6.05	7.70	6.60	6.93
	Fine aggregate/total aggregate	(%)	50.00	60.45	43.98	57.79	48.52	50.00	38.9
Strength	Compressive, 3-day	(psi)	1,810	5,460	5,090 ₃	3,046	3570	3866	--
	Compressive, 28-day	(psi)	6,050	7,900	6,100	4,946	5,220	5,157	8,368
	Flexural, 3-day	(psi)	525	690	611 ₃	493	--	--	--
	Flexural, 28-day	(psi)	770	900	702	638	--	--	--
	Ratio 28-day flexural/compressive	(%)	11.39	11.39	--	12.90	--	--	--

Notes:

1. 7 percent silica fume blended portland cement
2. Water content is total water based on oven-dried weight of aggregates, except for Canada and Chattanooga mixes, where reported water is free water based on saturated surface dry condition of aggregates.
3. 7-day compressive and flexural strength

2.3 Workability of RCC

ACI 116R-90 defines workability as “that property of freshly mixed concrete which determines the ease and homogeneity with which it can be mixed, placed, consolidated, and finished”. Workability is an important property that governs the ease of placement and provides an indication of production consistency. Workability of RCC is the main parameter that differentiates it from conventional concrete. RCC has usually lower volume of paste and lower water content that makes it much drier than conventionally vibrated concrete. Even though the

RCC has much lower workability than the near zero-slump concrete used in pavement construction, it has to have an adequate consistency to be properly compacted in the field.

RCC with adequate consistency for compaction can spread homogeneously under the roller passes. If the RCC is too wet for proper compaction, the surface will appear shiny and pasty, and the RCC will exhibit “*pumping*” behavior under the roller and even under foot traffic. Excessive consistency is also indication of too much paste or water in the mix that can lead to lower mechanical properties and durability. In contrast, dryer mixtures will increase the volume of voids during compaction. If the RCC is too dry, the surface will appear dusty or grainy and may even shear (tear) horizontally. In addition, aggregate segregation is likely to occur and sufficient density will be difficult to obtain, especially in the lower portion of the lift.

Due to the dry nature of RCC and the method by which the RCC is being compacted, the traditional workability test methods are not suitable for evaluating consistency of fresh RCC. The workability of an RCC mixture is determined experimentally by measuring the time required to consolidate a given volume of RCC at a specified energy level.

2.3.1 Vebe test

RCC workability is measured using a Vebe apparatus according to ASTM C1170, *Standard Test Method for Determining Consistency and Density of Roller-Compacted Concrete Using a Vibrating Table*. The Vebe apparatus has been modified by the U.S. Corps of Engineers and the Bureau of Reclamation in order to make it more suitable for use with RCC. It consists of a vibrating table of fixed frequency and amplitude, with a metal container having a volume of approximately 0.33 ft³ (0.0094 m³) securely attached to it. The Vebe apparatus used in this experiment is shown in Figure 4.

The procedure consists in placing loosely a representative sample of RCC of approximately 13 kg in a standardized cylindrical steel mould. The mould is fixed on a vibrating table, and a circular plastic plate is placed on top of the concrete sample. In order to consolidate the concrete, a removable mass of 29.5 or 50 lb is applied to the plate, and the vibrating table is turned on. The measure of consistency corresponds to the time of vibration required to fully

consolidate the concrete, as evidenced by the formation of a ring of mortar between the surcharge and the wall of the container. The Vebe Consistency Time is expressed to the nearest 1 second [ASTM C1170]. The Vebe test provides a simple, fast evaluation technique for determining RCC workability. The results from the Vebe tests can be greatly influenced by the operator, the type of apparatus, and the procedure followed. Care is needed when performing the test and interpreting the results.



Figure 4- Vebe test Apparatus for evaluating consistency of fresh RCC

Field experience has demonstrated that concrete workability must generally fall between 40 and 90 sec (Vebe consistency time) when the RCC is placed [Gauthier and Marchand, 2005]. These values appear to provide for adequate placement and avoid the workability problems described above. Limited laboratory research indicates that the modified Vebe time, as determined under a 50-lb (22.7 kg) surcharge, of 30 to 40 seconds is more appropriate for RCC pavement mixtures [ACI 325.10]. However, it should be emphasize that the range of workable mixtures can be broadened by adopting compaction techniques that impart greater energy into the mass to be consolidated. Figure 5 provides an example of a dry RCC mixture with a Vebe

time > 90 sec, as well as a properly proportioned RCC with a Vebe time of 45 sec after being compacted by Vebe apparatus.



Figure 5- Concrete surface after Vebe test, left) dry RCC with Vebe >90 sec, right) RCC with adequate consistency with Vebe=45 sec

2.3.2 Sampling procedure of RCC

The procedures for making RCC specimens for compressive and flexural strength testing are different from the practice used for conventional concrete. Compaction is the main factor affecting the properties of RCC. The substantial difference between the compaction procedure on the job site and the procedure used in laboratory sampling may result in a significant difference. Therefore, the concrete samples taken from the compacted pavement in the field are preferred over the laboratory samples. However, the difficulty of obtaining sawed beam specimens from actual paving sites requires developing and adopting a sampling procedure for RCC.

One technique for making RCC specimens has proven itself in recent years both in the field and laboratory, and has earned the recognition of contractors, consulting engineers, and testing/control laboratories. The technique provides for RCC cylinders (compressive strength), prisms (flexural strength), and several other specimen geometries, such as rectangular prisms for scaling resistance testing. It involves consolidating fresh RCC with an impact hammer with

an appropriate compaction head in steel molds. The procedure for producing RCC specimens for compressive testing using vibrating hammer and vibrating table are described in ASTM C1435 and ASTM C1176, respectively. The equipments, including hammer, rectangular head and circular heads used for sampling RCC are shown in Figure 6.



Figure 6- Hammer, rectangular head and circular heads used for sampling RCC

2.4 Mechanical characteristics of RCC

The following sections describe testing procedure that could be used to evaluate mechanical properties of RCC as well as typical value for the various test methods.

2.4.1 Compressive strength

Compressive strength is the main qualitative measure of mechanical properties of concrete and is usually used by design codes and standards for determining whether a concrete mixture is acceptable for a specific application. The compressive strength of RCC is comparable to that of conventional concrete, typically ranging from 4,000 to 6,000 psi (28 to 41 MPa). Some projects reported compressive strengths higher than 7,000 psi (48 MPa); however, practical construction and cost considerations would likely specify increased thickness rather than strengths of this nature. Missouri Standard Specifications for Highway Construction requires

that the RCC mix design shall have a minimum compressive strength of 3,500 psi (24 MPa) at 28 days when specimens prepared according to ASTM C 1176 or ASTM C 1435.

The densely graded aggregates used in RCC mixtures help the concrete achieve high levels of compressive strength. The low w/cm of RCC mixtures produces a low-porosity cement matrix that also contributes to the high compressive strength of the concrete. However, very low w/cm will result in a dry mix that cannot be compacted thoroughly. This increases the porosity and reduces the compressive strength of the hardened mixture. Every mixture proportion has an optimum moisture content at which it achieves the maximum dry density. This peak density most often provides the maximum strength.

2.4.2 Flexural strength

Flexural strength is one of the key parameters in designing a concrete pavement - conventional or RCC. The fatigue criteria (i.e. controlling cracking in a slab subjected to repetitive loading caused by heavy traffic) is influenced by the concrete's flexural strength.

Flexural strength is directly related to the unit weight and compressive strength of the concrete mixture. The presence of densely packed aggregates impedes crack propagation since more energy is required for cracking to occur. In properly constructed RCC pavement, the aggregates are densely packed and can reduce the development of fatigue cracking. The density of the paste and the bond strength of the paste to the aggregate particles are high due to the low water-to-cementitious materials ratio (w/cm). As a result, the flexural strength of RCC is generally high ranging from 500 to 1,000 psi (3.5 to 7 MPa). The ratio between flexural strength and compressive strength in RCC is about 0.15, as compared with 0.10 to 0.12 in the case of conventional concrete.

Having the compressive strength of the concrete, the flexural strength could be estimated from the following equation given by ACI 318 and ACI 325.10:

$$f_r = C \sqrt{f_c} \quad (\text{Eq. 1})$$

where:

f_r is flexural strength of concrete, psi

f_c is compressive strength of concrete, psi

C is a constant factor

The constant factor is $C=7.5$ for conventionally vibrated concrete. Due to the density of the paste in RCC and the strength of its bond to the aggregate particles, the constant value is usually higher than the conventional concrete. The recommended value is between 9 and 11 depending on actual RCC mix [ACI 325.10].

2.4.3 Splitting Tensile strength

Tensile strength of concrete is an important factor in designing thickness of pavement. Regarding the loading type on concrete pavement, the tensile stresses that are developed on the bottom of pavement are induced by bending of the pavement. Therefore, flexural test is generally used for determining the tensile strength of RCC pavement instead of the splitting tensile test.

2.4.4 Modulus of elasticity

The modulus of elasticity expresses the ratio between the applied stress and strain in the linear region. This constant is a measurement of the material's rigidity. The modulus of elasticity of RCC is similar to or slightly higher than that of conventional concrete when the mixes have similar cement contents.

The measured modulus of elasticity is compared with the estimated modulus of elasticity given by ACI 318:

$$E_c = 57000 \sqrt{f_c} \quad (\text{Eq. 2})$$

where E_c is the modulus of elasticity [psi], and f_c is compressive strength of the concrete [psi].

The AASHTO LRFD Bridge Design Specifications code provides an alternative way to estimate the modulus of elasticity:

$$E_c = 33000 w_c^{3/2} \sqrt{f_c} \quad (\text{Eq. 3})$$

where E_c is the modulus of elasticity [ksi], w_c is the unit weight of concrete [kip/ft³] and f_c is compressive strength [ksi].

It should be emphasized that the relation given in Eq. 2 and Eq. 3 are developed for conventional concrete. These equations may underestimate the modulus of elasticity of RCC.

2.4.5 Coefficient of Thermal expansion

The coefficient of thermal expansion (CTE) is used for determining the expansion or contraction of concrete pavement by the seasonal or daily changes of ambient temperature. The extent of longitudinal, transverse, and corner cracking associated with thermal curling on jointed concrete pavements is believed to depend on the CTE of the concrete. Thermal expansion and contraction properties of RCC are believed to be similar to those of conventional concrete made with similar materials. The typical values of concrete CTE ranges from about $8 \mu\text{m}/\text{m}/^\circ\text{C}$ to $12 \mu\text{m}/\text{m}/^\circ\text{C}$ depending on the aggregate volume and properties, binder content, and binder compositions. Thermal expansion and contraction properties of RCC are believed to be similar to those of conventional concrete made with similar materials [ACI 207.5].

2.4.6 Drying Shrinkage

Concrete shrinkage can be defined as decrease in either length or volume of a material resulting from changes in moisture content, temperature, or chemical changes. The temperature expansion/contraction is estimated using the coefficient of thermal expansion discussed in section 2.3.5. Any significant change in isothermal volume contraction experienced with RCC pavements is due to drying shrinkage. The main factors in drying shrinkage are the w/cm and aggregate volume. Drying shrinkage increases with the increase in w/cm , as well as, the rate of drying. Rigid aggregates can restrain paste shrinkage and deformation and reduce the drying shrinkage. The degree to which deformation is restrained depends on aggregate elastic properties.

The volume change associated with drying shrinkage is normally less than that in comparable conventional concrete mixtures due to the lower water content and lower paste volume of RCC. The significant volume of compacted skeleton of aggregates in RCC reduces drying shrinkage more than lowering the w/cm does. In fact, the greater the volume of aggregate, the less affect the w/cm has on drying shrinkage. The maximum drying shrinkage in a typical RCC

mix generally falls between 400 and 500 $\mu\text{m}/\text{m}$, compared with values for conventional concrete of 700 $\mu\text{m}/\text{m}$ or more.

Lower shrinkage of RCC reduces crack width compared to conventional concrete, also helps reduce curling and warping stresses. Thus, transverse cracks in RCC pavements are spaced considerably farther apart than transverse cracks in conventional concrete pavements. That is why sawed contraction joints for controlling random cracking are not usually required in RCC pavements.

2.5 Durability characteristics

Durability is the ability of concrete to endure in harsh environment. Concrete's durability is linked to its ability to resist aggressive ingredients penetration into its pore network. Minimizing the air void content in the RCC mixture through increasing its density is crucial to its durability. Excess porosity allows the penetration of air, water, and aggressive ingredients and reduces the durability of concrete in harsh environment.

Despite the various advantages offered by RCC, there are some issues regarding its long-term durability in severe environment. One of the main concerns associated with RCC is its frost durability in cold climates. Concrete structures, such as RCC pavements, exposed to cold climate are generally subjected to two types of damage caused by freeze-thaw cycles: 1) internal cracking and 2) surface scaling. While they may occur simultaneously, these phenomena are distinct and independent. In a concrete that has a critical moisture content, freeze-thaw cycles can produce internal cracking if the concrete is not properly air-entrained and if it does not have sufficient strength to resist the force caused by freezing of internal water. Surface scaling can also occur during freeze-thaw cycles when the concrete is exposed to deicing salts and if the exposed upper part of the pavement is not properly air-entrained. RCC mixtures must therefore be designed to resist both of these types of attack caused by freeze-thaw cycles.

In RCC, it is difficult to entrain air due to the low water content in RCC. Most laboratory test results that have been published during the last two decades have indicated that the frost and

particularly the Deicing salt-scaling resistance of RCC are not always satisfactory. Contrary to the laboratory test results, many field surveys tend to indicate that non-air entrained RCC can be quite resistant to frost action under severe exposure conditions when placed and cured properly. Some field surveys also indicate that non-air-entrained high-performance RCC even can be resistant to Deicing salt-scaling, particularly when certain supplementary cementitious materials are used [PCA, 2004].

2.5.1 Freeze and thaw resistance

Field performance studies have indicated that RCC has performed well in harsh weather conditions. Studies in the United States and Canada indicate that RCC mixtures, whether air entrained or not, have performed well for more than three decades. Piggott (1999) inspected and reported on 34 RCC pavements in United States and Canada. The study concluded that RCC pavements in varied climatic conditions and ranging in age from 3 to 20 years have performed well. The study notes that non-air entrained RCC pavements can provide reliable and durable performance in freeze and thaw environments as long as the mix has adequate cement content, sound aggregates, proper mixing, adequate compaction, and proper curing.

2.5.2 Deicing Salt-Scaling Resistance

According to most laboratory data, RCC appears to be more susceptible to Deicing salt-scaling than conventional Portland cement concrete mixtures of the same compressive strength. A series of scaling tests carried out on specimens taken from test areas indicates that binder type plays a significant role in Deicing salt scaling resistance. Mineral admixtures (fine particles), especially silica fume, improve RCC scaling resistance. Furthermore, it appears that fly ash did not contribute to the scaling resistance of these mixes.

2.5.3 Porosity and the permeability

Porosity and the permeability of the hydrated cement paste fraction of the material have a strong influence on the durability of concrete. Porosity and pore size distribution of RCC depend on the w/cm and the degree to which the concrete is compacted. Permeability is defined as the ease with which fluids can penetrate concrete. This can be accomplished through the lowering w/cm, improved curing, and the use of SCMs. Pavements with low

permeability resist penetration of moisture into the concrete matrix, leading to improved freeze-thaw resistance and improved resistance to physical and chemical attacks.

Paste distribution in RCC is less homogeneous than in conventional concrete due to the difficulty of dispersing mixing water in a stiff mix. As a result, RCC contains a certain number of compaction voids that can affect its freeze-thaw resistance. The irregular shape and larger size of compaction voids clearly differentiates it from the spherical voids produced by air entraining agents. A high number of compaction voids may form an interconnected network that seriously jeopardizes durability. On the other hand, compaction voids can play a positive role if they are sufficiently small and well distributed. Optimizing the aggregate skeleton, proper selection of binder composition and volume and more importantly fine-tuning the w/cm of the mixture reduce the number of compaction voids and improve the durability of RCC.

2.5.4 Electrical resistivity

Indirect testing of corrosion resistance of concrete can be evaluated using the electrical conductivity approach that plays a key factor in the electro-chemical reaction. The electrical conductivity is usually evaluated using the RCPT (AASHTO T277, ASTM C1202) by determining the electrical charge passing through the ionic pore solution of a concrete sample. Recently, other test methods have been developed to evaluate the electrical properties of concrete: the surface resistivity (SR) and the bulk electrical conductivity test methods.

The resistivity results from this test method must be used with caution, especially in RCC where few data are available. The qualitative terms in the left-hand column of Table 5 that shows the risk of chloride corrosion in terms of surface resistivity could be used in most concrete types. It should be emphasized that these tests are basically used for measuring corrosion resistance of concrete against chloride attacks. RCC pavements are usually made without reinforcement; therefore, chloride permeability of RCC is not a concern in pavement construction. However, these tests also give information on connectivity of pores which is key parameter in durability of concrete. Therefore, the resistivity test is also performed on RCC samples and the results are used to evaluate durability resistance of RCC.

Table 5- Relation between surface resistivity and risk of corrosion in concrete

Chloride Ion Penetrability	Surface Resistivity Test	
	100-mm × 200-mm (4 in. × 8 in.) Cylinder (KOhm-cm) a=1.5	150-mm × 300-mm (6 in. × 12 in.) Cylinder (KOhm-cm) a=1.5
High	< 12	< 9.5
Moderate	12-21	9.5 - 16.5
Low	21 - 37	16.5 – 29
Very Low	37 - 254	29 – 199
Negligible	> 254	> 199

3 Testing protocols

3.1 Compressive strength

The compressive strength of RCC is determined in the same procedure as conventional concrete following ASTM C39 or AASHTO T22. The testing apparatus used in this research program is shown in Figure 7.



Figure 7- Compressive Strength test

3.2 Flexural strength

Flexural strength can be evaluated depending on where the load is applied: cantilever, center point, or third point. The first two evaluate flexural strength at a single point, whereas the third

method determines the flexural strength at the middle third of the specimen. Following ASTM C78, a third-point loading setup was used for testing the flexural strength, as shown in Figure 8. Two rigid supports were located 1 in. away from each side of the specimen. The load is applied gradually to the concrete prism, and the failure load (P) is recorded. The flexural strength is calculated using the following equation:

$$f_r = \frac{PL}{bh^2} \quad (\text{Eq. 4})$$

where P is the failure load (maximum load), L is the flexural span between the support, and b and h are the width and height of concrete prism, respectively.

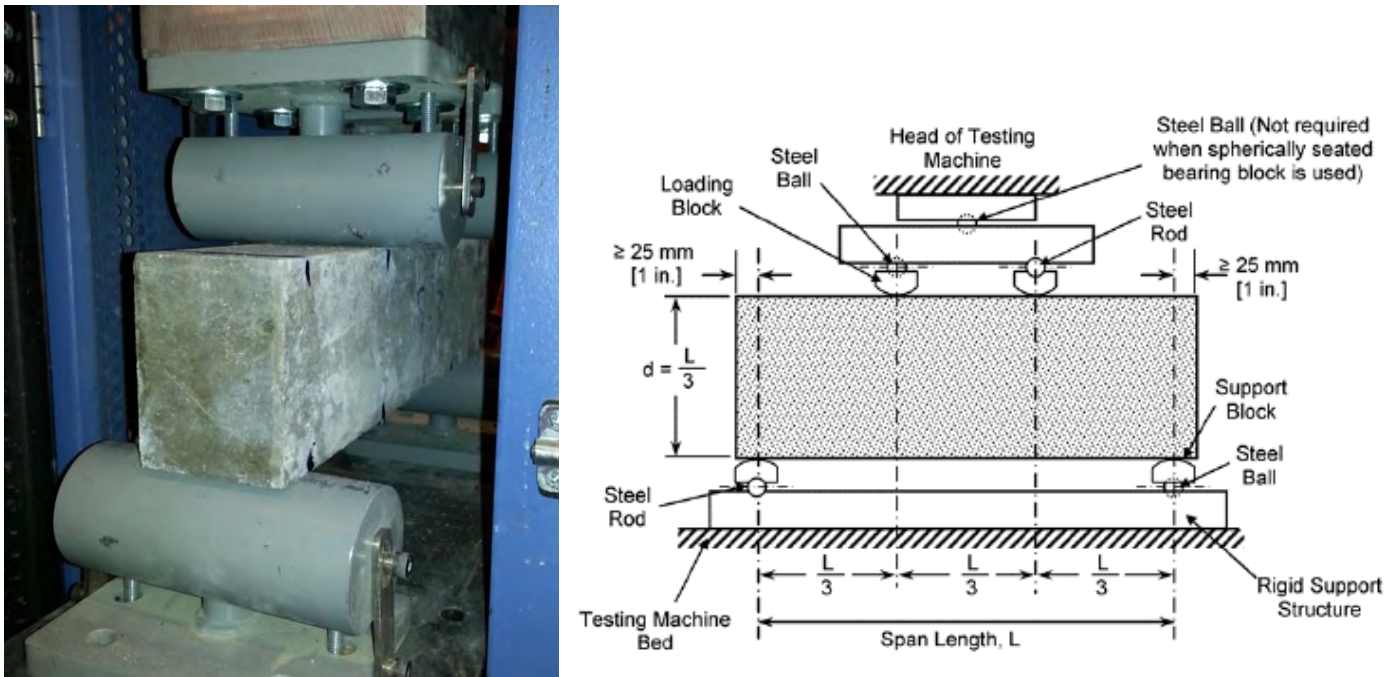


Figure 8- Setup of flexural strength test (ASTM C78)

3.3 Splitting Tensile strength

The standard procedure of splitting tensile strength is described in ASTM C496. The setup used for measuring the splitting tensile strength is shown in Figure 9. Compressive loads (P) are applied on the top and bottom of the specimens where two strips of plywood are placed to

distribute tensile strength along the vertical axis of the specimens. The load at failure is recorded as the peak load, and the tensile strength is calculated using the following equation:

$$f_t = \frac{P}{\pi DL} \quad (\text{Eq. 5})$$

where P is the peak load, L is the length of the specimen, and D is the diameter of the specimen.



Figure 9- The splitting tensile test setup used in this program

3.4 Modulus of elasticity

The modulus of elasticity is determined using ASTM C469. The MTS machine used in this investigation for measuring the modulus of elasticity is shown in Figure 10. For each testing age, three 4x8 in. cylindrical specimens were used for determining the static modulus of elasticity according to ASTM C469. All the specimen end surfaces were grinded to ensure uniform load distribution over the specimen surfaces.

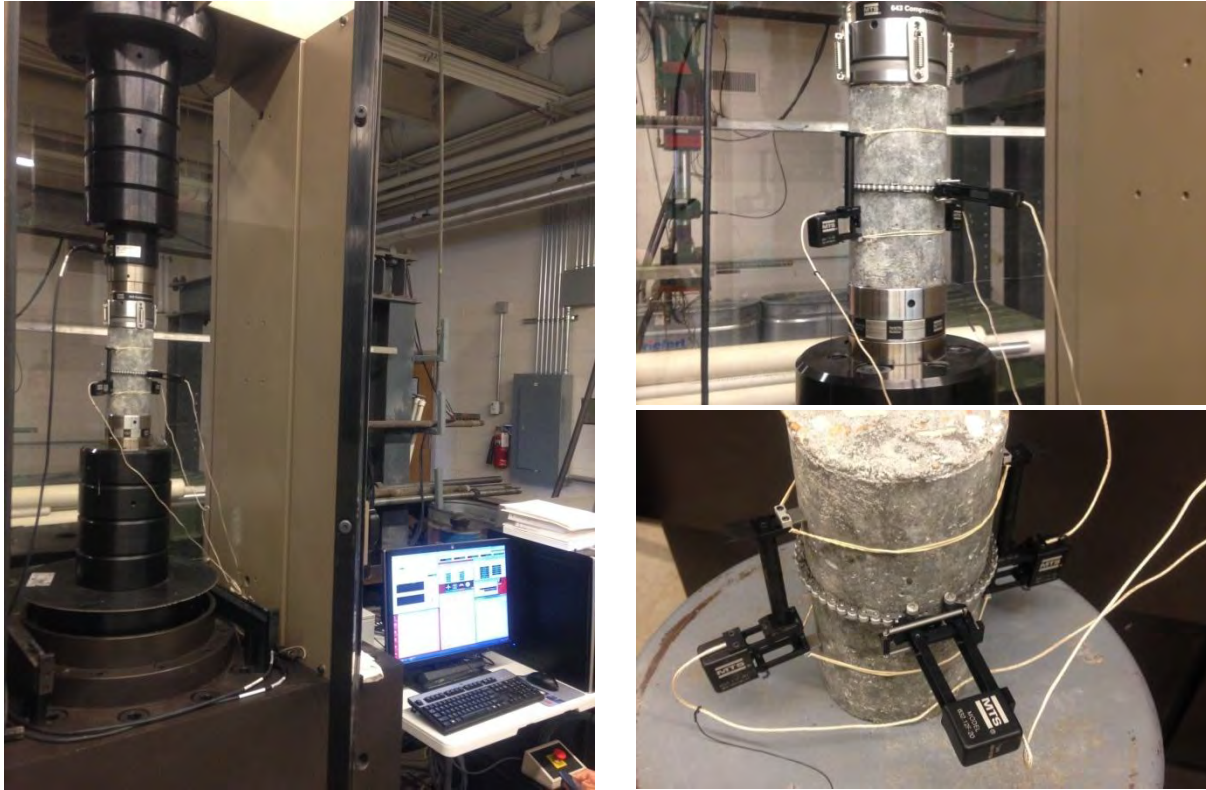


Figure 10- The test setup used for measuring modulus of elasticity

3.5 Coefficient of thermal expansion

This parameter can be determined according to AASHTO TP60, *Coefficient of Thermal Expansion of Hydraulic Cement Concrete*. Concrete samples were cured in the Missouri S&T lab until testing age then shipped to MoDOT for conducting the test.

3.6 Drying Shrinkage

The drying shrinkage of concrete specimens in this research project were measured in accordance to ASTM C157, *Standard Test Method for Length Change of Hardened Hydraulic-Cement Mortar and Concrete*. The testing apparatus is shown in Figure 11. This initial length was registered and used as the reference for determining the shrinkage deformation of the specimens. The same device was used for measuring the length of specimens at different time intervals after moving them to the environmental chamber.

Three 3×3×11.3 in. prisms were used for monitoring drying shrinkage of each of the concrete mixtures according to ASTM C157. The concrete specimens were demolded 24 hours after

casting and placed in the lime-saturated water of 70 ± 3 °F for 7 days. The samples were then kept in an environmental chamber with a temperature of 70 ± 3 °F and a relative humidity of $50\% \pm 4\%$.



Figure 11- Measurement of drying shrinkage

3.7 Freeze and thaw resistance

The freeze-thaw resistance of RCC samples were evaluated in accordance to ASTM C666, *Resistance of Concrete to Rapid Freezing and Thawing, procedure A*. This test method covers the determination of the resistance of concrete specimens to rapidly repeated cycles of freezing and thawing in the laboratory.

This test procedure consists of subjecting concrete specimens to 300 cycles of rapid freezing and thawing in water. The freezing and thawing cycles have to be adjusted so that the temperature decreases from 5°C to -18°C and increases back to 5°C in no less than 2 hours and no more than 5 hours. To conduct the test, the specimens are placed in metal containers and surrounded by approximately 5 mm of clean water. Freezing is generated with a cooling plate at the bottom of the apparatus while thawing is produced by heating elements placed between the containers. The basic concept is measuring the dynamic modulus of elasticity of concrete

specimens subjected to freeze-thaw cycles. It has been shown that internal cracking caused by repeated cycles of freezing and thawing reduces the dynamic modulus of elasticity. Therefore, reduction in dynamic modulus of elasticity is an indicator of damage caused by freeze-thaw cycles.

The ultrasonic pulse velocity test was used for determining the dynamic modulus of elasticity of the specimens and its variation with the increase in freeze-thaw cycles as shown in Figure 12. The Freeze-thaw chamber according to ASTM C666, procedure A are shown in Figure 13.

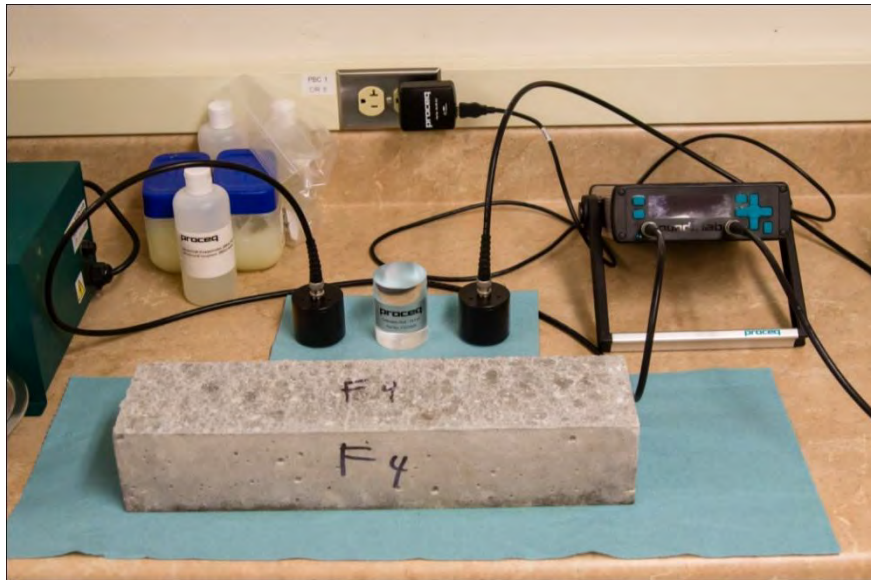


Figure 12- Dynamic modulus of elasticity testing apparatus for freeze-thaw test



Figure 13- Freeze-thaw chamber according to ASTM C666, procedure A

3.8 Deicing Salt-Scaling Resistance

The test methods generally used to evaluate RCC scaling resistance is ASTM C672, Scaling Resistance of Concrete Surfaces Exposed to Deicing Chemicals. In this test, the surface of concrete is covered with approximately 6 mm of salt solution and the specimens are subjected to freezing and thawing cycles. The salt solution is a 4% sodium chloride solution (i.e., 4 g of NaCl for each 100 ml of water). The specimens are subjected to a minimum of 50 freezing and thawing cycles by alternately placing them in a freezing environment ($-17.8 \pm 1.7^{\circ}\text{C}$) and a thawing environment ($23 \pm 1.7^{\circ}\text{C}$). The chamber used for this purpose is shown in Figure 14. At the end of each series of 5 cycles, the salt solution is renewed and the scaling residues is recuperated, dried, and weighed. The extent of surface scaling is assessed visually. The visual rating ranges from 0 for concrete surfaces showing no scaling to 5 for concrete surfaces suffering severe scaling with coarse aggregates visible over the entire test surface.



Figure 14- Chamber used for Deicing salt-scaling resistance test

3.9 Permeable voids

Permeable voids of RCC specimens were determined in accordance to ASTM C642, *Standard Test Method for Density, Absorption, and Voids in Hardened Concrete*. Compared to other test methods for permeability, the test method described in ASTM C642 is simple to perform and does not require any specialized equipment. The testing apparatus used in this investigation is shown in Figure 15.



Figure 15- The apparatus used for measuring permeable voids in concrete

3.10 Electrical resistivity

Bulk electrical resistivity and Surface electrical resistivity of RCC specimens is measured in accordance to ASTM C1760, *Standard Test Method for Bulk Electrical Conductivity of Hardened Concrete* and AASHTO T95, *Standard Method of Test for Surface Resistivity Indication of Concrete's Ability to Resist Chloride Ion Penetration*, respectively. Test method described in ASTM C1760 covers the determination of the bulk electrical conductivity of saturated specimens of hardened concrete to provide a rapid indication of the concrete's resistance to the penetration of chloride ions by diffusion. The test method described in AASHTO T95 is based on the same concept but measures the surface resistivity which is applicable to the surface of currently build structures in the field. The equipment used for bulk and surface resistivity is shown in Figure 16.



Figure 16- Testing apparatus of surface and bulk resistivity of concrete

The surface resistivity test method consists of measuring the resistivity of 4 x 8 in. cores or cylinders by use of a 4-pin Wenner probe array. An AC potential difference is applied in the outer pins of the Wenner array generating current flow in the concrete. The potential difference generated by this current is measured by the two inner probes. The current used and potential obtained along with the area affected are used to calculate the resistivity of the concrete.

4 Field evaluation of concrete used for RCC Pavement

RCC used as a part of the modernization of Highway 160. The project includes the addition of shoulders from Route 21 near Doniphan to the west of Route JJ. The total length of the improvement is 8.35 miles (see Figure 17).

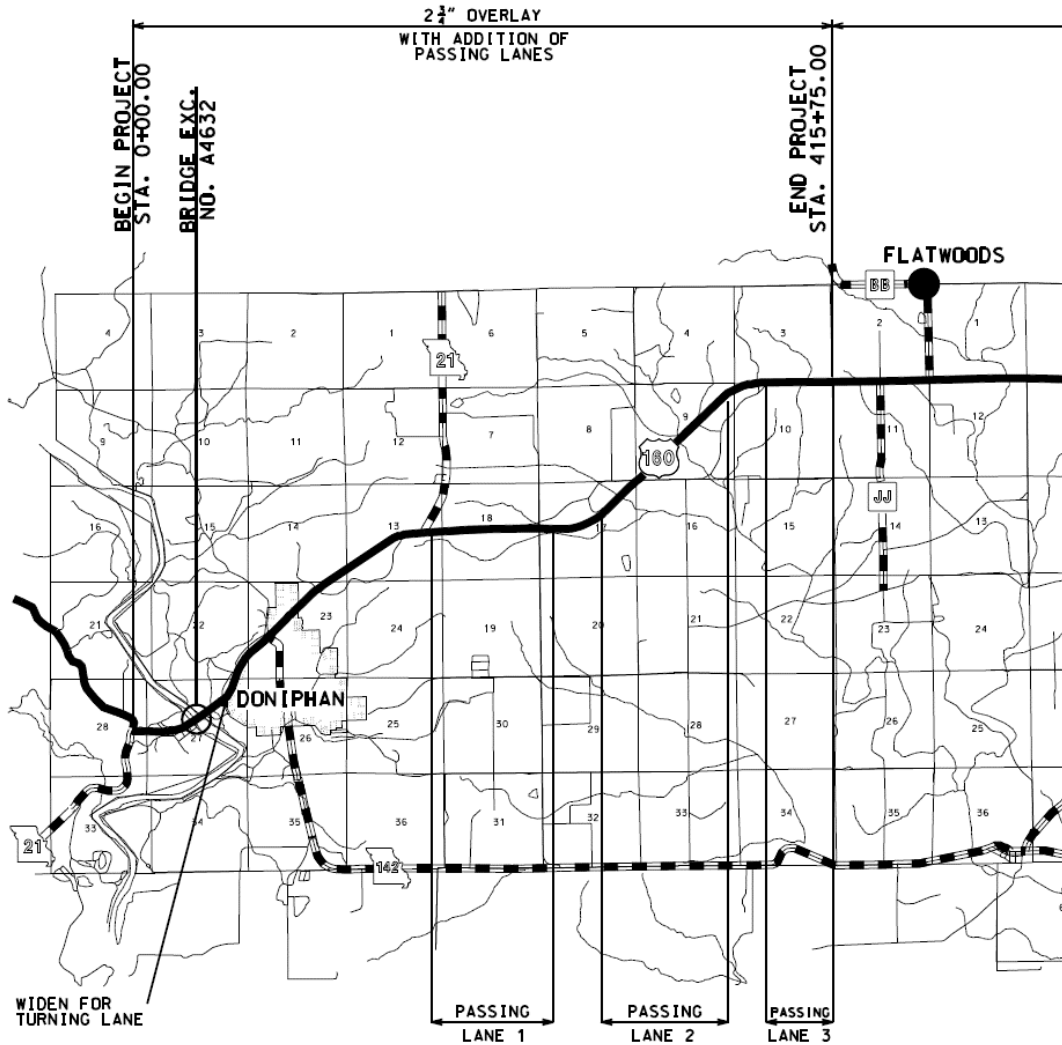


Figure 17: Overview of the highway 1600 Job J9P2186 near Doniphan, MO

The concrete shoulder has 10 ft wide and the thickness of pavement is 8 in., which was constructed in two lifts. The concrete constituents were a coarse aggregate with maximum nominal size of 3/4 in., natural sand, cement, and water. The RCC made without chemical

admixture or SCMs. The concrete was batched in a pug mill mixer and delivered by trucks to the job site. The RCC production facilities are shown in Figure 18.



Figure 18- RCC production facilities used for widening Route 160

Roller Compacted Concrete Field evaluation and mixture development

The RCC was placed with two road wideners and a vibratory roller behind each roller compacting the lifts. The vibratory rollers were 13 ton rollers. The curing compound was standard SS-1 tack that were used on hot mix sprayed from an Etnyre distributor. The lag time between concreting each lift was about 10-15 minutes. The RCC pavement construction are shown in Figure 19.



Figure 19- RCC pavement construction in Route 160

4.1 Concrete sampling

Concrete samples were taken at the jobsite to test fresh concrete properties and cast specimens. Before sampling, a practice was carried out to optimize the sampling process and fine-tune test procedure on August 1st 2013 (first day of production). The first sampling was taken on August 1st 2013 while the second one was carried out on August 2nd.

In this report, results obtained on second and third batch will be referred to as RCC2 and RCC3, respectively (see Table 6). The first sampling was performed to optimize the sampling procedure and the samples were not tested. All samples were taken from the same mix design as developed by the contractor.

Concrete specimens were cast to evaluate the mechanical properties, drying shrinkage, and key durability characteristics. Some pictures of the sampling procedure are shown in Figure 20. All specimens were compacted according to ASTM C1435 by using a vibrating hammer. The cylindrical specimens were cast in three layers, and each layer was fully compacted until mortar was formed on the top surface. Cylinder specimens, 6 x 12 in., were used for compressive strength, splitting tensile strength and modulus of elasticity testing. Flexural strength was determined using 3 x 3 x 16 in. prisms and 3 x 3 x 11.25 in. prisms were used for monitoring drying shrinkage. Concrete workability were evaluated by the Vebe apparatus in accordance to ASTM C1170.

Table 6- Nomenclature of test specimens

Name	Sample taken	Description
RCC1	08/01/2013 1.00 pm	Practice to optimize sample process and test procedures
RCC2	08/01/2013 4:00 pm	Sample taken for fresh concrete tests and casting specimens
RCC3	08/02/2013 11:30 am	Sample taken for fresh concrete tests and casting specimens



Figure 20- Sampling of concrete specimens

Specimens were stored on-site in moist conditions for 24 to 48 hours before being transported to the CIES laboratory at Missouri S&T. On site, the specimens were covered with saturated sand and plastic sheets, as shown in Figure 21. The specimens were placed into a water container during the 5-hr transport to Rolla, MO. The specimens were demolded in the laboratory and placed in lime-saturated water at a temperature of 70 ± 3 °F until the age of testing. Table 7 summarizes the sampling and testing program.

Table 7- Sampling and testing program

Test	Test method	Age of testing	Sample size	# samples
Consistency of concrete (Vebe Consistency Time)	ASTM C1170	Fresh	9.5x7.75 cylinders	1
Compressive strength	ASTM C39	7, 28, 91 days	6x12 in. cylinders	9
Splitting tensile strength	ASTM C496	28 days	6x12 in. cylinders	2
Modulus of elasticity	ASTM C469	28 days	6x12 in. cylinders	2
Flexural strength	ASTM C78	91 days	3x3x16 in. prisms	2
Shrinkage	ASTM C157	Continuous	3x3x11.25 in. prisms	2



Figure 21- Storage of concrete specimens at the job site

4.2 Fresh concrete properties determined in-situ

The workability of the RCC was measured using a Vebe vibrating table test (according to ASTM C 1170). The Vebe cylindrical container was filled with loosely compacted concrete and the surface of the specimens was leveled. A 50-lb surcharge was placed on top of the leveled concrete surface. The time for a mortar ring to appear, around the surcharge under vibration, was determined. The testing procedure is shown in Figure 22. All the tested concretes showed no mortar ring after 2 minutes of vibration (Table 8), thus indicating a very low workability. The low workability of concrete made it difficult to sample the mixture and achieve the proper consolidation. The low compaction of concrete was visible in the specimens where some honeycombing were observed after demolding.

Table 8- Results consistency measurements by means of Vebe consistency measurements

Sample	Vebe time
RCC2	> 120 s
RCC3	> 120 s



Figure 22- RCC workability test

4.3 Mechanical properties of samples specimens

A summary of the mechanical test results up to 91 days is presented hereafter. The results include compressive strength, modulus of rupture, splitting tensile strength, and modulus of elasticity. All the test samples were water-cured until the age of testing.

4.3.1 Compressive strength

The compressive strengths are determined on 6 x 12 in. cylinders at 7, 28, and 91 days of concrete age. Three concrete specimens were tested at each age and the mean values are

considered as the compressive strength at a given age. The results, are summarized in Table 9 and plotted in Figure 23. The results obtained for the RCC3 mixture are slightly higher at 28 and 91 days than those for the RCC2 mixture. However, the spread in the compressive strength of the two concretes was limited to 10%.

Table 9- Compressive strength of the specimens cast in the field

Mix	Age	Compressive strength, f_c (psi)	
		Mean	C.O.V. (%)
RCC2	7 days	3610	5.7
RCC3		3540	7.9
RCC2	28 days	4170	1.3
RCC3		4460	2.2
RCC2	91 days	4090	-
RCC3		4590	4.3

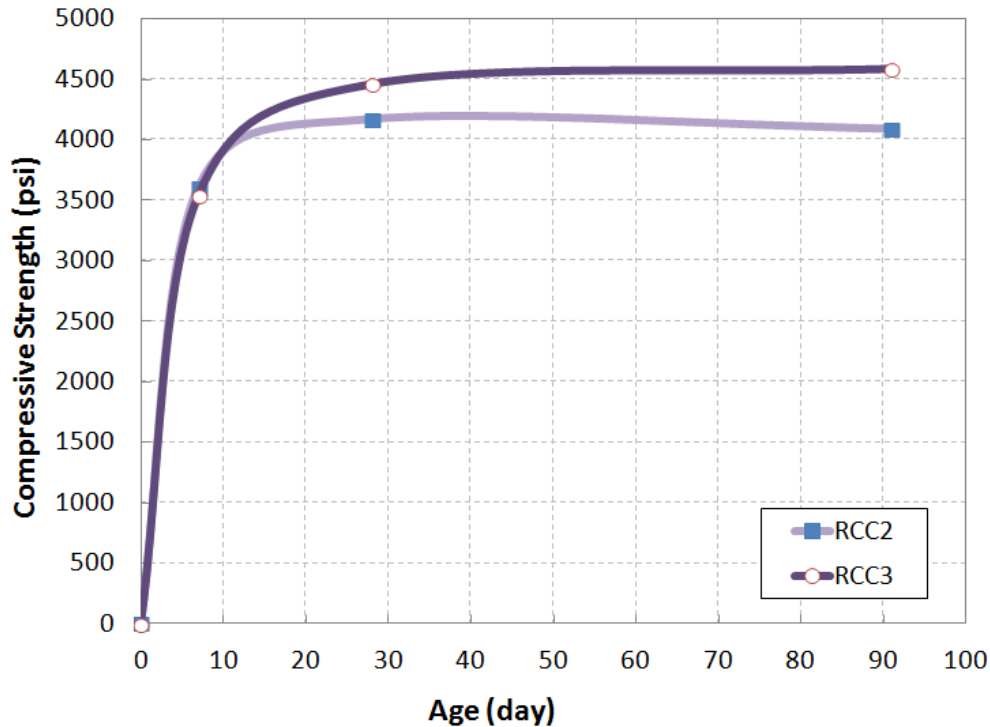


Figure 23- Development of Compressive strength in field RCC

4.3.2 Flexural strength

The flexural strength was measured on 3 x 3 x 16 in. prism specimens at 91 days. Two specimens were tested and the mean values were reported as flexural strength of the concrete. The flexural strength results are given in Table 10. The two mixtures showed comparable flexural strengths (only 8% difference).

Table 10- Flexural strength of concrete specimens cast in the field

Mix #	Flexural strength of specimens (psi)			Estimated, ACI (psi)
	A	B	Mean	
RCC2	980	950	970	650
RCC3	860	920	890	670

The flexural strength estimated based on ACI 325.10 using the constant factor of C=10 are also added to Table 10. The measured flexural strengths are higher than the values estimated by ACI 325.10 even when C=10 is selected in the formula.

4.3.3 Splitting tensile strength

Splitting tensile strength was measured on 6 x 12 in. cylinder specimens at 28 days. Three concrete specimens were tested and the mean values were determined. The two mixtures exhibited almost the same tensile strength of 410 psi and 420 psi, as presented in Table 6.

Table 11- Tensile strength of concrete specimens cast in the field

Mixture	Splitting Tensile Strength		
	Average (psi)	C.O.V (%)	ft/fc * (%)
RCC2	420	18.6%	10.2%
RCC3	410	3.1%	9.0%

*Tensile/Compressive ratio

4.3.4 Modulus of elasticity

The modulus of elasticity was determined in accordance with ASTM C 469. Two 6 x 12 in. cylinder specimens were used for measuring the modulus of elasticity at 91 days of age. The results are presented in Table 12. The measured modulus of elasticity is compared with the

estimated value given by ACI 318 and AASHTO LRFD Bridge Design Specifications. The results presented in Table 12 show that the measured values of the modulus of elasticity are about 20% to 25% higher than the estimated values either by ACI or AASHTO equations.

Table 12 – Modulus of elasticity of concrete specimens cast in the field

Mixture	Modulus of Elasticity			
	Average (ksi)	C.O.V (%)	Estimated, ACI (ksi)	Estimated, AASHTO (ksi)
RCC2	4530	7.0%	3680	3780
RCC3	3810	8.8%	3810	3930

4.4 In-situ mechanical properties

For the evaluation of the in-situ properties of the RCC pavement, cores were drilled from the shoulder. These cores were obtained on August 20th 2013 (being 14 to 19 days after placement). In total 10 cores of 3.75” diameter (5 pairs of 2 cores) were drilled out of the RCC shoulder slab (~ 8 in. in thickness) along the length of the job site. The locations of the core drillings are schematically shown in Figure 24.

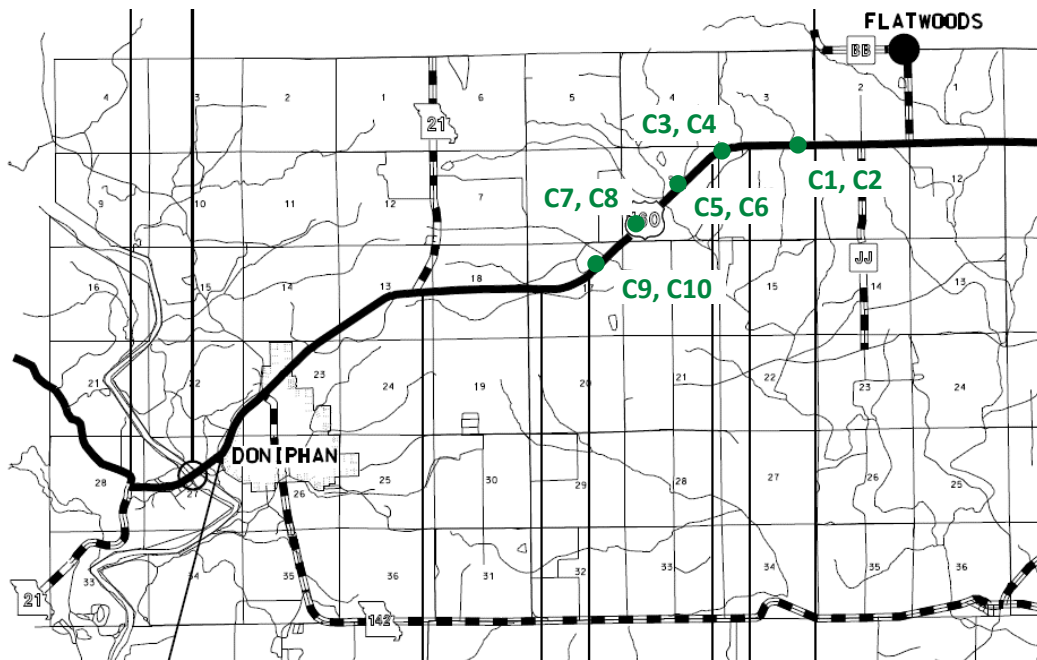


Figure 24- Location of core drilling

The C3 and C4 cores were drilled close to the location of the installed vibrating wire gage sensors. These cores can be related to the concrete sample RCC2. The C5 and C6 cores can be related to the concrete sample RCC3.

All cores were cured in lime-saturated water at 70 ± 3 °F until the age of testing. A visual inspection of the cores shows that the cores are close to or higher than 8 in. In most cores, the seam of interface between the two cast layers is visible. As described before, the total thickness of pavement is 8 in. which was paved in two lifts each has a 4 in. thickness. The time lag between lifts was about 10 to 15 minutes. Concrete at the bottom of the top layer was loosely compacted compared to the other parts of the cores. A typical seam between two layers are shown in Figure 25. Based on the failure pattern, this joint is not affecting the compressive strength test result to a high extend.



Figure 25: Joint between two casting layers showing increased porosity as observed for core C2

4.4.1 Compressive strength

The in-situ compressive strength was determined on two cores at 28 and 91 days. According to ACI recommendation, the compressive strengths of core specimens were corrected by applying the drilling damage factor of 0.85. The results are summarized in Table 13. The corrected compressive strengths of core specimens are very close to the compressive strength of the cast in the field specimens (RCC2).

Table 13- Compressive strength of the core specimens

core #	ages	Compressive strength (psi)		
		Measured	Corrected	Relative *
C3	28 days	3580	4210	101%
C4		3040	3580	86%
C2	91 days	3730	4390	107%
C1		3910	4600	113%

** Corrected compressive strength of core specimens divided by the average compressive strength of specimens cast in the field*

4.4.2 Relative bond strength

Relative bond strength was also determined using the drilled cores in which the bond surface is normal to the longitudinal axis at approximately the mid-length of the specimen. A splitting tensile stress normal to the bond surface is produced by applying a point load at the joint (see Figure 26).

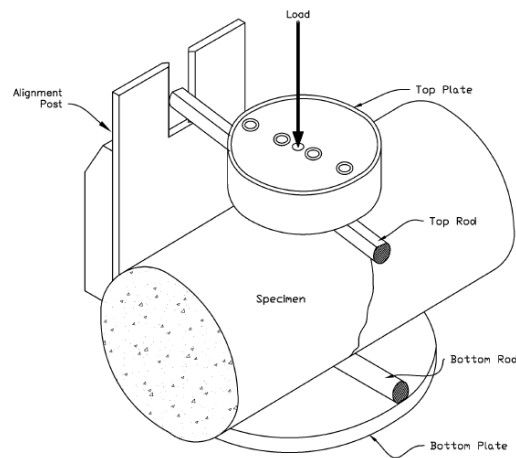
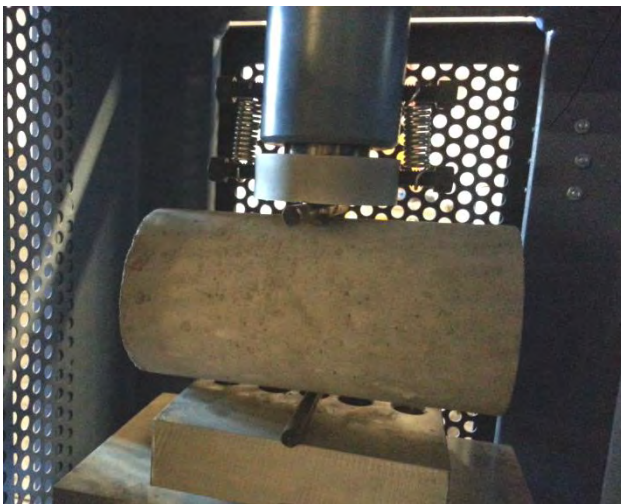


Figure 26- Apparatus used for testing the relative bond strength

This test was performed in accordance to ASTM C1245 [6] and is intended for the determination of the relative bond strength between successive layers of RCC in multiple-lift forms of construction. It should be noted that this test gives the relative bond strength and is not intended to provide tensile strength results of the RCC tested. This test is also performed on the middle of the lift, and the results are compared with those of testing at the joint between two concrete lifts. The results summarized in Table 14 show that the relative bond strength between two lifts of tested RCCP is about half of the corresponding strength determined within a single lift. Typical failure surface is shown in Figure 27. The failure surface at the joint between layers (left specimen) shows higher porosity compared to the failure surface at the middle of lift (right specimen).

Table 14- Results of relative bond strength tests on core specimens

Core #	diameter (in.)	length (in.)	L ⁺ (in.)	* <i>f_{tb1}</i> (psi)	** <i>f_{tb2}</i> (psi)	<i>f_{tb1} / f_{tb2}</i>
C7	3.71	7.48	3.54	80	230	0.35
C8	3.71	7.87	3.78	88	154	0.57
C9	3.71	8.46	3.70	96	202	0.47
Average				88	195	0.46

⁺ Distance of the joint from top surface of core specimens

* Relative bond strength at the joint between two lifts

** Relative bond strength at the mid height of the lift



Figure 27- Failure surface in the bond strength test, (left) joint between two lifts, (right) inside the lift

Bond strength at the interface of RCC lifts is a critical property and determines whether the RCC pavement constructed in multiple lifts can behave as a monolithic section or as partially bonded or un-bonded section. According to ACI 325.10 [7], the bond strength at the interface of two lifts should be at least 50 percent of the strength of the parent RCC material based on good engineering practice.

4.4.3 Coefficient of thermal expansion (CTE)

The coefficient of thermal expansion is determined on two 4"×8" cylindrical cast-in-place specimens as well as two cores taken from the paved RCC in the field. Concrete specimens were water cured in Missouri S&T then shipped to MoDOT construction laboratory for lab for testing. The results that are presented in Table 15 show both cast-in-place specimens and drilled cores have the same coefficients of thermal expansion.

Table 15 – Coefficient of thermal expansion of cast-in-place specimens and drilled cores

Code	Type	CTE ($\mu\text{m}/\text{m}/^\circ\text{C}$) (temp increment)	CTE ($\mu\text{m}/\text{m}/^\circ\text{C}$) (temp decrement)	CTE ($\mu\text{m}/\text{m}/^\circ\text{C}$) (Average)
RCC2	Cast-in-place	9.56	9.59	9.57
RCC3		9.43	9.55	9.49
C12	Drilled core	9.53	9.48	9.51
C6		9.58	9.50	9.54

4.5 Drying shrinkage

Four 3 × 3 × 11.25 in. prisms were used for monitoring drying shrinkage of concrete. Two specimens were cast from each RCC2 and RCC3. The concrete specimens were demolded two days after casting and placed in the lime-saturated water of 70±3 °F for three weeks. The samples were then kept in an environmental chamber with a temperature of 70±3 °F and a relative humidity of 50% ± 4%.

Drying shrinkage was determined in accordance with ASTM C 157 using a digital-type extensometer, as shown in Figure 11. The results of shrinkage measurement are presented in Figure 28. These results are the average of two specimens taken from each RCC mixture. The measured shrinkage values of two sampling data were nearly identical, as presented in Figure

28. The average measured shrinkage of RCCP specimens 300 days after demolding was about 400 $\mu\text{m}/\text{m}$. These results are in accordance with those reported in the literature stating that the volume change from drying shrinkage in RCC is lower than that of conventional concrete because of the reduced paste content and reduced water content of RCC [1].

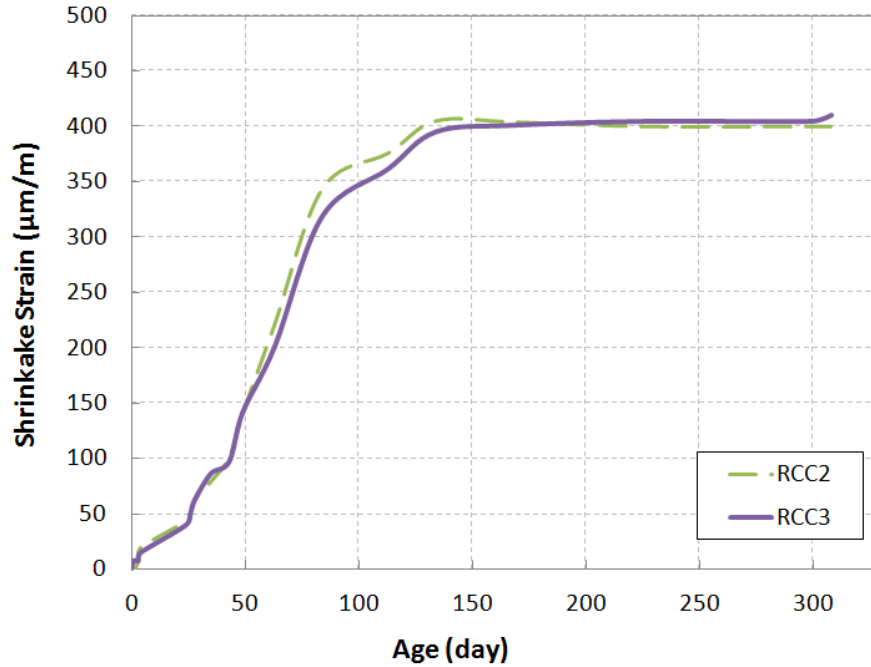


Figure 28- Shrinkage of concrete specimens in the lab

4.6 Durability characteristics

The resistance to freezing and thawing, freeze-thaw (ASTM C666), Deicing Salt-Scaling Resistance (ASTM C672) and permeable air voids (ASTM C642) are determined and discussed in the following sections.

4.6.1 Freeze-thaw resistance

Three prismatic samples measuring 3×4×16 in. were used to evaluate frost resistance according to ASTM C666, Procedure A. Three specimens were cured in lime saturated water before conducting freeze-thaw testing. The PUNDIT test was used for determining the dynamic modulus of elasticity of the specimens and its variation with the increase in freeze/thaw cycles.

Table 16 summarizes the variations of the durability factor of the concrete as a function of freeze-thaw cycles. Such a factor reflects the residual dynamic modulus of elasticity of the concrete. Drop in durability factor reflects the presence of internal cracking of the concrete due to damage from repetitive cycles of freezing and thawing. Values of durability factor greater than 80% after 300 cycles of freezing and thawing reflect adequate frost durability. However, all RCC samples failed before 60 cycles of freezing and thawing. Cracks appeared in some specimens after 30 cycles (Figure 29).

Table 16 – Frost durability of sampled RCC (ASTM C666, procedure A)

Mixture Specimen	Relative Dynamic Modulus of Elasticity (%)										
	0 cycles	30 cycles	60 cycles	90 cycles	120 cycles	150 cycles	180 cycles	210 cycles	240 cycles	270 cycles	300 cycles
RCC2	1	100	73	Fail	-	-	-	-	-	-	-
	2	100	70	Fail	-	-	-	-	-	-	-
	3	100	48	Fail	-	-	-	-	-	-	-
RCC3	1	100	Fail	-	-	-	-	-	-	-	-
	2	100	Fail	-	-	-	-	-	-	-	-
	3	100	Fail	-	-	-	-	-	-	-	-



Figure 29- Cast in field RCC specimens after 30 cycles of freezing and thawing

4.6.2 Deicing salt scaling resistance

Five concrete slabs (11"×10"×3") were cast for salt scaling testing according to ASTM C672. Concrete specimens were cured in water up to 91 days then were sent to MoDOT for salt scaling testing. The curing procedure is applied to the specimens was longer than that recommended by ASTM C672. The results of visual observation of surface quality after subjecting to freeze-thaw cycles are summarized in Table 17. All concrete slabs failed after 15 cycles of freezing and thawing. Cracks propagated through the concrete slabs that caused leaking of the salt solution. Concrete specimens were then pulled out before reaching to the standard 50 cycles. Severe surface scaling was also observed in the tested slabs. It should be noted that the ASTM C666 and C672 tests are harsh tests and the results of these two tests may not be a good predictor of freeze-thaw durability of RCC.

Table 17 – Deicing salt scaling test results of cast-in-place RCC

Sample Number	Visual Rating of Scaled Surfaces (ASTM C 672)									
	5 Cycles	10 Cycles	15 Cycles	20 Cycles	25 Cycles	30 Cycles	35 Cycles	40 Cycles	45 Cycles	50 Cycles
RCC-1	4	5	5	*	-	-	-	-	-	-
RCC-2	4	4	4	*	-	-	-	-	-	-
RCC-3	5	5	5	-	-	-	-	-	-	-
RCC-4	4	4	4	-	-	-	-	-	-	-
RCC-5	4	5	5	*	-	-	-	-	-	-

* Sample was pulled from testing after 15 cycles due to panel was leaking all solution

4.6.3 Permeable air voids

Permeable void volume was determined on cast-in-place cylindrical specimens according to ASTM C642. Four 6"×12" specimens were used. Each cylinder was sawed into three equal parts. The top part was tested for surface abrasion resistance and the middle and bottom parts were used for the permeable air void. Specimens were placed at the oven (105 °C) for 48 hours until mass loss was stabilized. This was followed by 4 days of immersion in water before being submerged in boiling water for 5 hours. Table 18 summarizes the results of the permeable void volume tests. The total volume of permeable air voids is almost the same in all eight specimens. For Portland cement concrete pavements, a volume of permeable pores less than or equal to 12% is desirable for long-term durability. The average value of permeable air voids is 10.1% that

is lower than the maximum value, thus indicating a relatively low value of permeable air voids in the tested RCC.

Table 18 – Permeable air voids of cast-in-place RCC

Specimen	Bulk density (lb/ft ³)			Apparent density	Volume of permeable air voids (%)
	Dry	After immersion	After boiling		
R1	148.9	154.2	154.3	163.1	8.70%
R2	147.5	153.7	153.8	164.2	10.20%
R3	147.5	153.1	153.3	162.7	9.40%
R4	149.0	155.3	155.4	166.2	10.30%
R5	147.3	153.6	153.8	164.4	10.40%
R6	146.3	153.0	153.4	165.0	11.30%
R7	146.9	153.3	153.4	164.1	10.50%
R8	147.6	153.5	153.8	163.9	9.90%
Average	147.6	153.7	153.9	164.2	10.10%
C.O.V.	0.61%	0.47%	0.45%	0.66%	7.79%

4.6.4 Surface electrical resistivity

The surface resistivity of four 4”x8” cylinders were measured at 91 days according to AASHTO T95. The results summarized in Table 19 show that the tested RCC has low electrical resistivity. The average surface resistivity was 10.3 kΩ-cm. According to the information provided in Table 5 this value corresponds to relatively high risk of corrosion. It should be noted that the corrosion is not critical in RCC because RCC pavement are usually constructed without reinforcements. However, this test could provide information on permeability, which is important parameter in characterizing durability of concrete.

Table 19 – Surface resistivity of cast-in-place RCC

	Surface resistivity (kΩ-cm)			
	RCC1	RCC1	RCC1	RCC3
Ave	9.9	9.9	9.7	11.9
C.O.V.	7.1%	7.9%	9.7%	5.7%

4.7 Summary of RCC characteristics

The tested RCC showed adequate mechanical properties. Compressive strength of RCC determined on cast-in-place samples or drilled cores were higher than the minimum acceptable values required for pavement construction. Even after 7 days, compressive strength was 3,580 psi, which is higher than the minimum 3,500 psi specified by Missouri Standard Specifications for Highway Construction. Shrinkage measurements up to 300 days show that the tested RCC has lower shrinkage values compared to the shrinkage of typical pavement concrete.

5 Instrumentation of RCC pavement

Long-term in-situ deformation characteristics of the pavement layer were investigated using vibrating wire strain gages to monitor strains in the concrete pavement as well as temperature variations. The gages consist of vibrating, tensioned wires. The strain is calculated by measuring the resonant frequency of the wire (an increase in tension increases the resonant frequency). The instrumentation is used to monitor deformation caused by temperature variations and shrinkage induced deformation in the longitudinal and perpendicular directions in the pavement. All gages and sensors are placed in the pavement during casting and were connected to a data acquisition system.

5.1 Installation of the monitoring system

In total, six vibrating wire gages were embedded in the RCC pavement. These are grouped in 3 x 2 sensors. Each group was mounted to a tower which is configured to hold one sensor at about 1 in. from the bottom of the slab, and one sensor at about 3 in. from the bottom of the slab (Figure 30). Due to the placement method (casting the slab in 2 layers of approximately 4 in.), all the sensors were installed on the first bottom layer of about 4 in. thickness.



Figure 30: Tower with two installed vibrating wire gages Figure 31: Installed DAQ system powered by solar panel

The sensors are connected to a local data acquisition system that can be remotely accessed to retrieve the data. Power to the system is provided by an installed solar panel (Figure 31). The location of installation of the monitoring system can be seen in Figure 32.

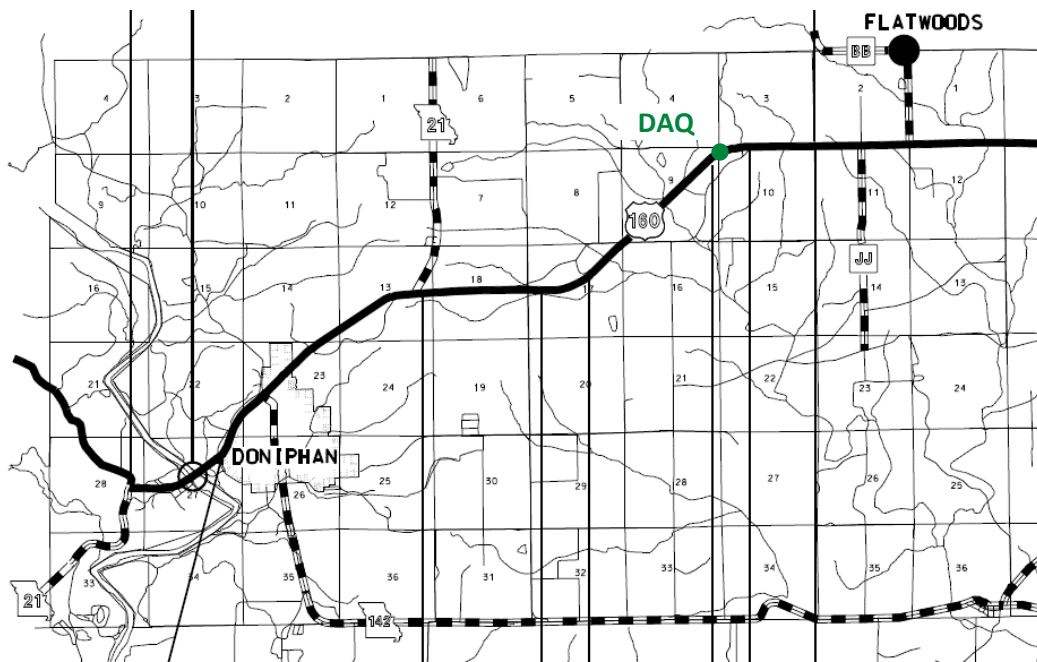


Figure 32: Location of installed monitoring system

The orientation and exact location, along this section of the shoulder, of the different sensor towers is schematically shown in Figure 33. The strains measured by sensor tower A, are strains in the transverse direction (perpendicular to the direction of traffic), while strains measured by towers B and C are parallel to the direction of travel.

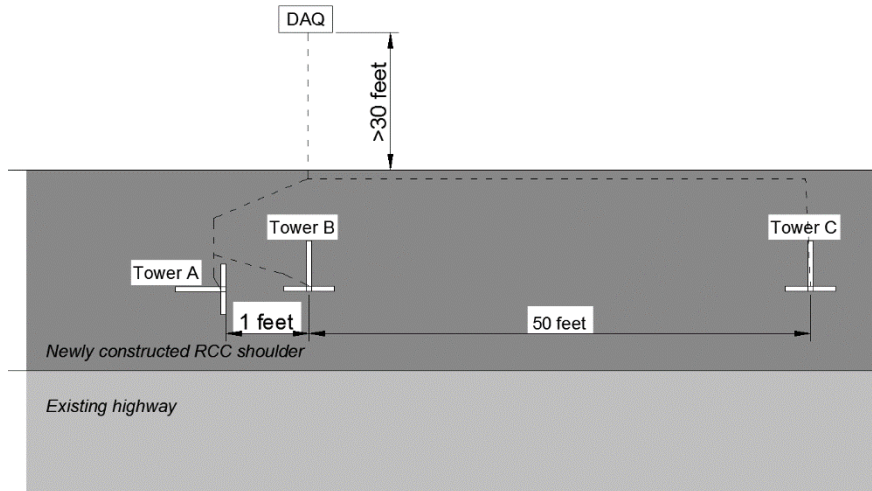


Figure 33: Schematic representation of sensors locations (plan view)

During placement of the concrete, the first pass of the roller compactor were executed without vibration in order to protect the sensors from being damaged. All other passes and the compaction of the second layer were performed with vibration (Figure 34).



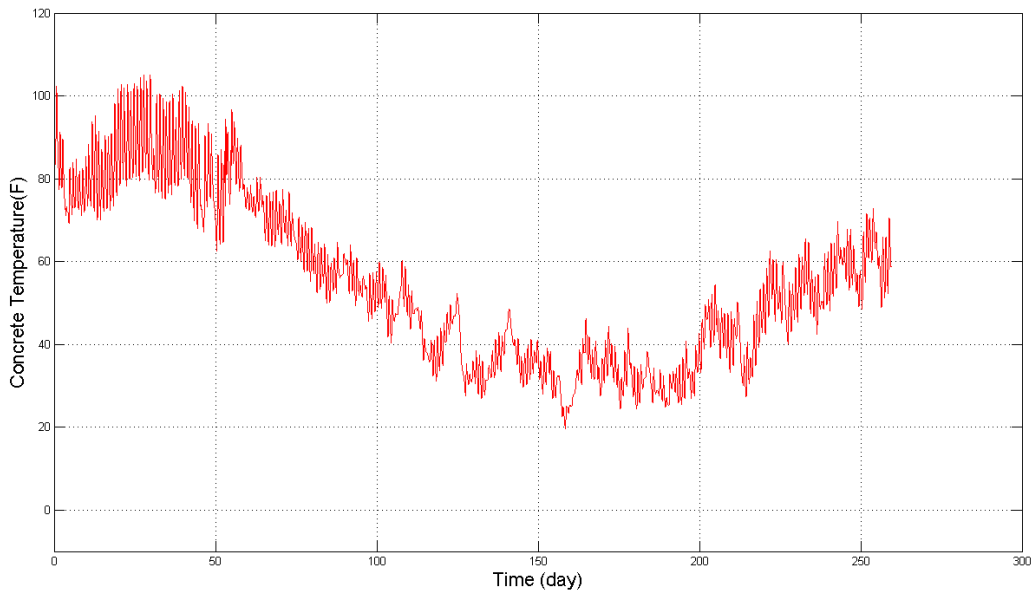
Figure 34: Compaction of RCC above installed sensors

5.2 Long-term deformation monitoring

The installed gages measure total strain of concrete (ϵ) which includes the elastic strain due to applied effective stress (ϵ_e), thermal strain due to the change in temperature (ϵ_t) and the isothermal strain due to creep, shrinkage or other long term deformation of concrete (ϵ_s). To determine the thermal deformation, the temperature of concrete at the point where the strains are measured should be known. The ambient and concrete temperatures at all sensors locations were measured and considered in the analysis. The variations of ambient and concrete temperature are shown in Figure 35.

Temperature of concrete pavement was measured using the six vibrating wire gages. The ambient temperature was recorded at data acquisition system. The temperatures of concrete pavement were almost identical at different locations and different depths.

The ambient temperature varied from 113 °F (45.2 °C) to -3 °F (-19.6 °C), while the temperature of concrete pavement varied from 106 °F (41.4 °C) to 19 °F (-7.2 °C) over the 9 month observation in the period of August 2013 to May 2014. The maximum one-day variation of temperature in the concrete pavement was about 60 °F (15 °C). The maximum one-day variation of ambient temperature in was about 77 °F (25 °C).



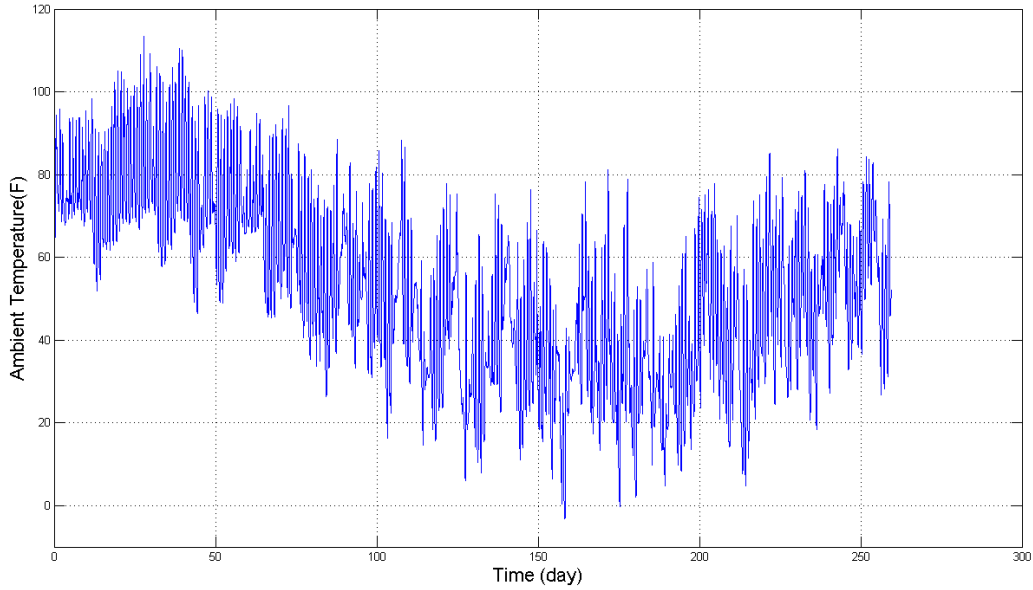


Figure 35- Temperature of concrete pavement (top) and ambient temperature (bottom)

5.2.1 Shrinkage deformation in pavement

The recorded temperature values of concrete pavement were used to calculate thermal strain. Thermal strain was then subtracted from the total strain to capture the net shrinkage strain of the concrete (iso-thermal strain). Shrinkage strain of concrete was obtained from the following equation:

$$\varepsilon_{iso} = \varepsilon + (\alpha - \beta) \times \Delta T \quad (\text{Eq. 6})$$

where α is the coefficient of thermal expansion of gage, β is the coefficient of thermal expansion of the concrete, and ΔT is the change in temperature. ε_{iso} is the iso-thermal strain and ε is the total strain measured by vibrating wire gages. The coefficient of thermal expansion of the wire gage is $11.5 \mu\text{m}/\text{m}/^\circ\text{C}$ as given by the gage manufacturer. The coefficient of thermal expansion of concrete is $9.5 \mu\text{m}/\text{m}/^\circ\text{C}$ as determined in the coefficient of thermal expansion test.

Figure 36 shows the total strain recorded by the gage C-top located at the top of tower-C. This strain is separated into thermal strain and iso-thermal strain by using Eq. 6. The separated iso-thermal strain is also shown in Figure 36. Even though there are still some fluctuations in the separated iso-thermal strain, it is relatively smoother than the measured total strain.

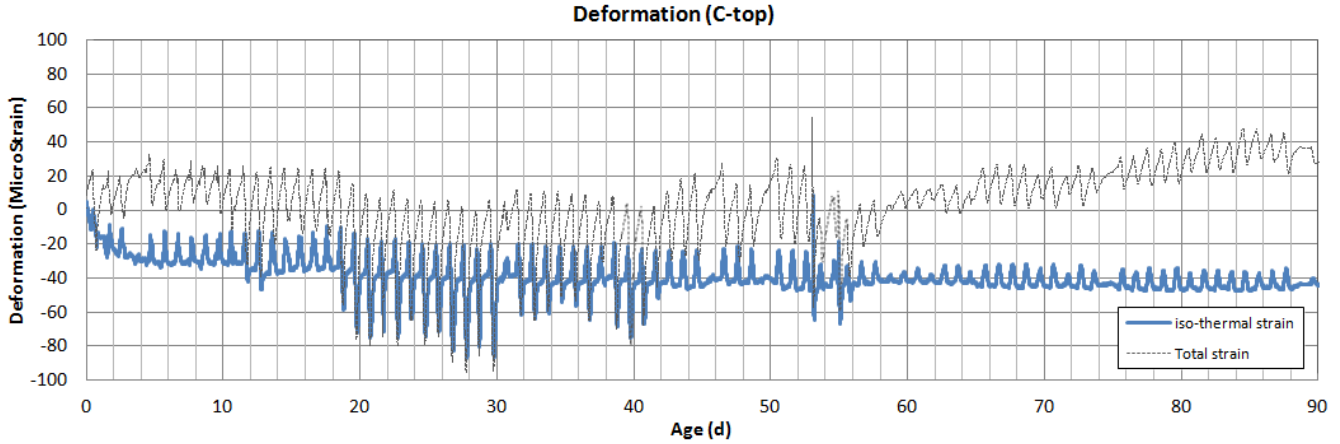


Figure 36- Total strain and iso-thermal strain recorded by the C-top gage

The measured strain is also studied by the Fourier analysis to reveal its major frequency. The Fourier transform of the total strain recorded by the C-top gage are shown in Figure 37. The results indicate that the major frequency of the measured total strain is about $9.2E-6$ Hz (period 1.2 day). In other words, there is a periodical function with the period of about one day, which causes fluctuation in the measured strain. The temperature variation is usually a periodic function with 1-day period (frequency of $11E-6$). The frequency analysis of measured strain confirms that the fluctuations observed in the recorded data are due to the variation of temperature which are repeated periodically every day.

The results of strain measurements presented hereafter, are separated by Eq. 6 to achieve the iso-thermal strains. The results of filtered iso-thermal measurements of all installed gages are given in Figure 38.

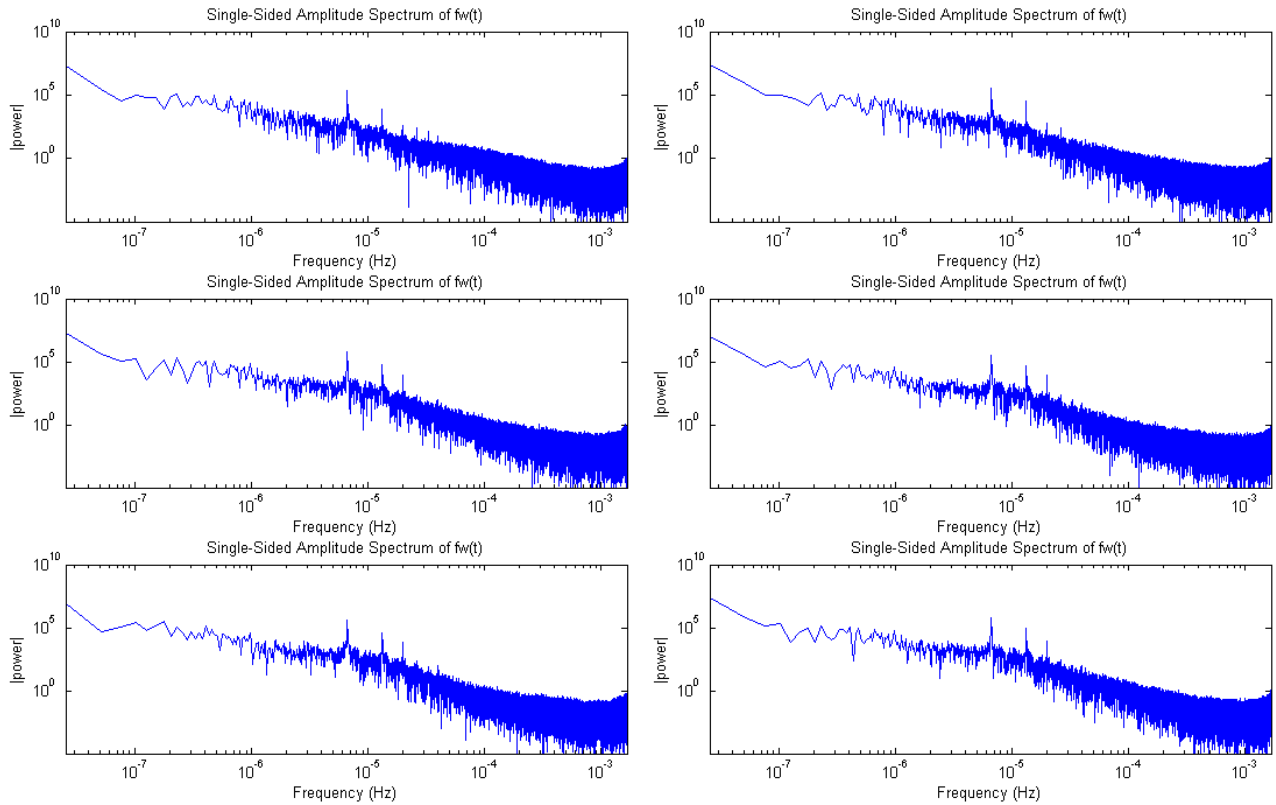


Figure 37- Frequency analysis of the total strain recorded by the C-top gage

The strains measured by the gage located at tower-A are almost constant with respect to time and are lower than those measured at tower-B and tower-C. It is worth to note that the gages in tower-A are perpendicular to axis of road while the gages at tower-B and tower-C are parallel to the axis of road. The maximum strain at the gage A is $-22 \mu\text{m/m}$ and the maximum isothermal strain at gage B and C is $-112 \mu\text{m/m}$ and $-63 \mu\text{m/m}$, respectively. The in-situ shrinkage of concrete pavement is lower than the shrinkage measured in the lab that is about $-400 \mu\text{m/m}$. This could be explained through the fact that the laboratory concrete specimens that were stored in the environmental chamber with a temperature of $70 \pm 3 \text{ }^\circ\text{F}$ and a relative humidity of $50\% \pm 4\%$ are drying constantly in a relatively low humidity environment. In contrast, the concrete in the field pavement is experiencing wetting and drying cycles that prevent it from being dried totally. Also, surface-to-volume ratio of drying shrinkage specimens is higher than that of concrete pavement in the field.

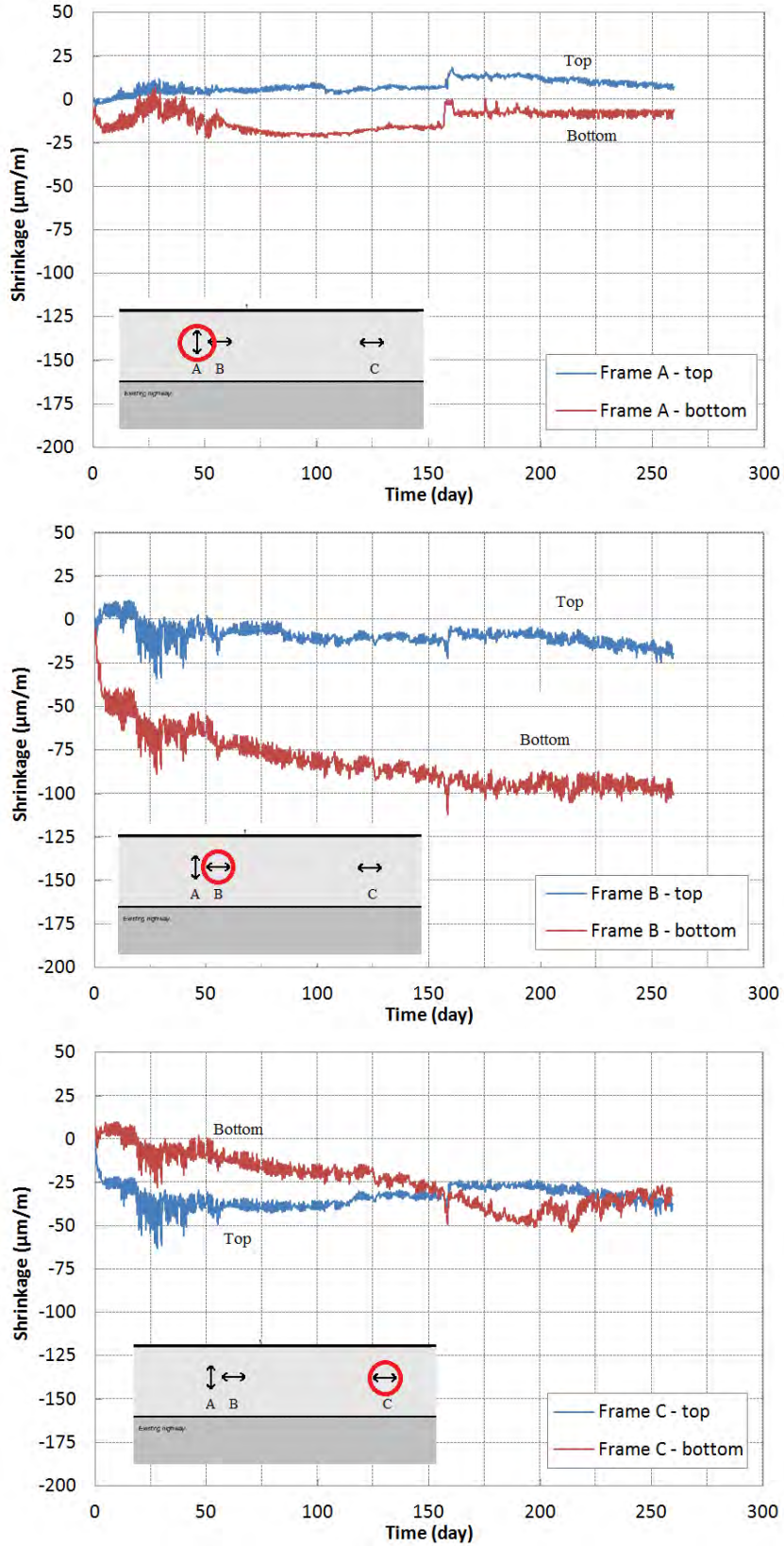


Figure 38- Iso-thermal strains measured by installed gages in the concrete pavement

5.2.2 Total deformation in RCC pavement

The investigated pavement is used as the shoulder and is not under traffic load; therefore, the elastic strain could be negligible. However, the ambient temperature could vary in a large interval; Thus, the thermal strain cannot be ignored in the analysis. Figure 39 shows the mean shrinkage strain (ϵ_s) and total strain of concrete measured by vibrating wire gages in the longitudinal direction. It is clearly visible that the shrinkage strain in the RCC pavement is much lower than the total strain. In other words, contribution of thermal deformation in RCC pavement is much higher than shrinkage deformation in the monitored RCC pavement.

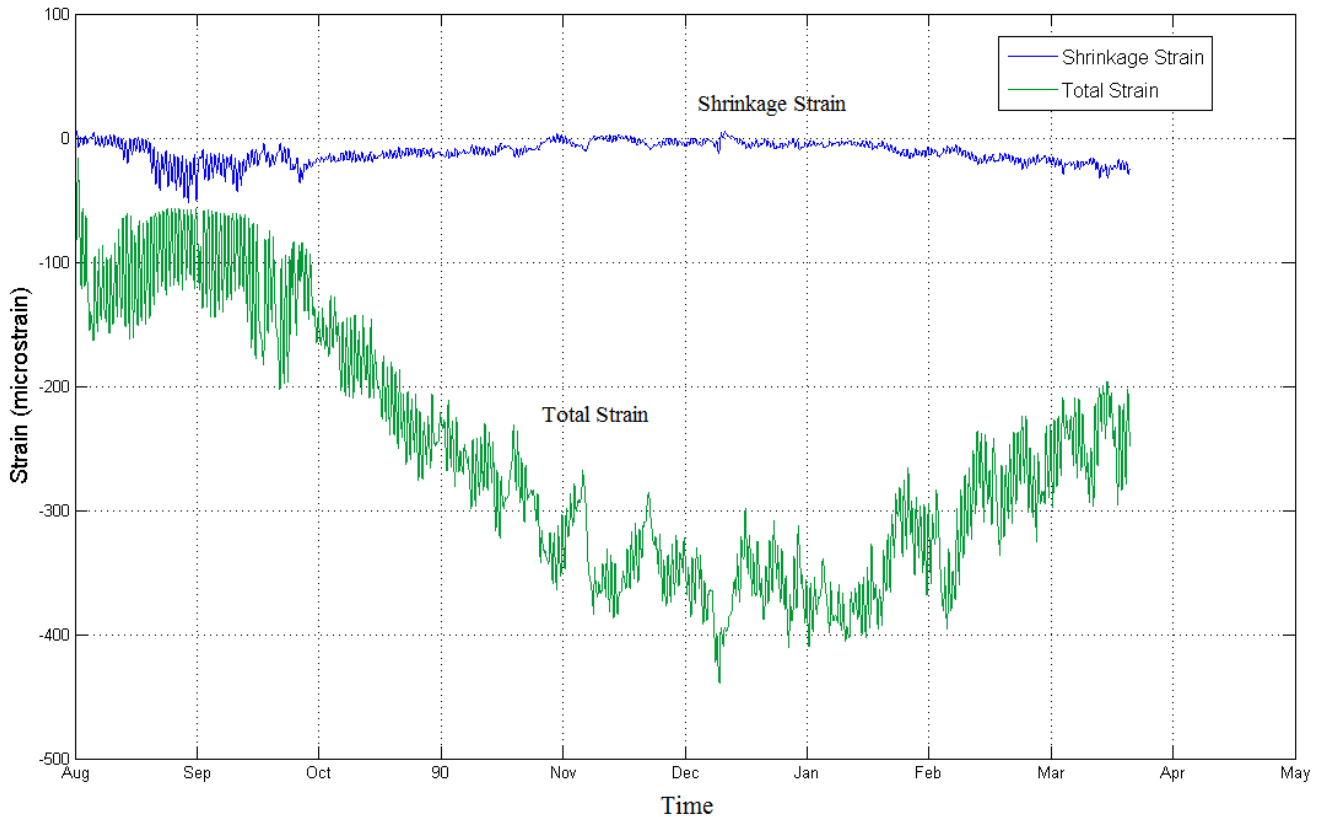


Figure 39- Mean shrinkage strain and total strain in RCC pavement

6 Development of RCC mix design

The aim of this task is to develop an optimized RCC mixture using materials that are locally available in Missouri. The materials selected for this purpose are described in Section 6.1. Section 6.2 discusses the selection of the optimum combination of aggregates as the solid skeleton of RCC materials. Pre-optimization of binder composition and binder volume is discussed in Section 6.3. Final optimized RCC mixture proportions are presented in Section 6.4. Mechanical and durability properties of the optimized concrete is reviewed in Chapter 7. The obtained results are compared with the mechanical and durability properties of reference mixture that typically used in the pavement, as well as the RCC mixtures used for widening Rout 160.

6.1 RCC Materials Selection

6.1.1 Aggregate

Crushed or rounded aggregates or blends of both may be used in RCC mixtures, depending primarily on their availability. The use of crushed aggregate reduces the risk of segregation and increases the quality of the paste-aggregate bond, thereby enhancing the concrete's mechanical properties. On the other hand, RCC made with rounded aggregate yields more workable mixtures and higher packing density.

Both crushed and rounded coarse aggregates were investigated in this research program to evaluate the effect of physical characteristics of aggregates on packing density. Rounded aggregate in the form of 1" coarse gravel and 5/16" intermediate gravel were obtained from the Capital Sand Company in Jefferson City. Crushed aggregate samples were procured from an aggregate production facility (Capital Quarries) near Rolla, MO. Photographs of aggregate Quarries are shown in Figure 40. In all laboratory-made RCC mixtures, the same river sand, with finenesses modules of 2.7, was used. Fine aggregate were also taken from the aggregate production facility at Rolla. Aggregate samples are shown in Figure 41.



Capital Quarries in Jefferson City



Capital Quarries in Rolla

Figure 40- Aggregate quarries



Figure 41- Aggregate samples investigated in the research program

Approval and use of aggregates are based upon the meeting of physical test requirements. The testing protocols that are conducted to check the quality of aggregates are summarized in Table 20. Aggregate properties were characterized to ensure compliance with ASTM C33 as well as MoDOT requirements, as described in Missouri Standard Specifications for Highway Construction, Division 1000.

Table 20- Proposed materials test methods and protocols

Property	Test Method	Test Title/Description
Density, Relative Density, and Absorption	ASTM C127	Standard Test Method for Density, Relative Density (Specific Gravity), and Absorption of Coarse Aggregate.
Gradation	ASTM C136	Standard Test Method for Sieve Analysis of Fine and Coarse Aggregates
Gyratory Compaction	ASTM D6925	Standard Test Method for Preparation and Determination of the Relative Density of Hot Mix Asphalt (HMA) Specimens by Means of the Superpave Gyratory Compactor

The aggregate gradation and the percent retained on each sieve are shown in Figure 42 and Figure 43, respectively. The gradation limits, as given by the Missouri Standard Specifications For Highway Construction, Section 1005 “AGGREGATE FOR CONCRETE” are also indicated in the figures. It should be emphasized that the particle-size distribution of a given aggregate combination may be outside the prescribed limits, but the particle-size distribution of the combined aggregate should be optimized to be within the recommended limits. The combined aggregate gradation will be discussed in detail in Section 6.2. The physical properties of aggregates are given in Table 21.

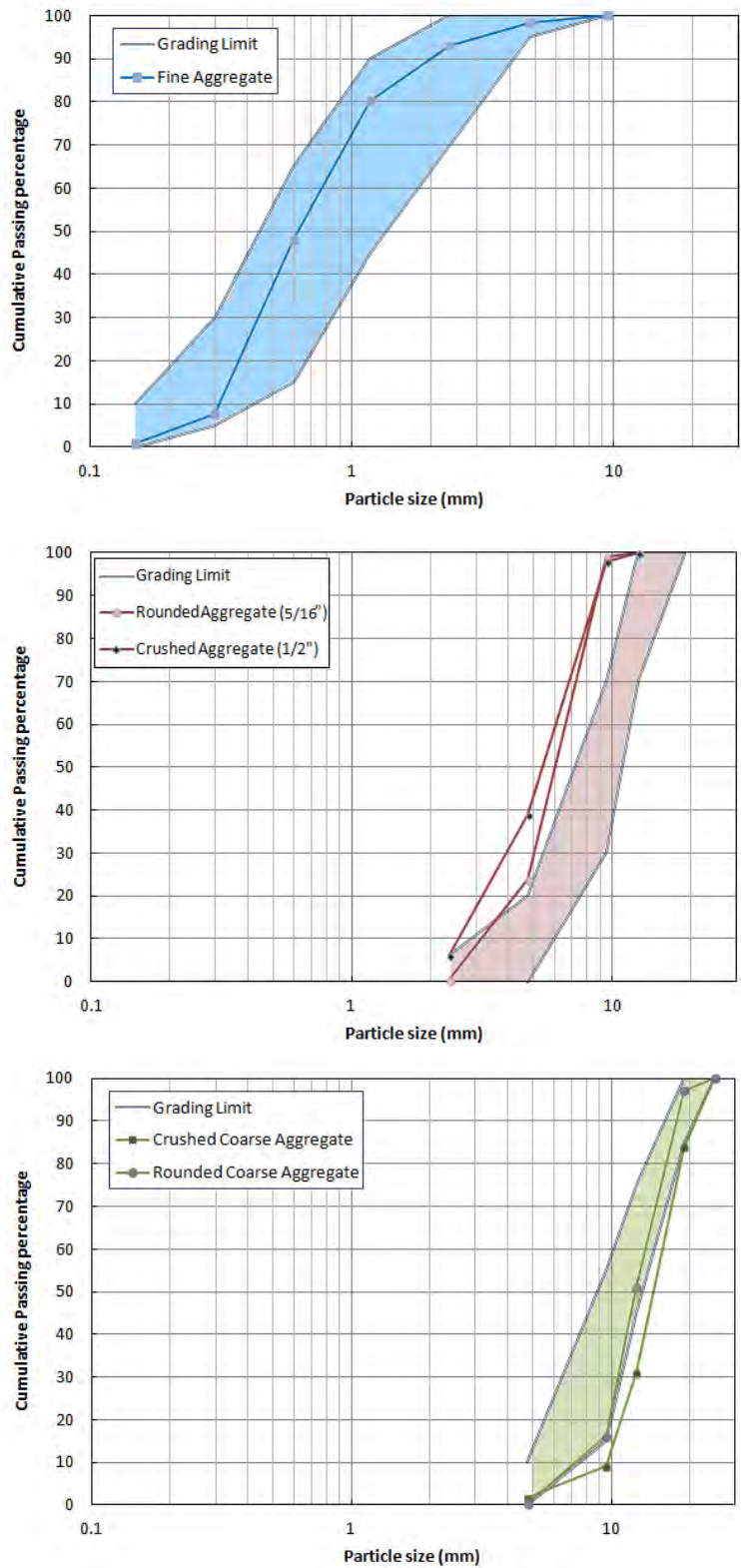


Figure 42- Particle size distribution of sand, intermediate and coarse aggregates, and grading limits given by the Missouri Standard Specifications For Highway Construction

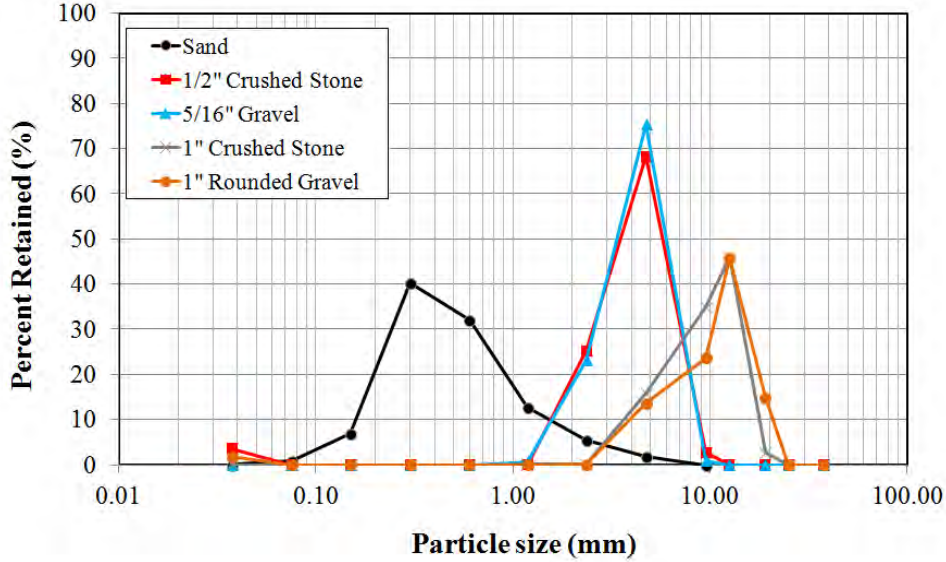


Figure 43- Percent of aggregate retained on each sieve

Table 21- Physical properties of investigated aggregates

Aggregate	Texture	Angularity	Absorption (%)	Specific gravity
Fine aggregate 0-4 mm	Smooth	Rounded	0.62	2.52
Rounded gravel (5/16 ")	Smooth	Rounded	1.13	2.54
Crushed stone (1/2")	Rough	Crushed	3.06	2.46
Rounded coarse gravel (1")	Smooth	Rounded	2.54	2.04
Crushed stone (1")	Rough	Crushed	2.74	2.57

6.1.2 Cementitious materials

Type I Portland cement, supplied by Holcim Inc., was used in all RCC mixtures. A Class C fly ash (FA) was also used in the binary system to develop different binder compositions in selected mixtures. Figure 44 shows the particle-size distribution of all cementitious materials used in the current study. The physical and chemical characteristics of the cementitious materials are given in Table 22.

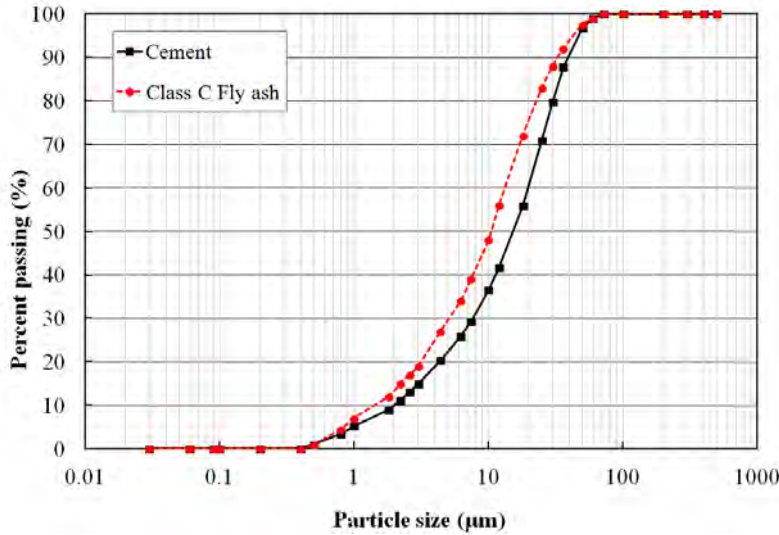


Figure 44- Particle size distribution of cementitious materials

Table 22- Physical and chemical characteristics of cementitious materials

Chemical Composition	Cement (Type I)	Fly Ash (Class C)
SiO ₂ , %	19.8	36.5
Al ₂ O ₃ , %	4.5	24.8
Fe ₂ O ₃ , %	3.2	5.2
CaO, %	64.2	28.1
MgO, %	2.7	5
SO ₃	3.4	2.5
Blaine surface area, m ² /kg	383	465
Specific gravity	3.1	2.71
LOI, %	1.5	0.5

6.1.3 Chemical admixtures

Chemical admixtures are rarely used in RCC. A commercially available air-entraining agent (AEA) was used in selected mixtures to entrain air in RCC. The AEA used in this study was supplied from Sika. The AEA is in a liquid solution with specific gravity of 1.05 and solid content 12%.

6.2 Optimization of particles size distribution

A mix design method that utilizes the optimum packing densities (and minimal binder content) was used. This method is used to determine the proportions of each of the dry solid ingredients (cement, fly ash, sand, and coarse aggregate) that can be used to optimize the dry packing density of a given RCC mixture. Using this optimized dry packing density, the amount of paste necessary to entirely fill the void spaces between the dry aggregates can be minimized. The optimized PSD is finally compared with the proposed limits for aggregate gradation given in various guidelines and specifications.

Two types of aggregates, including crushed stone aggregate and rounded aggregate are included in theoretical and experimental studies.

6.2.1 Empirical PSD optimization

The effect of aggregate characteristics on packing density was empirically evaluated to determine the optimum PSD of various blends of aggregates. Packing density of aggregate combinations was measured using the gyratory intensive compaction tester (ICT) that is shown in Figure 45. In general, the ICT is employed for the determination of compaction of granular materials, such as soil and concrete. The ICT compacts the sample with a shear-compaction principle. Shear movement under vertical pressure allows particles to get closer to each other, thus leading to achieve a higher packing density. The packing density of the tested mixture (ϕ) is calculated as follows:

$$\phi = \frac{\rho_d}{\rho_{d\max}}$$
$$\rho_{d\max} = \frac{1}{\frac{P_1}{\rho_1} + \frac{P_2}{\rho_2} + \frac{P_3}{\rho_3} + \dots}$$

where P_1 , P_2 , and P_3 are weight percentages of the ingredients used in the mixtures and ρ_1 , ρ_2 , and ρ_3 refer to specific gravities of these mixture ingredients. The specific gravities are determined for oven dried aggregates. Therefore, prior to ICT-testing, all aggregates were dried in oven to make sure that the packing density is accurately measured. The value of ρ_d is the measured density of the mixture as determined from the ICT. The ICT parameters selected in this examination, shown in Table 24, were kept constant in all testing. The number of cycles was selected due to the fact that the change in packing density was not significant after 256 cycles. The vertical pressure was adjusted to 2 bar (29 psi) to avoid aggregate crushing during the IC-testing.

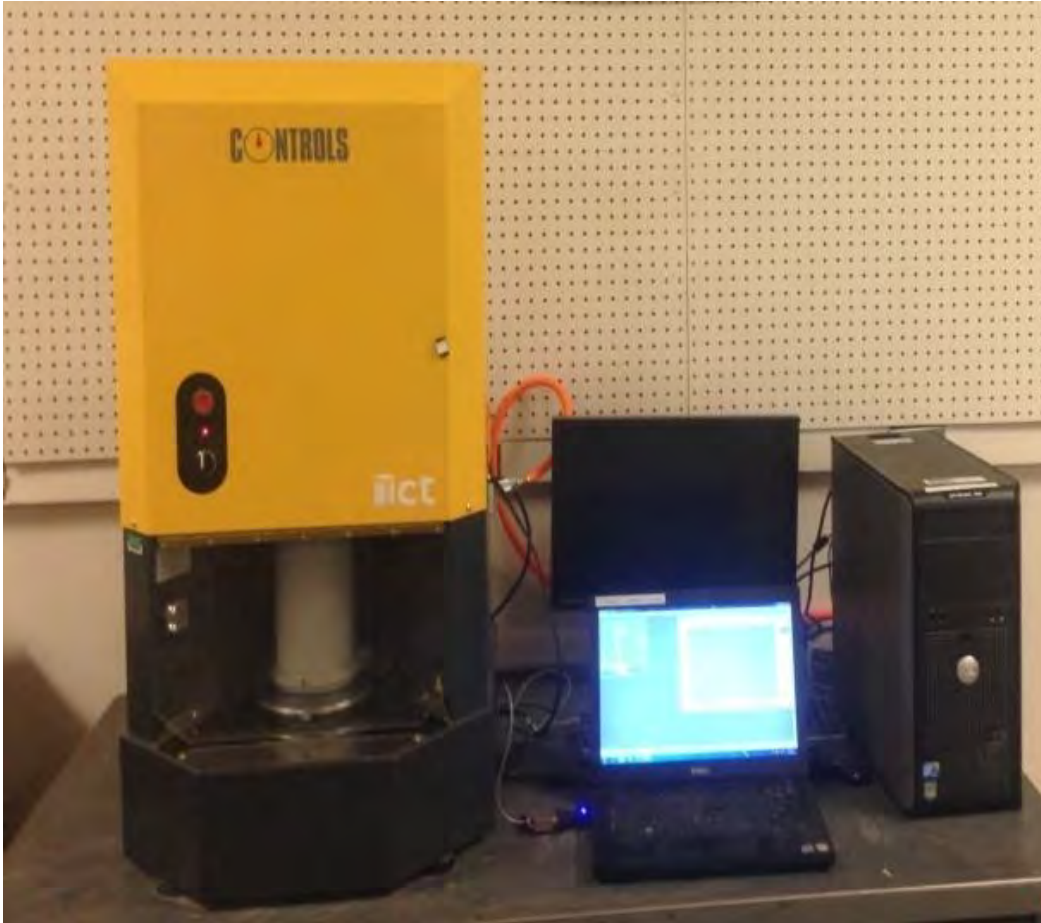


Figure 45- Gyratory intensive compaction tester (ICT)

Both crushed and rounded aggregates with various combinations of coarse/intermediate/fine aggregate ratio were investigated. In total, 26 different combined aggregates were selected to cover a wide range of ternary mixtures. The properties of aggregate used in this study are given in Section 6.1.1. Selected aggregate combinations are shown in Table 24. The packing densities of the various combination of aggregate varied from 0.713 to 0.815.

Table 23- IC-testing parameters

Parameter	Unit	Available range	Selected
Vertical pressure	bar	0.5-10	2
Number of cycles	Number	2-512	256
velocity	rpm	0-60	60
Gyratory angle	Micro-rad	0-50	40

Table 24- Aggregate combinations investigated in empirical PSD optimization

Type	Mix #	Sand (Sieve #4)	Rounded gravel (5/16 ")	Crushed Stone (1/2 ")	Rounded gravel (1 ")	Crushed Stone (1 ")	Packing density (ICT measurement)
Combination of crushed aggregates	C1	20%	0%	30%	0%	50%	0.713
	C2	30%	0%	20%	0%	50%	0.784
	C3	30%	0%	30%	0%	40%	0.756
	C4	30%	0%	10%	0%	60%	0.739
	C5	40%	0%	30%	0%	30%	0.796
	C6	40%	0%	20%	0%	40%	0.795
	C7	45%	0%	15%	0%	40%	0.794
	C8	48%	0%	32%	0%	20%	0.784
	C9	48%	0%	12%	0%	40%	0.801
	C10	50%	0%	33%	0%	17%	0.787
	C11	55%	0%	15%	0%	30%	0.797
	C12	55%	0%	5%	0%	40%	0.804
	C13	60%	0%	20%	0%	20%	0.786
	C14	60%	0%	10%	0%	30%	0.794
	C15	60%	0%	0%	0%	40%	0.793
Combination of Rounded aggregates	R1	30%	40%	0%	30%	0%	0.778
	R2	40%	30%	0%	30%	0%	0.785
	R3	50%	20%	0%	30%	0%	0.794
	R4	60%	10%	0%	30%	0%	0.791
	R5	30%	30%	0%	40%	0%	0.789
	R6	40%	20%	0%	40%	0%	0.815
	R7	50%	10%	0%	40%	0%	0.809
	R8	60%	0%	0%	40%	0%	0.794
	R9	30%	20%	0%	50%	0%	0.786
	R10	40%	10%	0%	50%	0%	0.81
	R11	50%	0%	0%	50%	0%	0.789

The measured packing densities of various combinations are shown in ternary packing diagrams (TPD) created by the PSD optimization software (see Figure 46). The variation of packing density is also plotted in 3D diagram in Figure 47. As shown in Figure 46, the measured packing density of blended aggregates can vary from the 0.71 in the poorly graded mixtures up to more than 0.80 for the mixtures with well graded aggregates. The difference between the packing densities of these two mixtures is 0.09 that needs to be filled with the cement paste in the concrete mixtures. Given the fact that the total paste volume of a RCC is about 0.15 to 0.25 of total volume of the concrete, the optimized PSD will greatly reduce the required paste volume and will result in a more economical mixture. This clearly shows the importance of PSD optimization in the design of RCC mixtures.

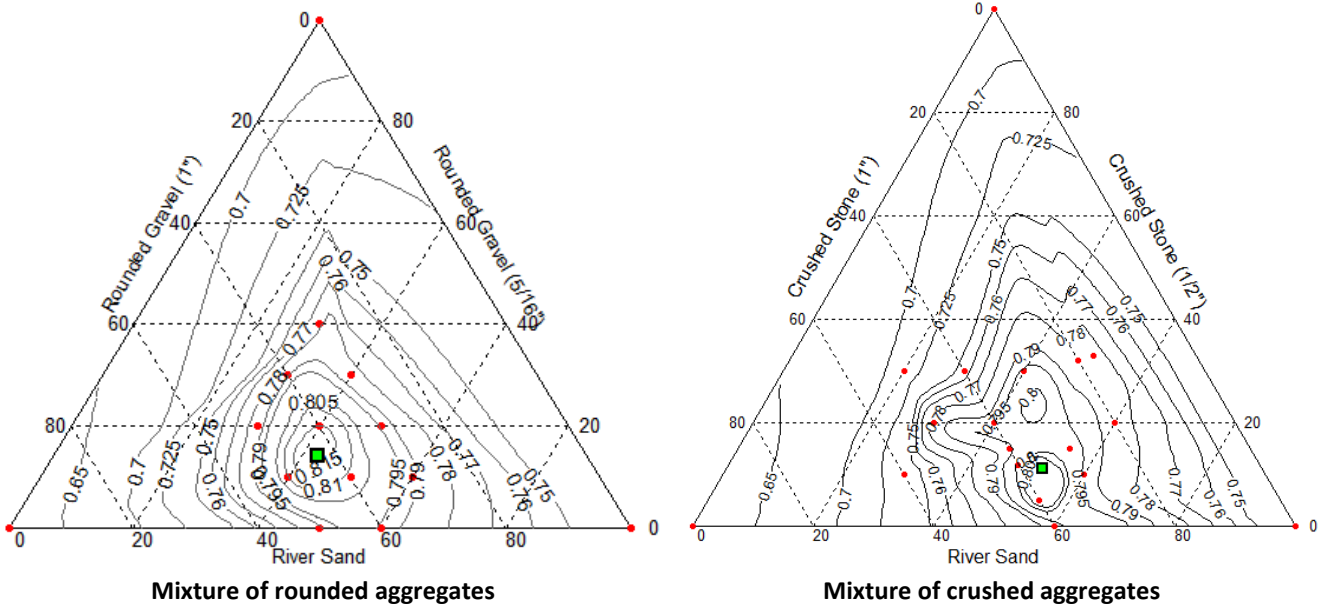


Figure 46- Ternary Packing Diagram (TPD) of blended aggregates (red points show the packing density measurements)

The maximum packing density (ϕ) in the blend of rounded aggregate is 0.815, which is slightly higher than the packing density of the mixture of crushed stone, $\phi=0.804$. For a given coarse to fine ratio, using smooth and rounded gravel resulted in a higher packing density compared to blended aggregates proportioned with crushed aggregates. However, the difference is not significant, and both crushed and rounded aggregates examined in this program could be used to produce a dense and well-packed solid structure. Mixture made with rough and angular aggregates needs more volume of sand to reach similar packing density compared to the mixtures proportioned with smooth and rounded aggregates. This can be attributed to the higher internal friction between crushed aggregates, which requires more fines to reduce the inter-particle friction and achieve maximum packing density.

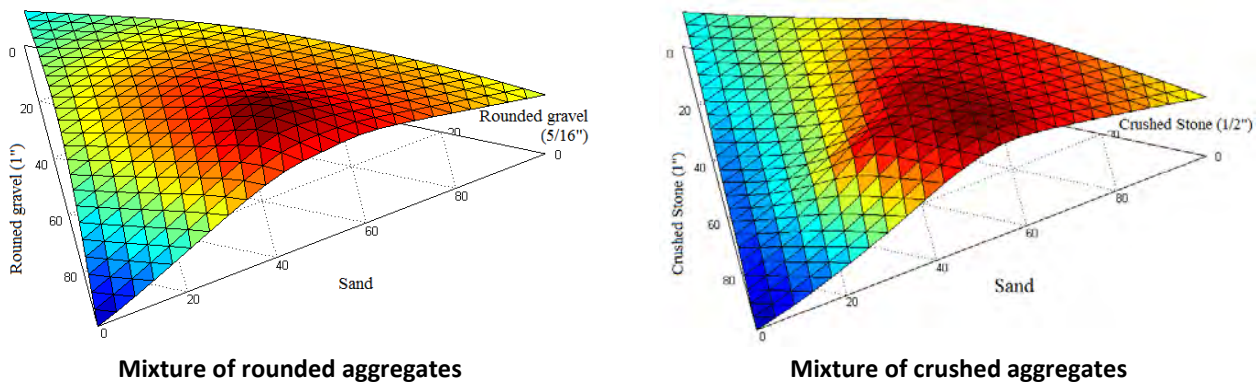


Figure 47- 3D representation of measured packing density in aggregate blends

6.2.2 Theoretical models for PSD optimization

Various packing models have been developed so far to find the optimum PSD of solid particles in concrete. The first studies on packing carried out to improve concrete mix design dates back to work of Fuller and Thompson in 1907. They proposed the following relation for the optimum particle size distribution:

$$P(d) = \left(\frac{d}{d_{max}} \right)^{1/2}$$

where $P(d)$ is a fraction of the total solids being smaller than size d , and d_{max} is the maximum particle size of the total grading. Another theoretical approach for the formulation of ideal grading is presented by Andreasen [Andreasen and Andersen, 1930] in which the optimum PSD is determined from the following equation:

$$P(d) = \left(\frac{d}{d_{max}} \right)^q$$

where q is the distribution modulus that controls the fineness of the grading. Andreasen and Andersen concluded from numerous experiments that the distribution modulus q should be between $1/3$ and $1/2$ for densest packing. In many publications afterwards, a distribution modulus of $1/2$ is referred to as 'Fuller curve' or 'Fuller parabola', based on the work of Fuller and Thomsen, and recommended by most design codes for conventionally vibrated concrete. The Andreasen packing model considers only a maximum particle size d_{max} in the system. This will not be the case under practical conditions as there will be always a minimum particle size depending on the ingredients used. Accordingly, a modified version of Andreasen packing model was introduced [Funk and Dinger, 1994] that prescribes the grading for continuously graded aggregates considering a minimum and maximum particle size in the mixture. This modified equation for the PSD (cumulative volume fraction) reads:

$$P(d) = \frac{d^q - d_{min}^q}{d_{max}^q - d_{min}^q}$$

where d_{max} and d_{min} are the maximum and minimum size of particles in the grading, respectively. These models usually assume dry packing of spherical particles. The contention of

the method is that the mechanical characteristic of the concrete at a fixed cement content, and w/c is mainly a function of the packing of the solid particles. The optimal mechanical characteristic was found to be when the combined aggregate proportions result in higher packing density.

6.2.3 PSD optimization software

PSD optimization software was developed to study the PSD of various blends of aggregates. The software provides an easy to use tool for optimizing the PSD of solid particles. Even though this software is primarily developed for RCC mixtures, it can be used for determining the optimum PSD of other types of concrete. This software enables the determination of the optimum coarse/fine aggregate in binary aggregates or coarse/intermediate/fine aggregate combination in ternary mixture for use in proportioning RCC, based on packing models. A screen shot of the software is shown in Figure 48. By knowing certain materials characteristics (such as gradation and specific gravity) for each of the dry solid ingredients, a fast verification can be run using various packing models. The main advantage of the developed software is that it can be used to quickly recalculate the optimum proportions of an RCC mixture without having to prepare a large number of laboratory trial batches.

Various packing models including the Fuller-Thompson model, the Andreasen and Andersen model, the 0.45 power chart, and the modified Andreasen and Andersen model can be selected for the optimization purpose. In this investigation, the modified Andreasen and Andersen model was selected since it considers both the maximum and minimum size of particles and gives higher flexibility in adjusting fineness of the combined aggregates.

The selection of distribution modulus (q) is important for the Andreasen packing model. Using a lower value of q results in a mixture with higher content of fine materials that can improve the packing density by reducing the inter-particle friction and reduces the risk of segregation. On the other hand, the particles size distribution of the combined aggregates can influence the mean particle size and specific surface area of the aggregate. For a given paste content, the increase in specific surface area will result in a smaller paste film thickness around the aggregates, thus leading to a lower workability. Investigations on highly flowable mixtures

showed that the Andreasen model with $0.22 < q < 0.30$ provides appropriate PSD for self-consolidating concrete. Limited reports, however, are available for selection of appropriate value of distribution modulus (q) in RCC mixtures. Hüsken and Brouwers [Hüsken and Brouwers, 2008] investigated zero-slump concrete and suggested that the appropriate values for q are in the range between 0.35 to 0.40.

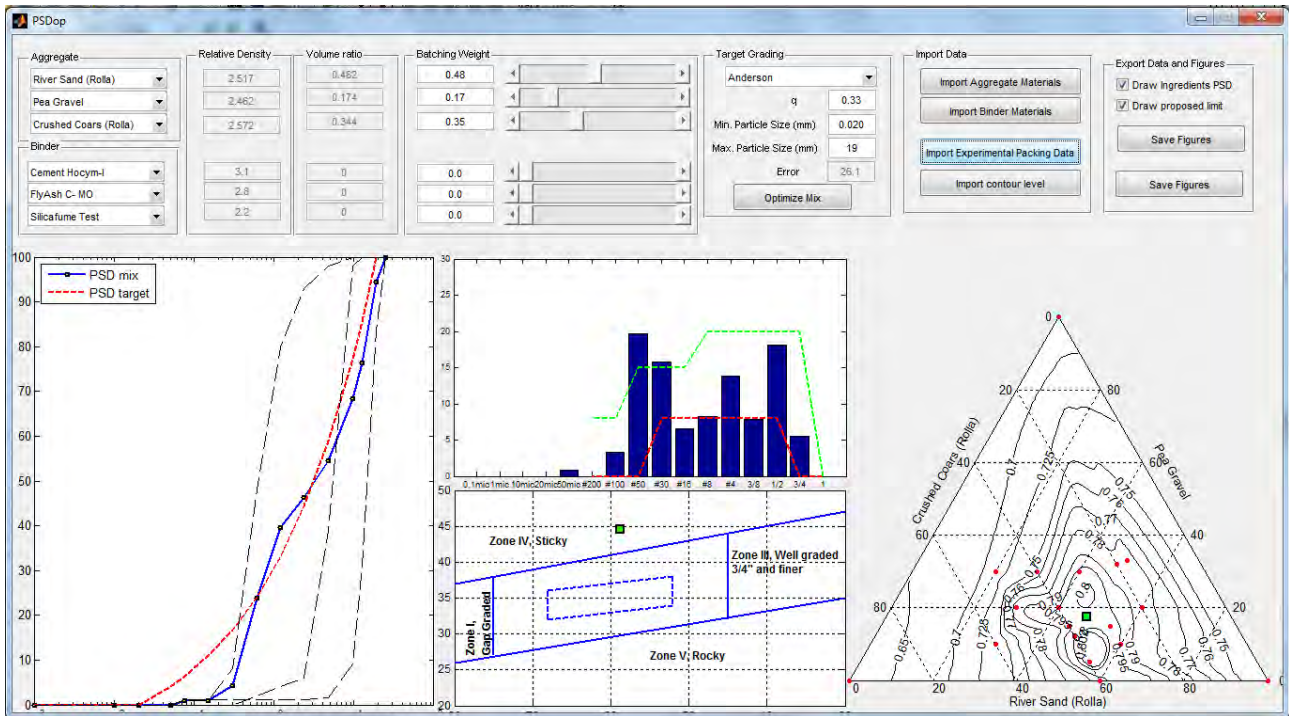


Figure 48- Screen shot of PSD optimization software

Numerical study using the PSD optimization software is performed to evaluate appropriate value of the distribution modulus (q) for RCC mixtures. Aggregate properties including gradation, specific gravity, and experimental packing data are the input of software. The results show that the q values of 0.17 and 0.42 are close to the upper and lower the boundary limits, respectively of aggregates proposed by ACI 325 for RCC mixtures for pavement. The ACI 325 aggregate gradation limits as well as the corresponding Andreasen models with q values of 0.17 and 0.42 are shown in Figure 49.

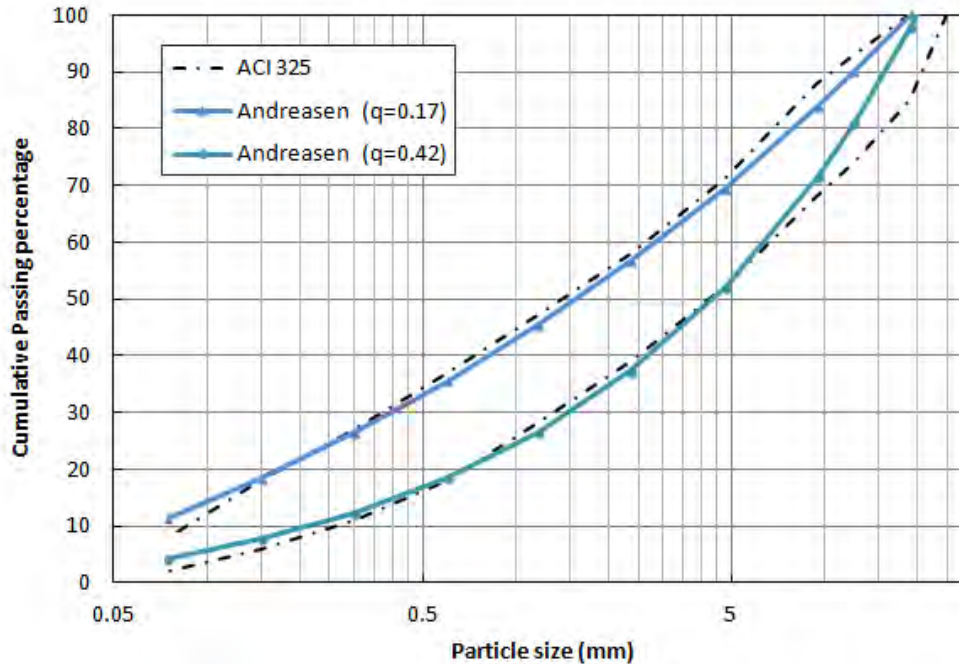


Figure 49- ACI 325 aggregate gradation limits for RCC and the corresponding Andreasen packing models

6.2.4 Selection of optimum aggregate type and proportions

In addition to maximum packing density criteria, there are some other factors that affect the selection of aggregate type and its optimum proportions. Given lower paste volume, segregation resistance is an important factor in the design of RCC mixtures. Crushed aggregates are preferred in this case since the interlocking friction between the particles reduces the risk of aggregate separation. Another factor that is important in segregation resistance of a blend of aggregate is the percentage retained on the each sieve. The general rule is that the amount of retained aggregate on each sieve should not differ significantly from the next sieve. This ensures that all size of aggregates are available in the mixture that reduces the risk of segregation. Therefore, all these factors should be considered to determine the optimum blend of certain aggregates.

Based on the obtained results from various aggregate proportions and types investigated in the current study, the combination of river sand, crushed stone 1/2", and crushed stone 1" with the proportions of 48%, 17%, and 35%, respectively, was selected as the optimum combination. The particle size distribution of the combined aggregate, depicted in Figure 50, show that the combined PSD is close to the optimum particle size distribution of Andreasen model with

distribution modulus of 0.35. In addition, the sieve analysis of combined aggregate, shown in Figure 51, show that the percentage retained on each sieve is well distributed and there is no gap in the aggregate gradation. The packing density of the selected mixture is 0.801 that is close to the highest packing measured in various blends of crushed aggregates ($\phi=0.804$).

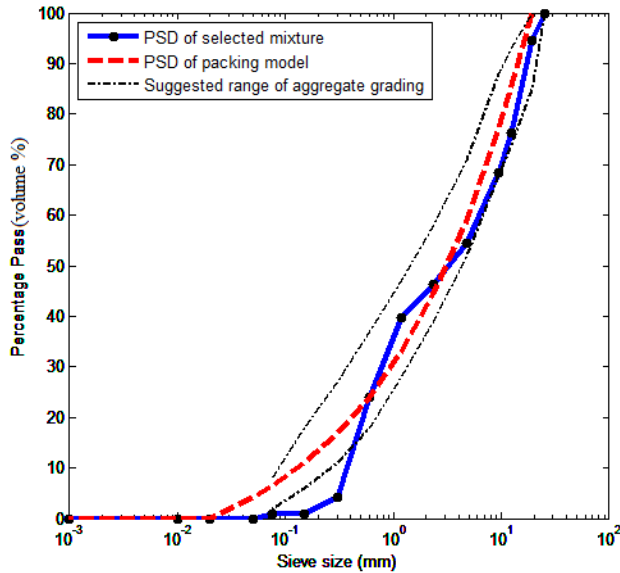


Figure 50- PSD of selected aggregate combination vs. PSD of Andreasen model with $q=0.35$

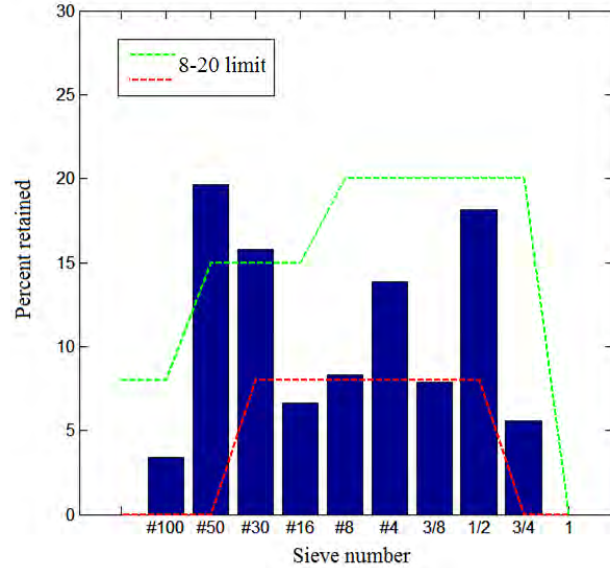


Figure 51- Percent retained on each sieve in selected aggregate combination

6.3 Optimization of paste volume and composition

The next step after determining the skeleton of aggregate, which was described in Section 6.2, is optimizing the volume and composition of the paste that should fill the voids between the aggregates. The mixture parameters that investigated in this step include the volume and composition of the cementitious materials and the water content. These mixture parameters are again determined following the concept of maximizing the packing density of the mixture. In addition to packing density, workability of fresh mixture, as well as the compressive strength of RCC is also considered in the selection of the binder composition.

Three steps are taken to find the optimum PSD. In the first step, the water-to-solid ratio is optimized through maximizing of the packing density of RCC. Various binder compositions and binder volumes are investigated in this stage. In the second step, the compressive strength is

evaluated to verify its compliance with the design requirements. Finally, the workability properties of fresh RCC are examined to determine the minimum water content needed for placing concrete in the pavement.

6.3.1 Experimental matrix

In total, 30 RCC mixtures were examined to determine the optimum binder composition for the RCC. Three different volumes of cementitious materials are considered. Regarding the minimum cement content allowed for RCC pavement by Missouri Standard Specifications for Highway Construction (400 lb/yd³), the lowest cementitious materials was selected as 420 lb/yd³ (250 kg/m³). The high and medium cementitious materials contents selected in this experiment were 495 lb/yd³ (295 kg/m³) and 590 lb/yd³ (350 kg/m³), respectively. Two binder compositions were investigated. The first binder was Type I cement, while the second binder contained 20% of class C fly ash replacement. The water-to-solid ratio (w/s) varied from 4% to 7%. Solid ingredients include aggregate and cementitious materials. Packing density, compressive strength, and Vebe time of all trial mixtures were evaluated according to the standard procedure previously described in Chapter 4. Details of experimental program are given in Table 25. A legend to the codes used for the trials mixtures are given in Figure 52.

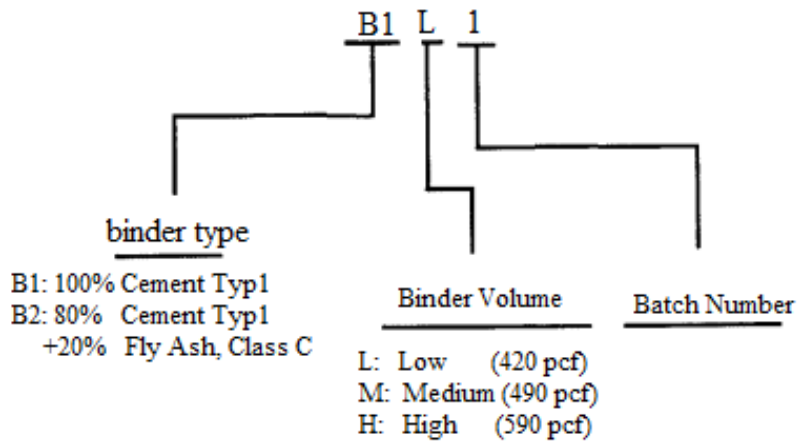


Figure 52- Identification code or RCC trial mixtures

Table 25- Details of experimental program used to optimize the binder content and composition

Mixture	Water-to-solid ratio					Binder composition		Binder content			Aggregate combination as optimized in Section 6-2	tests		
	4.5%	5.0%	5.5%	6.0%	6.5%	Type I Cement	80% Type I Cement + 20% FA class C	Low (420 lb/yd ³)	Medium (495 lb/yd ³)	High (590 lb/yd ³)		Unit weight	compressive strength	Vebe time
Binder Type I														
B1-M-1	x					x			x		x	x	x	x
B1-M-2		x				x			x		x	x	x	x
B1-M-3			x			x			x		x	x	x	x
B1-M-4				x		x			x		x	x	x	x
B1-M-5					x	x			x		x	x	x	x
B1-L-1	x					x		x			x	x	x	x
B1-L-2		x				x		x			x	x	x	x
B1-L-3			x			x		x			x	x	x	x
B1-L-4				x		x		x			x	x	x	x
B1-L-5					x	x		x			x	x	x	x
B1-H-1	x					x				x	x	x	x	x
B1-H-2		x				x				x	x	x	x	x
B1-H-3			x			x				x	x	x	x	x
B1-H-4				x		x				x	x	x	x	x
B1-H-5					x	X				x	x	x	x	x
Binder Type II														
B2-M-1	x						x		x		x	x	x	x
B2-M-2		x					x		x		x	x	x	x
B2-M-3			x				x		x		x	x	x	x
B2-M-4				x			x		x		x	x	x	x
B2-M-5					x		x		x		x	x	x	x
B2-L-1	x						x	x			x	x	x	x
B2-L-2		x					x	x			x	x	x	x
B2-L-3			x				x	x			x	x	x	x
B2-L-4				x			x	x			x	x	x	x
B2-L-5					x		x	x			x	x	x	x
B2-H-1	x						x			x	x	x	x	x
B2-H-2		x					x			x	x	x	x	x
B2-H-3			x				x			x	x	x	x	x
B2-H-4				x			x			x	x	x	x	x
B2-H-5					x		x			x	x	x	x	x

6.3.2 Optimum water-to-solid ratio

Adjusting the water-to-solid ratio to achieve a mixture with nearly optimum moisture content ensures optimum compaction and maximum density in the RCC. For a fixed cementitious materials volume, different water-to-solid ratios are examined to establish a moisture-density relation. For most of tested aggregates, the optimum moisture content is found to be within the range of 4% to 8%. The moisture content were varied from 4% to 7% in the trial mixes to determine the optimum water-to-solid ratio in all binders. The w/s is computed using the following formula:

$$W/S (\%) = \frac{\text{Weight of water}}{\text{Weight of cementitious materials} + \text{Oven dried aggregate}} \quad (\text{Eq. 7})$$

For each cementitious content and composition described in Table 25, the ICT was used to determine the maximum measured density of the RCC mixture in the wet state (γ_w). The dry density of RCC mixture (γ_d) is then calculated using the following formula:

$$d = \frac{w}{1+w/s} \quad (\text{Eq. 8})$$

where w/s is the water to solid ratio and γ_w is the wet density measured by the ICT. The relationship between the w/s and the dry density of RCC mixtures for various binder compositions is plotted in Figure 53. The ICT packing density might be over-estimated in the wet mixture. The paste leaking from the wet mixtures when the materials are being compacted in the cylinders may cause some errors in the density measurements. To overcome this issue, all packing measurements were stopped after leakage of paste was observed in the ICT. In addition, the measured dry density is limited to the theoretical maximum dry density ($\gamma_{d,max}$), which is the density of the mixture with zero-air content. The theoretical maximum dry density ($\gamma_{d,max}$) is also plotted in Figure 53. The maximum theoretical dry density ($\gamma_{d,max}$) could be obtained from the following equation:

$$d_{,max} = \frac{G_s}{1+w/s \times G_s} \quad (\text{Eq. 9})$$

where G_s is the average apparent density of solid ingredients of concrete. The average apparent density is obtained from the following equation:

$$G_s = \sum V_i \gamma_i \quad (\text{Eq. 10})$$

where V_i is the volume percentage of ingredients in the mixture proportions and γ_i is the apparent dry density of solid part of concrete ingredients (e.g. aggregates, cementitious materials).

The density-w/s curves, depicted in Figure 53, show that the maximum dry density in all binder types was obtained in the mixtures with w/s values of 5.5% to 6%. RCC mixtures made with Binder Type II in which part of cement was replaced with fly ash required a lower w/s to achieve the maximum density. However, the difference between the optimum w/s in two investigated binders was not significant.

6.3.3 Strength properties

Two 4"x8" concrete cylinders were cast from each mixture proportions. The ICT gyratory compactor was used for casting the specimens which provides high degree of compaction of the RCC material. The specimens were cured in water before being tested for compressive strength at 7 days. The compressive strength is plotted in Figure 54 versus the w/s for all binder types.

The maximum compressive strength varied from 5,000 MPa in the case of Mix B1-L mixture (Binder type I, Low volume) to 8,400 MPa for the Mix B1-H (Binder type I, high volume). All compressive strength results, even those measured for the RCC mixtures made with 420 lb/yd³ of cementitious materials are higher than the minimum target value of 3,500 psi needed for concrete pavements according to Missouri Standard Specifications for Highway Construction.

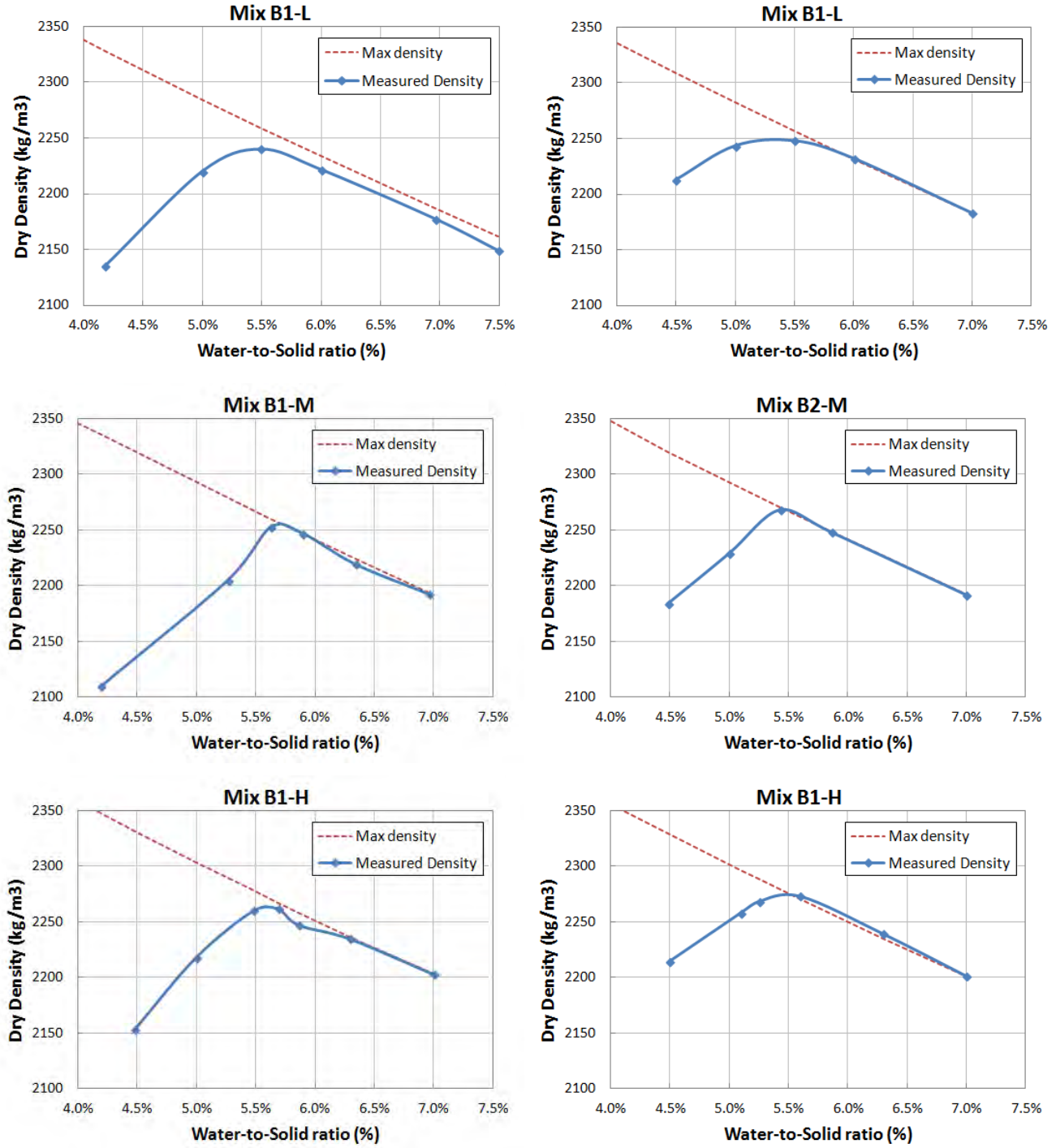


Figure 53- Dry density vs. w/s of RCC mixtures

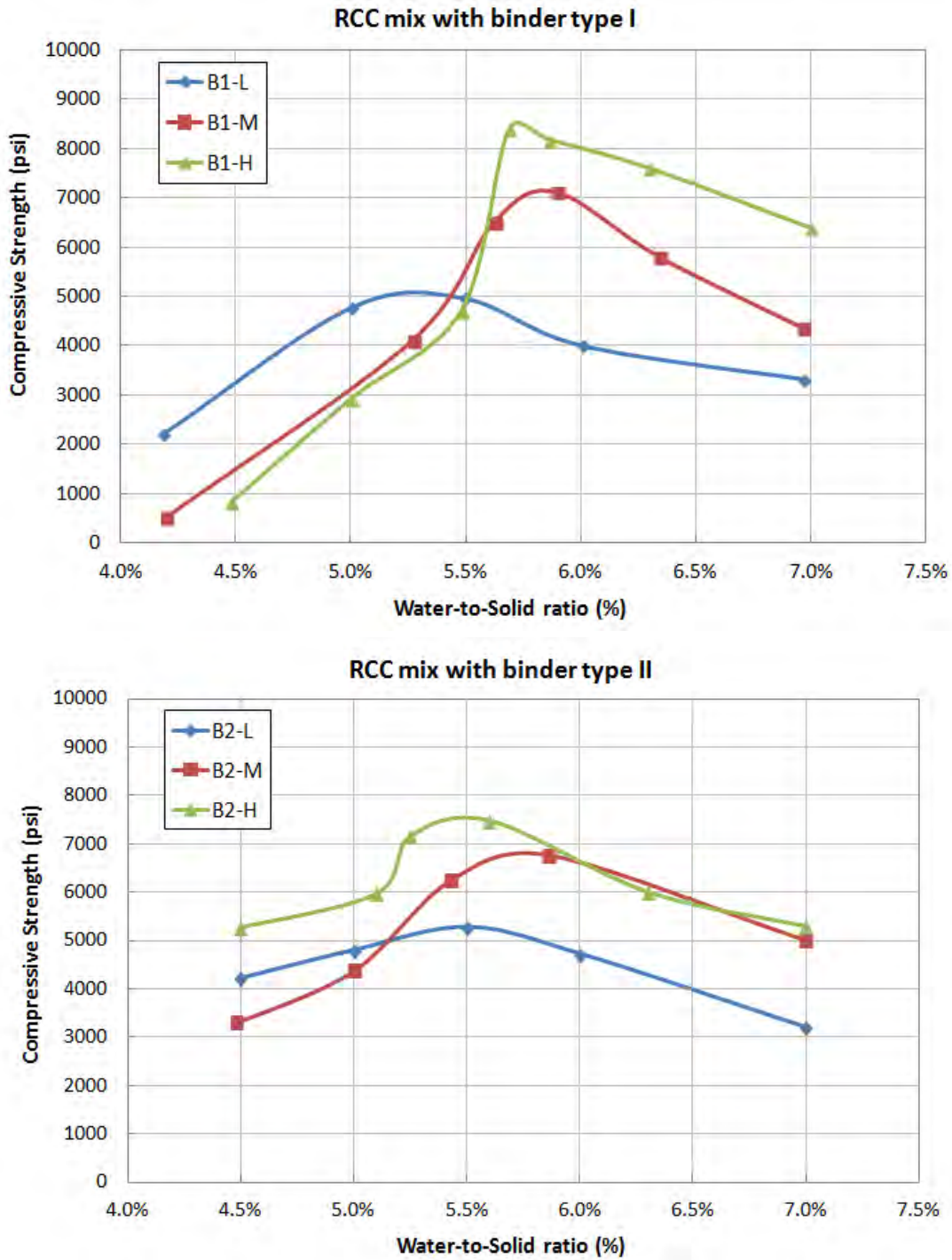


Figure 54- Compressive strength vs. w/s

The mixtures with w/s of 5.5% to 6% had the highest compressive strength. The density-w/s curve almost coincides with the strength-w/s curve. The too-dry mixtures made with w/s values lower than the optimum value have lower water-to-cement ratios but the mixtures are too dry

to be compacted well. The poor compaction leaves some entrapped air in the mixture that reduces the strength of RCC. On the other hand, in too-wet mixtures, the water-to-cement ratio increases that reduces the compressive strength of RCC. It is, therefore concluded that the maximum dry density provides often the maximum compressive strength.

It is worth noting that the slope of strength-w/s curve is much steeper where w/s is lower than the optimum value. In other words, a certain deviation from the optimum w/s causes more strength reduction in dry mixtures compared to wet mixtures. For instance in the mix B1-H, 0.6% increment in the w/s from the optimum value reduced the compressive strength from 8,400 psi to 7,500 psi. On the other hand, decreasing the w/s by the same magnitude from the optimum value reduced the compressive strength from 8,400 psi to 3,000 psi. Regarding the variation of moisture content of aggregate in the field, it is recommended to adjust the w/s a little higher than the optimum value. This ensures that there is enough water in the mixture to achieve proper compaction of the RCC and avoid a significant strength reduction in RCC mixtures.

6.3.4 Workability evaluation

The Vebe time was measured for all mixtures, and the results are depicted in Figure 55. The minimum and maximum acceptable Vebe time for the RCC mixtures is 30 and 90 seconds. These limits are also shown in Figure 55. The mixtures made with w/s lower than the optimum value were too stiff and the vebe time was higher than 90 seconds. The Vebe time of mixtures with w/s of 5.5% to 6% varied from 90 to 40 seconds in various mixtures. The B2 mixtures which made with 20% fly ash showed higher workability (lower Vebe time) at the same w/s. Increasing the binder volumes at the same w/s decreased the workability of RCC mixtures. It is reasonable because at the same w/s, by increasing the cement content, the w/cm is decreasing; therefore, lower workability is expected.

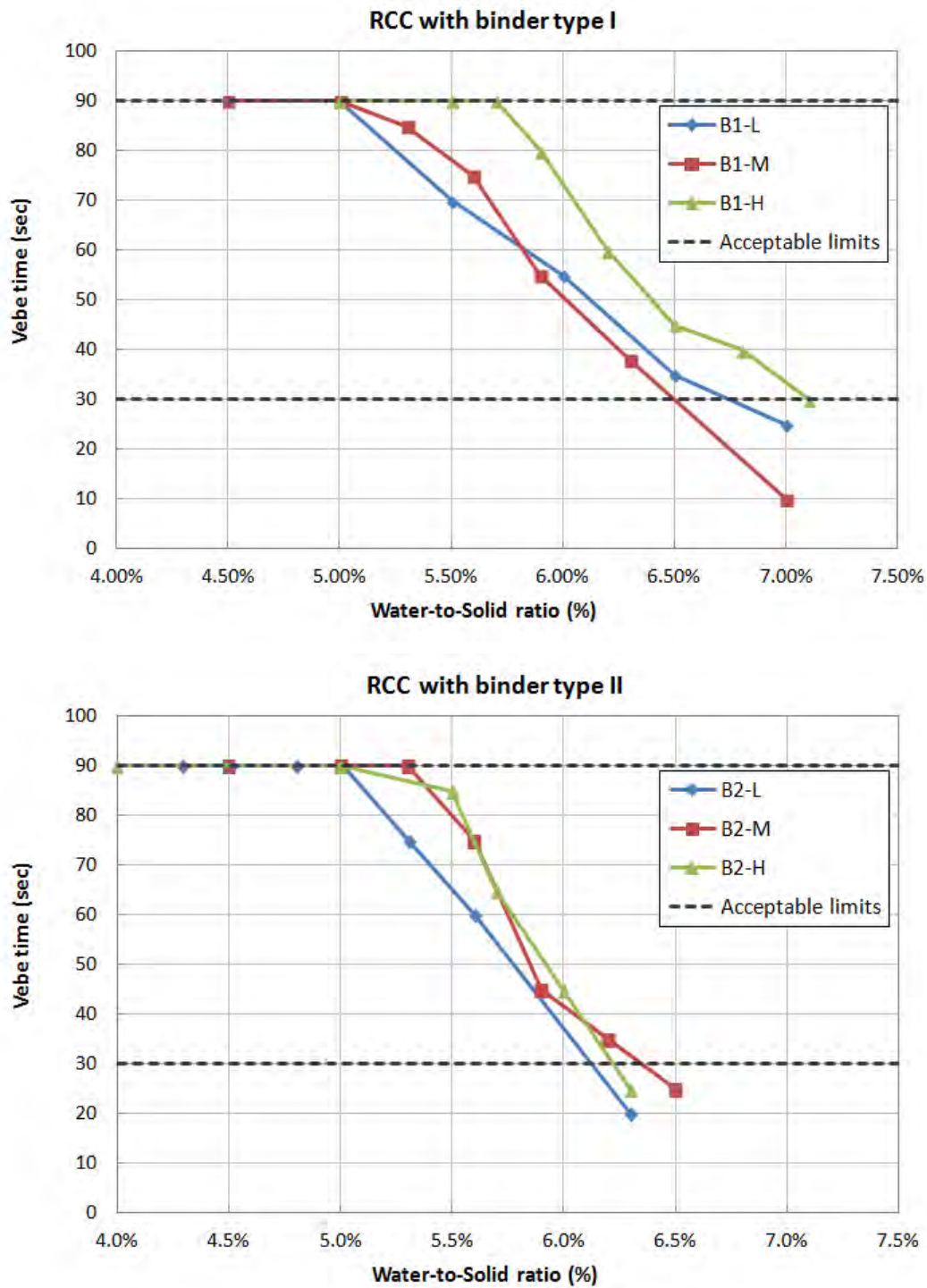


Figure 55- Vebe time vs. w/s

6.4 Selection of optimized RCC mixture proportion

The aggregate combination optimized in Section 6.2 is selected as the optimum solid structure for final RCC mixture proportions. Selection of the binder composition, however, requires considering the workability, density, strength, and durability criteria.

The compressive strength of mixtures made with low binder volume (420 lb/yd³) is higher than 3,500 psi required for pavement materials. However, at the optimum moisture content, the w/cm in these mixtures exceeds 0.50. The w/c is main factor controlling the permeability of concrete and its durability in severe environment. The w/c ratio should be limited to ensure good durability of RCC pavement in harsh environment. Therefore, the medium binder volume (495 lb/yd³) was selected in the final mix in which the w/cm at optimum moisture content is lower than 0.40.

Regarding the density-w/s curve presented in Figure 53, the optimum w/s is 5.5% to 6%. The same optimum range for w/s is concluded from the compressive strength-density curve that depicted in Figure 54. However, the workability criteria requires slightly higher w/s values (about 0.5% to 1%). RCC is compacted by heavy vibratory steel drum and rubber-tired rollers on the job site. The specimens prepared in this task are compacted by the gyratory compactor that compacts even dry RCC very well. Achieving such a degree of compaction in the lab by Vibrating Hammer or Vebe test is very difficult especially for dry concrete mixtures with high Vebe times. Based on our experience, the appropriate Vebe time of concrete required for proper compaction and sampling in the lab is about 20 to 40 sec. These values correspond to w/s of 6% to 6.5% which is higher than the optimum moisture content. Therefore higher w/s is selected to ensure that the concrete consistency is within the specified values. The final RCC mixture proportions are shown in Table 28.

An air-entrained RCC mixture is also considered in this research program. Incorporation of air bubbles in concrete increase the porosity and reduces the compressive strength of concrete. Thus, high volume of binder (590 lb/yd³) was considered in the air-entrained mixture to achieve the same class of compressive strength as the mixture without any AEA. Details of second mixture proportions are given in Table 28.

Table 26- Optimized RCC mixture proportions

Mixture proportions		Mix 1 CM	Mix 2 CH-AEA
Binder	Cement (pcy)	495	590
Aggregate	Maximum Aggregate size (in.)	1	1
	Crushed Stone (1") (pcy)	1155	1116
	Crushed Stone (1/2") (pcy)	561	543
	Sand (pcy)	1584	1534
	Fines (passing No. 200) (%)	1%	1%
Water	Total water (pcy)	251	249
	Free Water (pcy)	194	194
Admixture	Air Entraining Agent (oz/yd ³)	-	44
Compaction Parameters	Consistency (Vebe time) (sec)	30	30
	w/cm -	0.39	0.33
	w/s (%)	6.6%	6.6%
	Cementitious Materials/total solid (volume) (%)	11%	15%
	Fine Aggregate/Total Aggregate (%)	48%	48%

The important issues in the production of air-entrained RCC mixtures are difficulties in producing stable air bubbles in the dry RCC and lack of reliable test method to evaluate the air content in the fresh state. Efficiency of AEAs depends on how they are distributed in the mixture and how effectively air bubbles are produced. These strictly depends on the type of mixer and the duration of mixing procedure.

7 Performance of optimized RCC mixture

The mechanical and durability properties of both the air-entrained and non air-entrained RCC mixtures are examined according to the testing protocols described in Chapter 3. Mechanical properties and durability are discussed separately in Sections 7.1 and 7.2, respectively.

7.1 Physical and Mechanical properties of optimized RCC

The results presented and discussed herein include compressive strength, modulus of rupture, splitting tensile strength, and modulus of elasticity. All the test samples were water-cured until the age of testing. The mechanical testing is extended to continue up to 91 days; however, this

report covers results obtained up to 28 days. In addition to mechanical tests, the Coefficient of Thermal Expansion (CTE) and shrinkage measurement were also conducted on RCC samples.

7.1.1 Compressive strength

The compressive strength was determined using 4 x 8 in. cylinders consolidated by vibrating hammer. The strength is determined at 3, 7, and 28 days. Three concrete specimens were tested at each age, and the mean values are considered as the compressive strength at a given age. The results of the compressive strength are summarized in Table 27.

Figure 56 compares the mechanical properties of RCC mixtures made with and without AEA. At 3 days, the compressive strength of Mix #1 (without AEA) is 25% higher than the corresponding strength in Mix#2 (air-entrained). The compressive strength of both RCC mixeturs at 28 days was about 6,500 ± 300 psi. It should be noted that the air-entrained mixture (Mix #2 CH-AEA) had higher cement content and lower w/cm; however, the incorporation of air bubbles resulted in a mixture with the same level of strength as Mix #1 that had lower cementitious materials.

The coefficient of variation (C.O.V.) corresponds to strength results was higher in the air-entrained mixture at all testing ages. The higher C.O.V. shows that the air-entrained mixtures was more heterogeneous compared to the mixture without AEA. This is attributed to the difficulty of producing stable and uniform air-bubble in the very dry RCC mixtures.

Table 27- Compressive strength of optimized RCC mixtures

Mixture	Compressive Strength (psi)							
	3 days		7 days		28 days		91 days	
	Average	C.O.V.	Average	C.O.V.	Average	C.O.V.	Average	C.O.V.
Mix #1 (CM)	5300	4.9%	6250	4.4%	6770	7.8%	TBD	TBD
Mix #2 (CH-AEA)	4010	12.6%	6140	12.3%	6370	17.6%	TBD	TBD

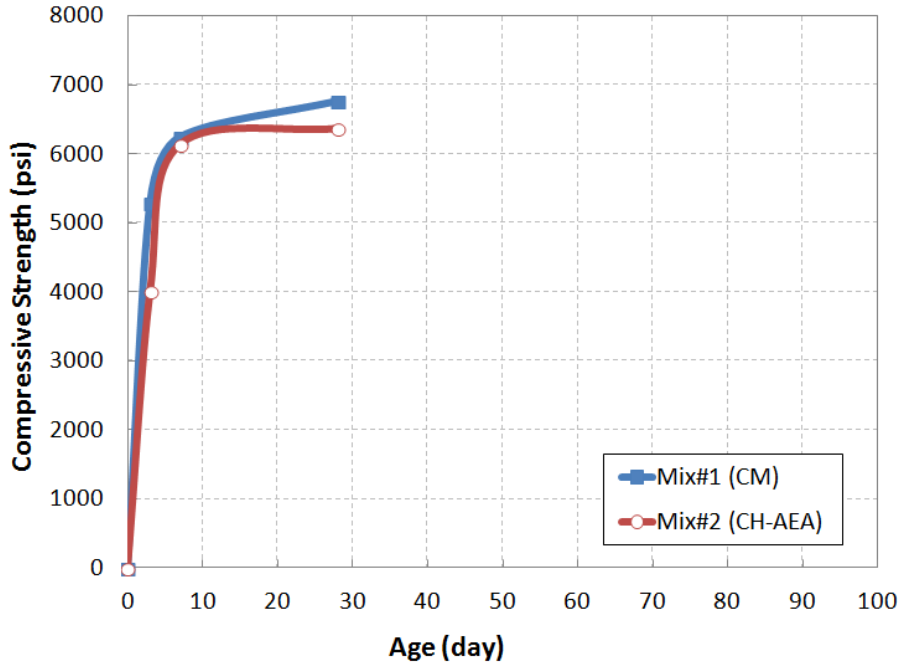


Figure 56- Compressive strength of optimized RCC mixtures

7.1.2 Flexural strength

The flexural strength, was determined on 3 x 3 x 16 in. prismatic specimens at 28 days. Three specimens were tested for each. The flexural strength results are given in Table 28. The flexural strength estimated based on ACI 325.10 (Eq. 1) using the constant factor of C=10 are also given. The measured flexural strengths are close to the values estimated by Eq. 1 given by ACI. Again, a higher C.O.V. was observed in the air-entrained mixture. However, the difference between the C.O.V. of two mixtures is not significant.

Table 28- Flexural strength of optimized RCC mixtures

Mixture	Flexural Strength			
	Average (psi)	C.O.V. (%)	f_t/f_c * (%)	Estimated, ACI (psi)
Mix#1 (CM)	785	4.0%	11.6%	825
Mix#2 (CH-AEA)	820	6.2%	12.9%	800

* Flexural/Compressive ratio

7.1.3 Splitting tensile strength

Splitting tensile strengths were measured on 4 x 8 in. cylinder specimens at 28 days. Three concrete specimens were tested, and the mean values were determined. The two mixtures exhibited almost the same tensile strength of 400 psi and 445 psi, as presented in Table 29.

Table 29- Splitting tensile strength of optimized RCC mixtures

Mixture	Splitting Tensile Strength		
	Average (psi)	C.O.V. (%)	f_t/f_c * (%)
Mix#1 (CM)	400	19.2%	5.9%
Mix#2 (CH-AEA)	445	19.6%	7.0%

*Tensile/Compressive ratio

7.1.4 Modulus of elasticity

The modulus of elasticity was determined in accordance with ASTM C 469. Two 4 x 8 in. cylindrical specimens were used for measuring the modulus of elasticity at 28 days of age. The results are presented in Table 30. The measured modulus of elasticity is compared with the estimated modulus of elasticity given by ACI 318 and AASHTO LRFD Bridge Design Specifications. The results presented in Table 30 show that the measured values of the modulus of elasticity are about 20% to 25% higher than the estimated values either by ACI or AASHTO equations.

Table 30 – Modulus of elasticity of optimized RCC mixtures

Mixture	Modulus of Elasticity		
	Average (ksi)	Estimated, ACI (ksi)	Estimated, AASHTO (ksi)
Mix #1 (CM)	5507	4690	4920
Mix #2 (CH-AEA)	5300	4550	4770

7.1.5 Drying shrinkage

Six 3 x 3 x 11.25 in. prisms were used for monitoring drying shrinkage of concrete. Three specimens were cast from each optimized RCC mixture. The specimens were demolded two days after casting and placed in the lime-saturated water of 70 ± 3 °F for 7 days. The samples were then kept in an environmental chamber with a temperature of 70 ± 3 °F and a relative humidity of 50% ± 4%.

The mean shrinkage results are presented in Figure 57. Mix #2 showed higher shrinkage deformation compared to Mix #1. The higher shrinkage observed is mainly due the higher volume of paste in Mix #2. It is worth noting that the observed shrinkage in both mixtures are lower than the typical values in conventional concrete. Detailed comparison between the optimized RCC in the lab, cast in the field RCC and a typical concrete pavement will be made in the concluding chapter.

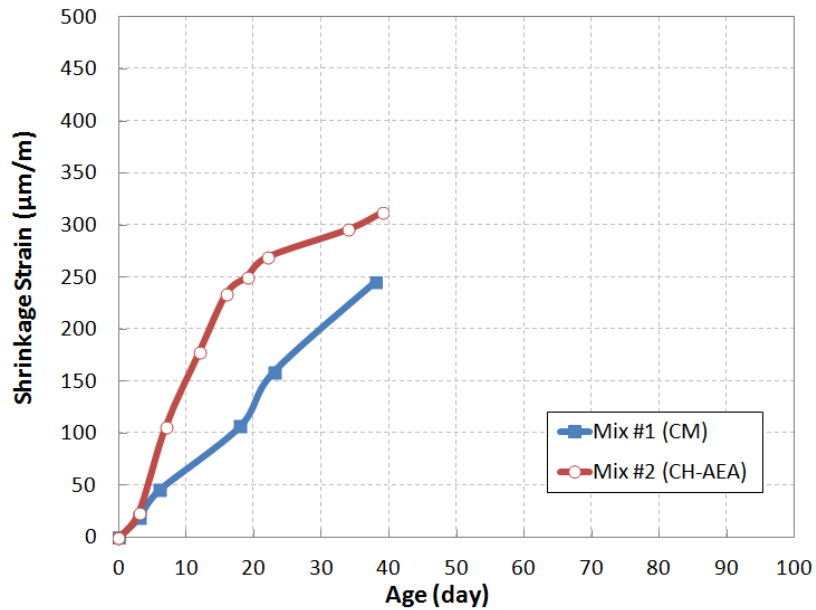


Figure 57- Shrinkage of optimized RCC mixtures

7.1.6 Coefficient of thermal expansion (CTE)

Two 4×8 in. cylindrical specimens were sampled from each RCC mixture to determine the coefficient of thermal expansion (CTE). Concrete specimens were water cured for 28 days before testing. The CTE results are summarized in Table 31.

Table 31 – Coefficient of thermal expansion of optimized RCC mixtures

Mix	CTE (µm/m/°C) (temp increment)	CTE (µm/m/°C) (temp decrement)	CTE (µm/m/°C) (Average)
Mix#1 (CM)	TBD	TBD	TBD
	TBD	TBD	TBD
Mix#2 (CH-AEA)	TBD	TBD	TBD
	TBD	TBD	TBD

7.2 Durability characteristics of optimized RCC

The durability of optimized RCC was evaluated in accordance to the testing protocols described in Chapter 3. The tests conducted for durability evaluation included electrical resistivity, permeable voids, freeze/thaw resistance and deicing salt scaling test.

7.2.1 Electrical resistivity

Three 4x8 in. cylindrical specimens were used for measuring the surface resistivity of RCC according to AASHTO T95. The measurement started at 3 days of age of concrete and will continue up to 91 days. Results are summarized in Table 32. The measured electrical resistivity in air-entrained mixture (Mix #2) at 28 days of age is 18% higher than that of Mix #1. This is due the higher cement content and lower w/cm in the air-entrained mixture. Again, higher C.O.V. were observed in the air-entrained mixture.

Table 32 – Surface resistivity of cast-in-place RCC

Mixture	Surface resistivity (kΩ-cm)											
	3 days		7 days		14 days		21 days		28 days		91 days	
	Average	C.O.V.	Average	C.O.V.	Average	C.O.V.	Average	C.O.V.	Average	C.O.V.	Average	C.O.V.
Mix#1 (CM)	7.42	5.20%	8.72	5.44%	9.68	2.03%	10.49	3.27%	11.08	0.99%	TBD	TBD
Mix#2 (CH-AEA)	8.18	5.35%	9.88	7.09%	10.75	8.18%	11.60	7.91%	13.06	9.92%	TBD	TBD

According to the established relation between surface resistivity and risk of corrosion in concrete (See Table 5) the optimized RCC mixture showed moderate to high risk of corrosion. The trend observed in the development of electrical resistivity of concrete (Figure 58) show that the resistivity is still increasing and higher values is expected at 91 days of age. Note that unlike conventional concrete pavements, RCC pavements are constructed without dowels, or reinforcing steel; therefore, risk of corrosion is not critical in RCC pavements. However, the electrical resistivity test gives some information about the pore structure of concrete and its permeability, which is an important factor in assessment of concrete durability. This test reveals that the air-entrained mixture had lower permeability even though the total volume of voids is higher in this mix. This is justified through the fact that the micro air bubbles formed by AEA break up the capillary structure within concrete and hence reduce its permeability.

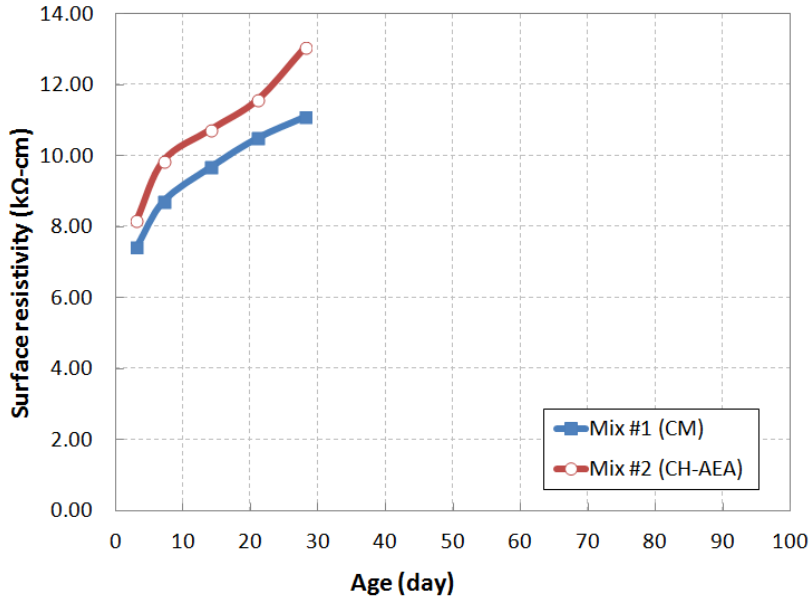


Figure 58- Electrical surface resistivity of optimized RCC mixtures

7.2.2 Permeable voids

Three 4x8 in. cylindrical specimens were used for measuring permeable voids of optimized RCC according to ASTM C642 (See Section 4.1 for details). Results are given in Table 33. The total volume of permeable voids, which is almost the same in both air-entrained and non air-entrained RCC mixtures, are lower than 10%. For Portland cement concrete pavements, a volume of permeable pores less than or equal to 12% is desirable for long-term durability. The result of this test confirms that both RCC mixtures have a dense solid structure. It also confirms the observation in surface resistivity test in which air-entrained RCC mix showed higher resistivity and therefore lower permeability is expected.

Table 33 – Water absorption, density and permeable voids of optimized RCC

Mixture		water Absorption		bulk density		Apparent density lb/ft ³	permeable voids %
		immersed	After boiling	Dry	After boiling		
		%	%	lb/ft ³	lb/ft ³		
Mix#1 (CM)	Average	3.6	4.3	146.2	152.4	162.4	9.98%
	C.O.V.	8.8	6.0	0.4%	0.2%	0.2%	5.6%
Mix#2 (CH-AEA)	Average	4.0	4.1	145.5	151.5	160.9	9.56%
	C.O.V.	3.0	3.7	1.0%	1.0%	1.3%	4.1%

7.2.3 Deicing salt scaling resistance

Deicing salt scaling tests were carried out using three slabs (11"×10"×3") for each RCC mixture. Concrete specimens were cured in lime-saturated water before being tested at 28 days. The visual observations were used for rating the surface of concrete after every five cycles of freeze-thaw. In addition, the scaling residues were collected and weighed to evaluate the surface deterioration, quantitatively. The visual ratings of concrete surfaces up 20 cycles of freeze-thaw are given in Table 34. The test is still running and the data will be collected up to 50 cycles. The surfaces of concrete slabs before exposure to freeze-thaw as well as after every five cycles are shown in Figure 59 and Figure 60. It should be emphasized that the mix #2 had a better initial surface condition due to better finishing applied on its surface.

Table 34 – Deicing salt scaling test results of cast-in-place RCC

Mix #	Sample #	Visual Rating of Scaled Surfaces (ASTM C 672)									
		5 Cycles	10 Cycles	15 Cycles	20 Cycles	25 Cycles	30 Cycles	35 Cycles	40 Cycles	45 Cycles	50 Cycles
Mix#1 (CM)	M1-1	1	2	2	3	3	3	3	-	-	-
	M1-2	1	2	2	3	3	3	4	-	-	-
	M2-1	1	2	2	3	3	3	3	-	-	-
Mix#2 (CH-AEA)	H1-1	0	1	1	1	1	1	1	-	-	-
	H1-2	0	1	1	1	1	1	2	-	-	-
	H1-3	0	1	1	1	1	1	2	-	-	-

The surface resistance of Mix #2 which was air-entrained was much better than Mix #1. It is attributed to the low w/cm of 0.33 as well as the better finishing applied to its surface during casting the specimens.

Figure 61 presents the cumulative mass of scaled-off particles up to 35 cycles. Again, the scaled-off mass collected from Mix #1 is higher than Mix #2 showing better resistance of the air-entrained mixture. The mass of scaling residues was found to vary between 0.08 kg/m² and 0.53 kg/m² after 35 cycles of testing. For both RCC mixtures, the average loss of mass after 35 cycles is lower than the 1 kg/m² limit [PCA-2004]. The results after 50 cycles will be used for final evaluation of RCC resistivity against deicing salt.

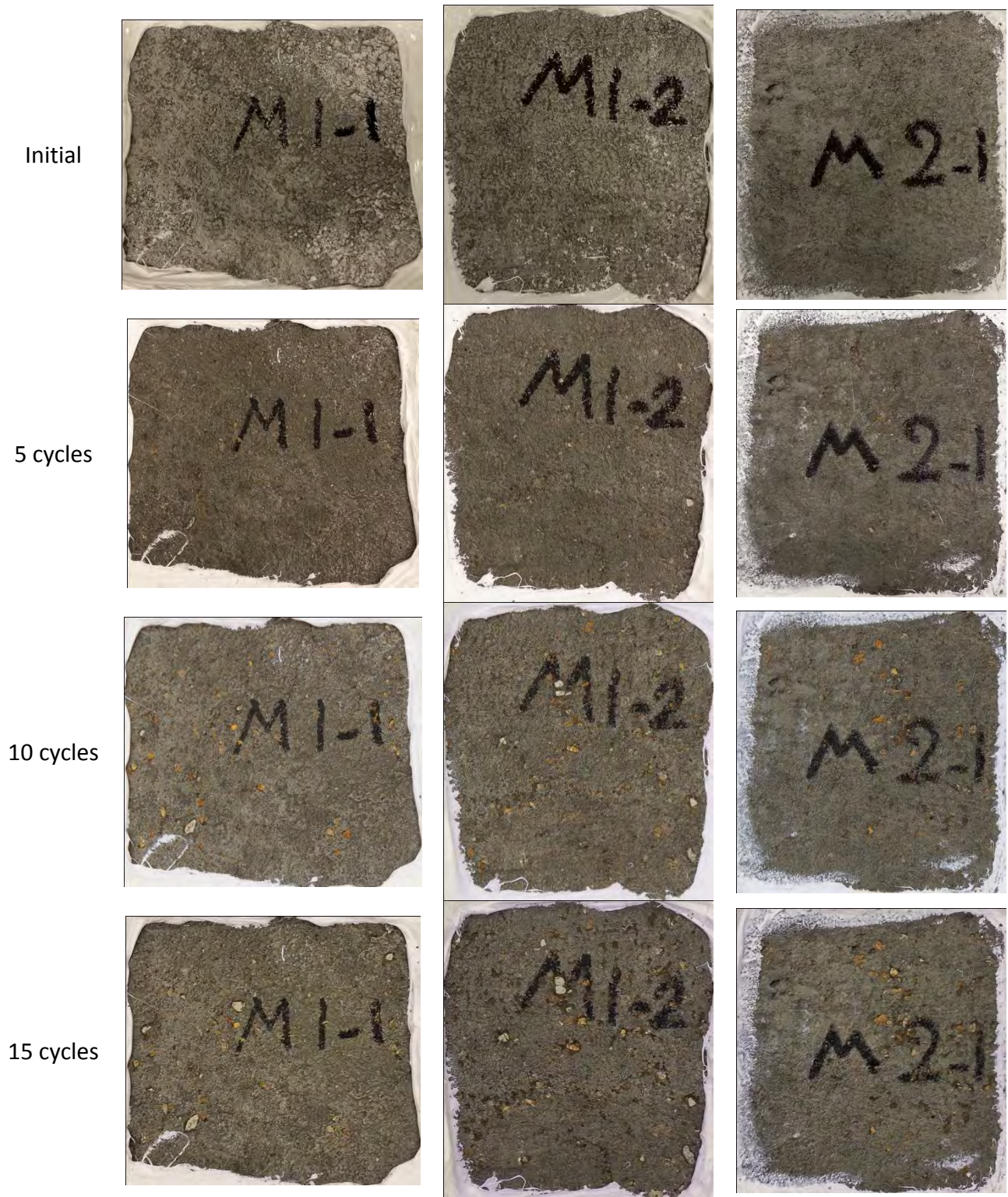


Figure 59- Surface of RCC specimens after subjecting to freeze-thaw cycles, Mix #1 (CM)

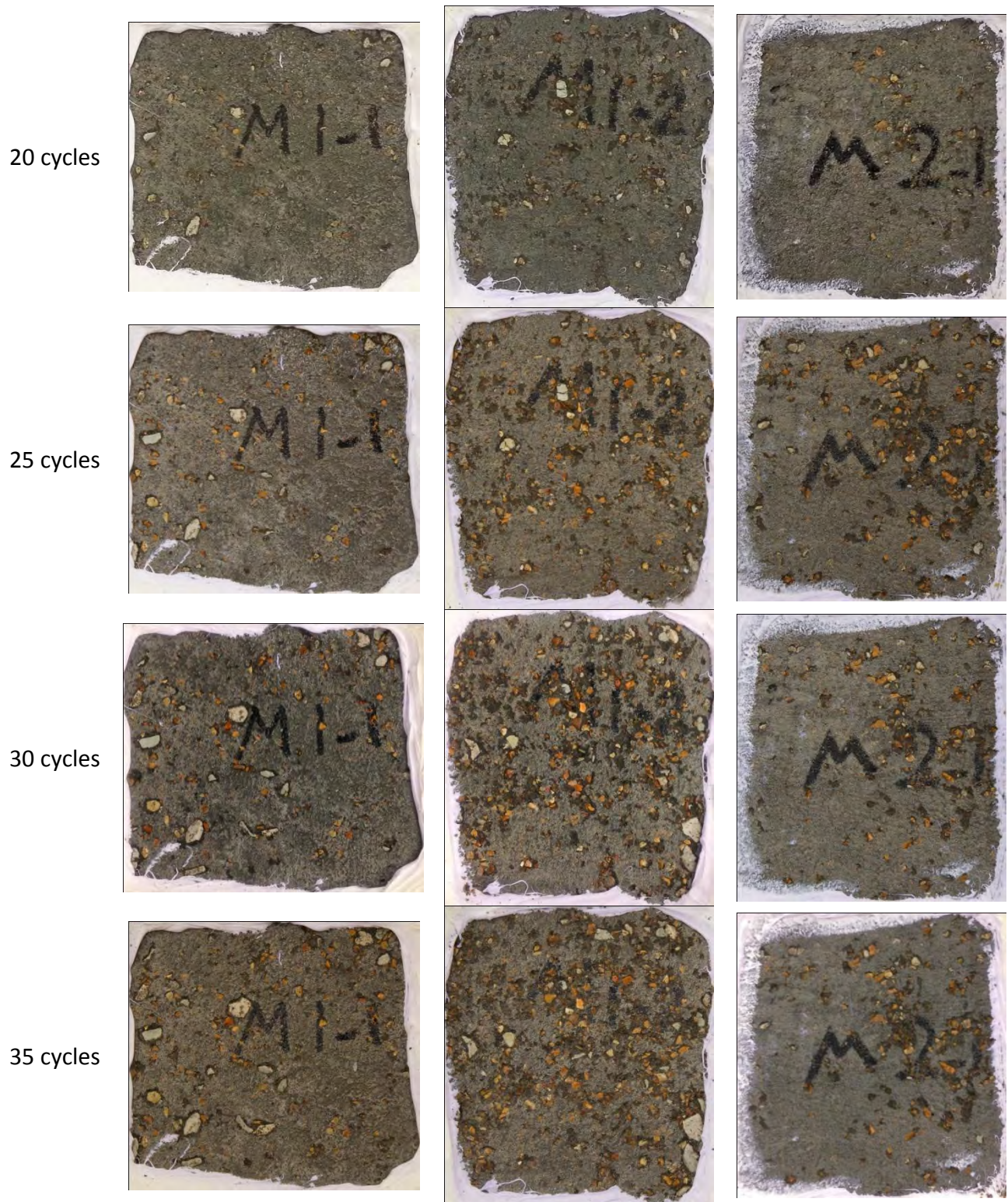


Figure 59- Surface of RCC specimens after subjecting to freeze-thaw cycles, Mix #1 (CM) (Continue)

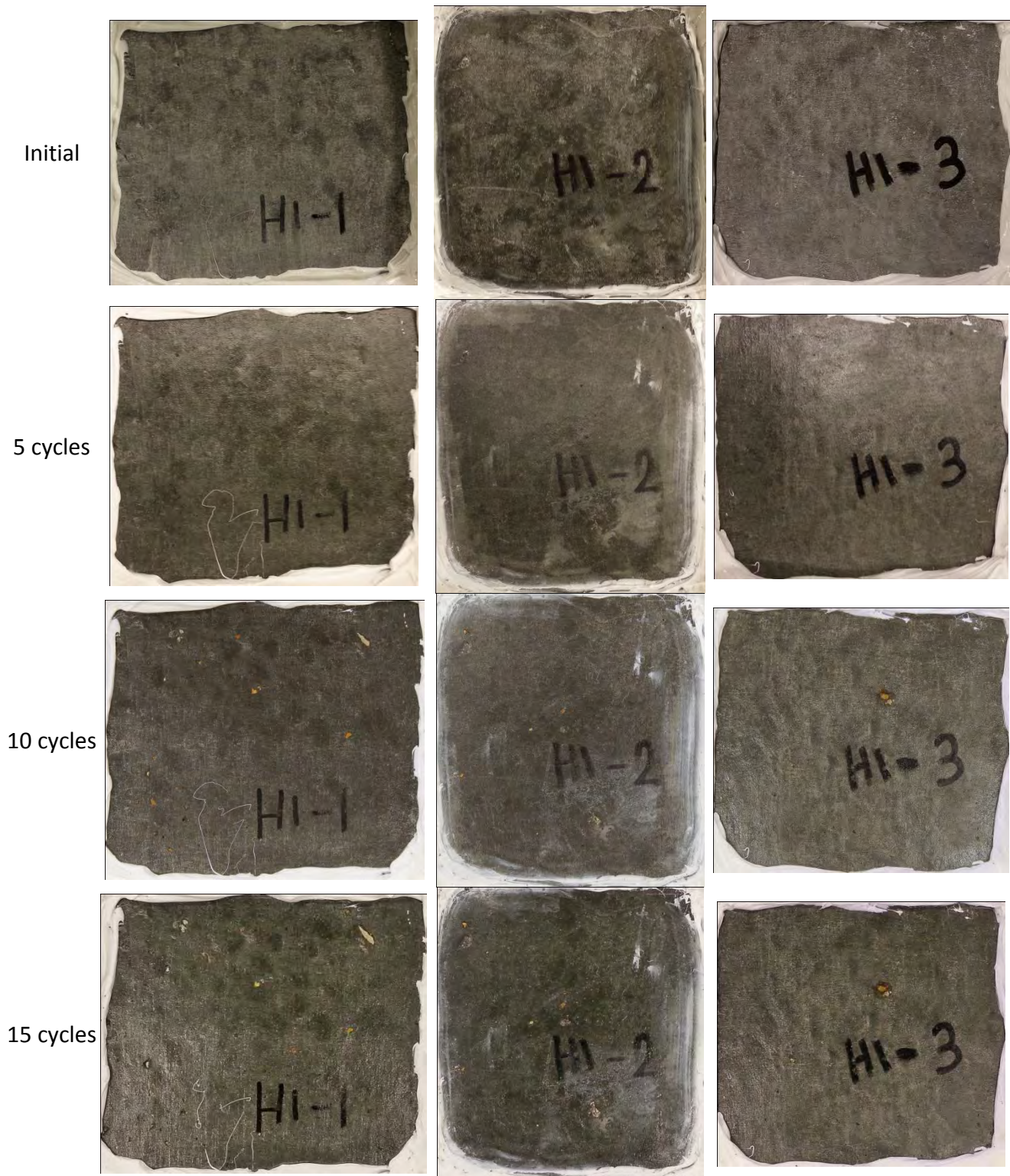


Figure 60- Surface of RCC specimens after subjecting to freeze-thaw cycles, Mix #2 (CH-AEA)

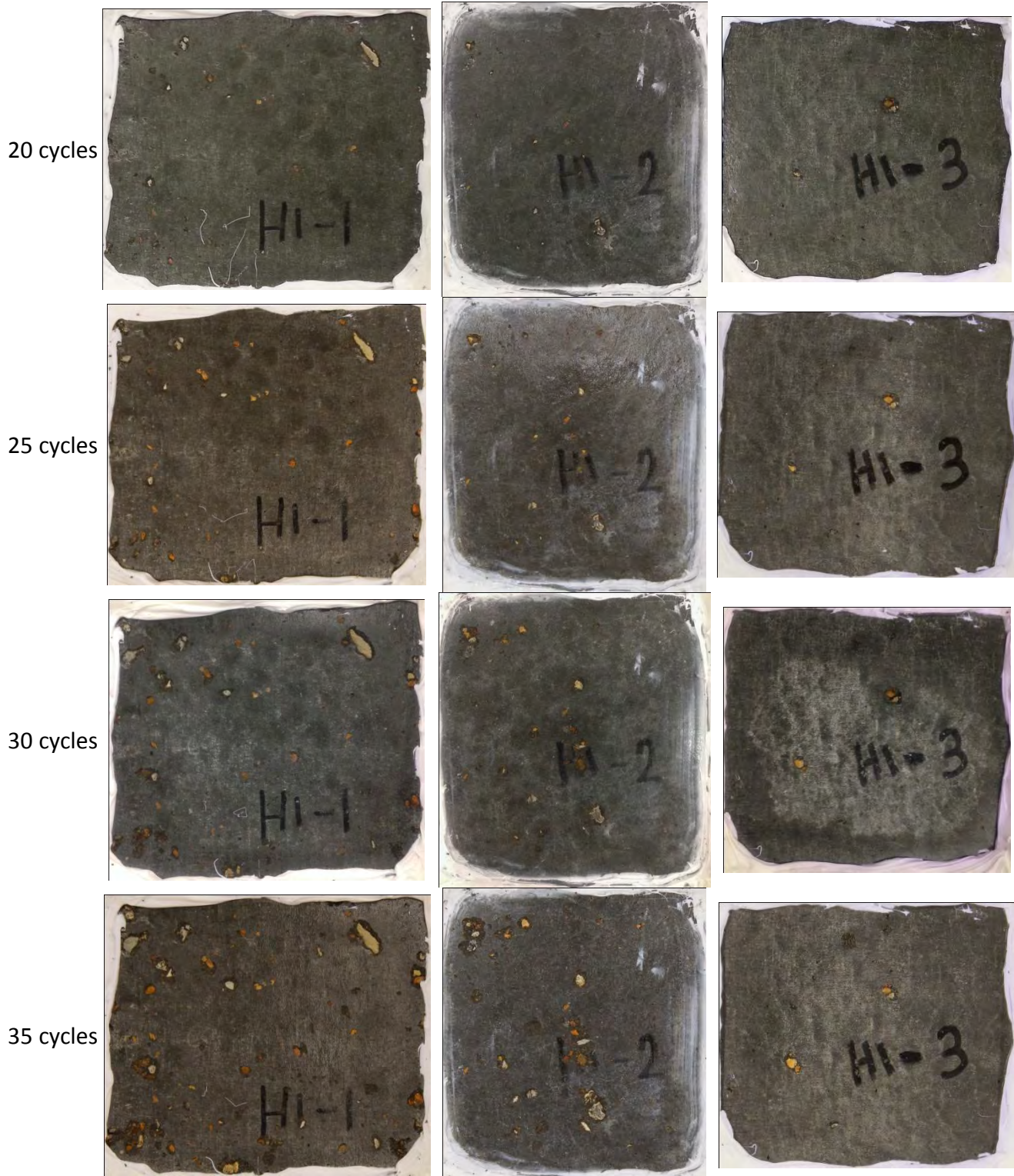


Figure 60- Surface of RCC specimens after subjecting to freeze-thaw cycles, Mix #2 (CH-AEA) (Continue)

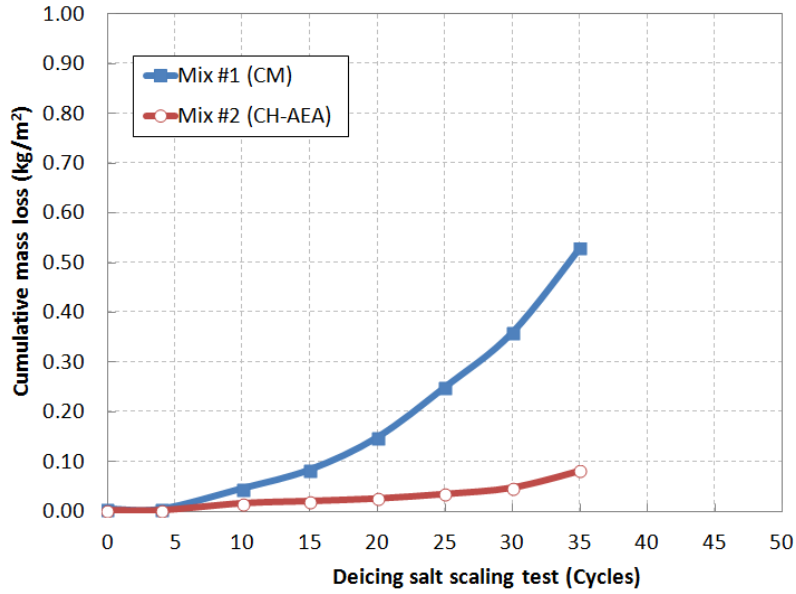


Figure 61- Cumulative scaled-off materials during salt scaling test in the optimized RCC mixtures

8 Comparison and conclusion

It is interesting to compare the results obtained on the two optimized RCC mixtures to data obtained from tests on the conventional pavement concrete. The data of conventional concrete used as the reference pavement material, were collected from the concrete materials used for the casting of the approach pavement to the Mississippi River Bridge (MRB) in St. Louis that was undertaken on April, 2013 by the MoDOT. The reference concrete which is the conventional MoDOT pavement concrete were used for the construction of a 22.5-ft wide ramp approach (outside lane and shoulder) from the Cass Ave. stub out to the EB Parkway Bridge over I-70 in St. Louis.

The slump of conventional concrete was 2 in. that is suitable for pavement construction. The optimized RCC had Vebe time of 30 seconds that provided adequate consistency for laboratory sampling by vibrating hammer. The mixture proportions of the optimized RCC and the reference concrete are summarized in Table 35. Type I/II Cement, river sand, and crushed stone used in all mixtures.

8.1.1 Mechanical properties

The development of compressive strength of the investigated concrete mixtures at various ages is compared in Figure 62. Other mechanical properties measured at 28 days, including, flexural strength and splitting tensile strength are shown in Figure 63. The investigated concrete mixtures developed 28-day compressive strengths ranging from 4,320 to 6,770 psi, which is higher than the minimum compressive strength required for pavement materials.

Table 35- Summary of Mixture proportions

Mixture proportions		Optimized RCC Mix #1	Optimized RCC Mix #2	Conventional concrete
Binder	Cement (pcy)	495	590	409
	Fly Ash, class C (pcy)	-	-	136
	Total Cementitious materials (pcy)	495	590	545
Aggregate	Maximum Aggregate size (in.)	1	1	1
	Aggregate type	crushed	crushed	crushed
	Coarse Aggregate (pcy)	1716	1659	1890
	Fine Aggregate (pcy)	1584	1534	1256
	Total aggregate	3300	3193	3146
Water	Free Water (pcy)	194	194	218
Admixture	Water Reducers (oz)	-	-	53
	Air Entraining Agent (oz)	-	44	4
Mix Parameters	Consistency (Vebe time or Slump) (sec/in.)	30 sec	30 sec	2.5 in.
	w/cm	0.39	0.33	0.40
	Cementitious Materials/total solid (volume) (%)	11	15	13
	Fine Aggregate/Total Aggregate (%)	48	48	40
	Air Content (%)	N.A.	N.A.	5.5

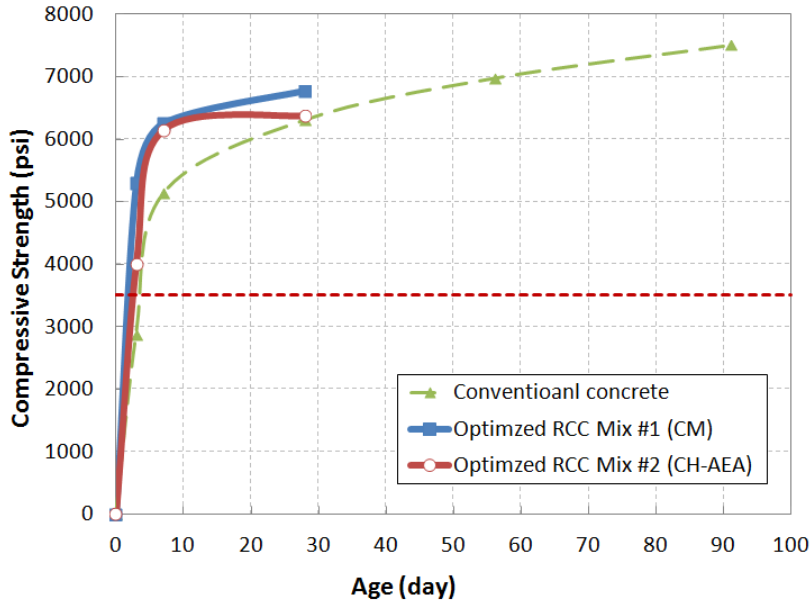


Figure 62- Comparison of compressive strength

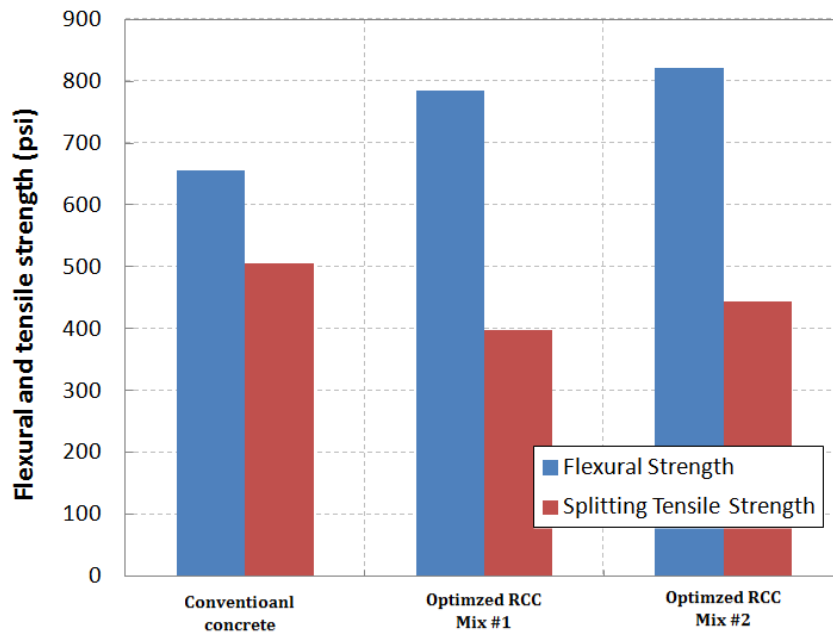


Figure 63- Comparison of flexural and tensile strengths

The optimized RCC mixtures made with 495 lb/yd³ of cement developed the highest 28-d compressive strength (6,770 psi) followed by the Mix #2 air-entrained optimized RCC. The average splitting tensile strength of RCC mixtures ranged between 400 and 500 psi and flexural strength ranging from 650 to 820 psi. The flexural strength of RCC was higher than that of the

reference mixture, while the splitting tensile strength is lower than the value measured in the conventional concrete. Thus, mechanical property of optimized RCC is not different from that of conventional concrete used in the pavement construction.

It should be emphasized that the mixture proportions are selected in a way to achieve almost the same class of strength in all mixtures. The optimized RCC Mix #1 achieved to the desired mechanical strength despite the 10% lower cement content than that of reference mixture. On the other hand, the air-entrained RCC mix (Mix #2) required 10% higher cement to achieve the same strength. It is worth noting that the water-to-solid ratio in the optimized RCC mixtures were adjusted higher than the optimum value to increase workability of mixture. This was necessary to produce RCC samples that can be properly compacted by using the standard laboratory procedure such as vibrating hammers. Such a high consistency is required for laboratory compaction but more dry concrete with water-to-solid ratio close to the optimum values may be successfully compacted by heavy vibratory steel drum and rubber-tired rollers at the job site. Therefore, higher mechanical and durability properties are expected for the optimized RCC mixtures at the job site if the RCC is produced with the optimum water-to-solid ratio.

8.1.2 Long-term deformation

Figure 64 compares the drying shrinkage of the two optimized RCC mixtures with that of conventional concrete. All RCC mixtures, including those produced with high cement content and air entraining agent, had equal or lower drying shrinkage value than that of conventional concrete. The optimized RCC Mix#1 showed the lowest. This can be attributed to the low volume of cement paste used in that mixture.

Long-term monitoring of the RCC pavement provides valuable information of the total deformation of the pavement. Over the period of 9 months, the shrinkage observed in the RCC pavement was limited to 100 $\mu\text{m}/\text{m}$, which is lower than the strain measured in the laboratory conditions (400 $\mu\text{m}/\text{m}$). Therefore, lower shrinkage value is expected if the optimized RCC Mix #1 is used for the pavement construction.

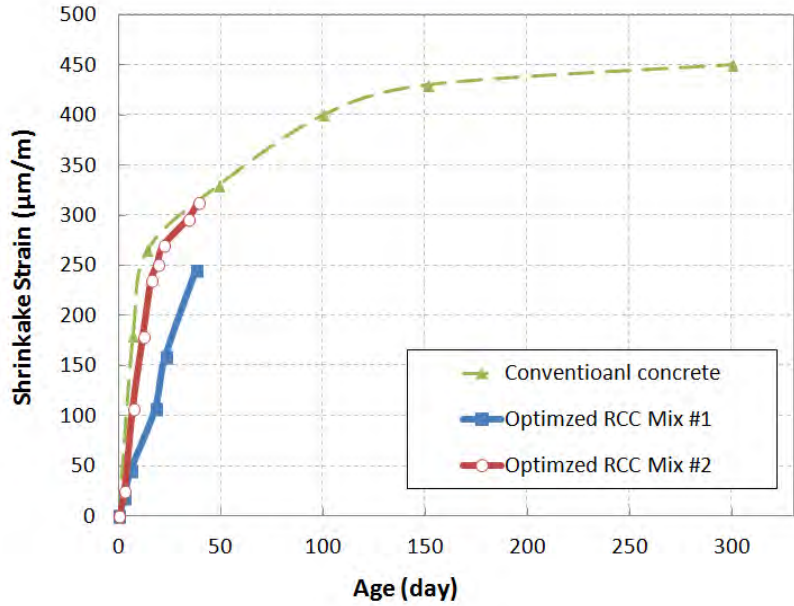


Figure 64- Comparison of shrinkage of investigated mixtures

8.1.3 Permeable voids and electrical resistivity

The volume of permeable voids of RCC mixtures was slightly lower than that of conventional concrete. The Surface resistivity results are in agreement with the results of permeable voids. The highest surface resistivity and the lowest permeable voids were obtained for the Mix #2 optimized RCC, which is the air-entrained RCC.

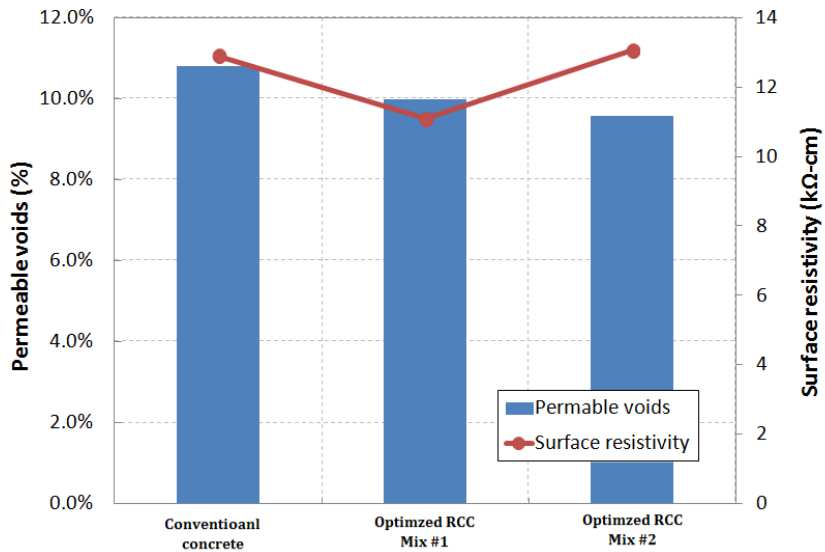


Figure 65- Comparison of Surface resistivity and permeable voids

The water absorptions of the RCC mixtures are compared with that of the conventional concrete in Figure 66. Again, lower water absorption were observed in the RCC mixture shows its lower permeability and better durability performance comparing to conventional concrete.

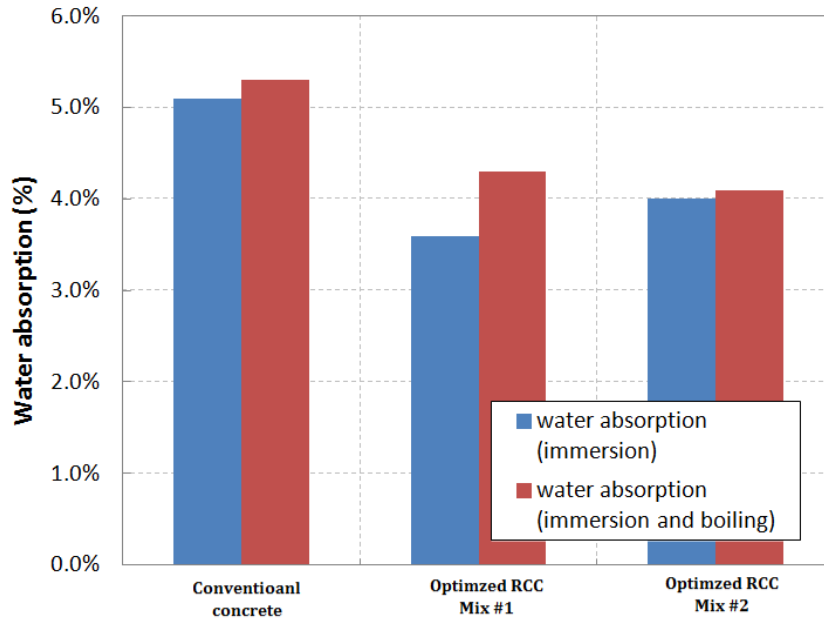


Figure 66- Comparison of water absorption

8.1.4 Frost resistance

Frost resistance of RCC mixtures was evaluated using the freezing and thawing test (ASTM C666) and deicing salt scaling resistance test (ASTM C672). Both tests are still underway but the data collected to date indicate acceptable performance of the RCC mixtures. The conventional concrete is only tested for freezing and thawing test (ASTM C666). Therefore, no quantitative and side by side comparison can be made between RCC and conventional concrete mixtures.

The results of salt scaling test indicate that it is possible to produce RCC with good resistance to Deicing salt-scaling. For both series, the loss of mass after 35 cycles is much lower than the 1 kg/m² limit [PCA, 2004]. The average results range from 0.08 kg/m² in air entrained RCC to 0.53 kg/m² in non air-entrained mixture. Even though the air entrained RCC showed superior performance, the non air-entrained RCC is performing acceptably under the severe conditions

of deicing salt scaling testing. The final conclusion on frost resistance of the optimized RCC will be made after completion of freezing and thawing tests.

8.1.5 Concluding remarks

The selection of proper aggregates combination to achieve a high packing density is crucial in optimizing the PSD of RCC. The mechanical properties of investigated RCC mixtures are comparable to those properties in conventional concrete. The compressive strength of the optimized RCC mixtures was almost equal to that of conventional concrete. The flexural strength, which used in pavement design were found to be 20% to 25% higher than the conventional concrete. Regarding the lower cement content used in the mixture proportioning of RCC to achieve the same level of strength as in the conventional concrete, the use of RCC could be beneficial in saving cement and reducing the carbon footprint associated with the cement production. In addition, when RCC is used in pavement, there is no need for the use of forms during placement and no need to finishing. These features speed up the pavement construction and result in a more cost saving.

All investigated durability factors showed that RCC has adequate durability compared to conventional concrete used in the pavement construction. The long-term deformation of either cast in the field RCC and laboratory optimized RCC was found to be lower than that of conventional concrete. The one-year monitoring of pavement deformation revealed that the field shrinkage strain is lower than shrinkage occurred in the laboratory specimens. The only exception is frost resistance of RCC in laboratory test evaluation.

8.1.6 Future work

Test results presented and discussed in this report confirm the importance of PSD of aggregates as the solid skeleton of RCC. Further research is still required to study the theoretical packing models and determining the proper packing parameters for RCC mixtures. In addition, it is recommended to investigate performance of RCC made with different aggregate types from various aggregate quarries to cover wide range of aggregates available in the state of Missouri. Binary, ternary and quaternary combination of aggregate is recommended in the future work. Recycled aggregate concrete may also included in the next research program.

The discrepancies between laboratory freeze-thaw tests and field behaviors in cold environment as well as the unresolved question of the necessity of air entrainment suggest the need for further research on the frost durability and scaling resistance of RCC mixtures. As reported in the literature and discussed in Chapter 5, it can be difficult to entrain air in RCC in the matrix because of its low paste content, and its low workability. The preliminary study presented and discussed in this report showed that air entrainment can be achieved in the RCC mixtures. Adjusting the amount of air content, the stability of air bubbles during the transport and compaction and uniformity of air-void distribution across the pavement, are among the important issues that should be addressed before using air-entrained RCC in the field applications.

Incorporation of supplementary cementitious materials in binary and ternary combination may also be helpful on improving long-term durability of RCC. Thus, further research is recommended to investigate the performance of binary and ternary binders in RCCP.

The degree of compaction for specimens that sampled manually either by vibrating hammer or by vibrating table is different from that of concrete pavement that have been compacted by the vibrating roller at the job site. The degree of compaction affects all mechanical and durability properties of RCC. Therefore, it is recommended to apply the optimized RCC mixtures in the field pavement construction and validate the performance of optimized RCC through testing on the specimens obtained from the RCC pavement. The lack of information on the frost durability of RCC also emphasizes the need for research in the field. The effect of the consolidation operations on the frost protection and salt-scaling resistance also needs to be elucidated. Further correlation between laboratory test results and field performance of RCC structures is required to be established.

Acknowledgment

The authors would like to thank to the Center for Transportation Infrastructure and Safety, a National University Transportation Center (NUTC) at the Missouri University of Science and Technology (Missouri S&T) as well as the Missouri Department of Transportation (MoDOT) for

providing the financial support (reference number r363). The authors also take this opportunity to express a deep sense of gratitude to Mr. Bill Stone and Ms. Jennifer Harper from MoDOT for their cordial support, and constant encouragement and monitoring throughout this project. We would like to give very special thanks to Dr. Pieter Desnerck and Dr. Soo Duck Hwang for their contribution and technical support. The authors are also grateful to Mr. Iman Mehdipour for his assistance in conducting the tests and analyzing the data. We also acknowledge Jason Cox and John Bullock for their valuable technical support in field evaluation of RCC. The cooperation and support from Abigayle Sherman, Gayle Spitzmiller, and Cheryl Geisler staff members of Centre for Infrastructure Engineering Studies (CIES) is greatly acknowledged.

References

- [1] ACI Committee 207, "207.5R-11 Report on Roller-Compacted Mass Concrete", American Concrete Institute, 2011, p. 71
- [2] ACI Committee 318, "ACI 318-11: Building Code Requirements for Structural Concrete and Commentary", American Concrete Institute, 2011, p. 503
- [3] ACI Committee 325, "ACI 325-10: Report on Roller-Compacted Concrete Pavements, 1995, p. 32
- [4] ASTM C39 (2010), Standard Test Method for Compressive Strength of Cylindrical Concrete Specimens, American Society of Testing and Materials, West Conshohocken, PA.
- [5] ASTM C78 (2010). Standard Test Method for Flexural Strength of Concrete (Using Simple Beam with Third-Point Loading) American Society of Testing and Materials, West Conshohocken, PA.
- [6] ASTM C469 (2002). Standard Test Method for Static Modulus of Elasticity and Poissons Ratio of Concrete in Compression. American Society of Testing and Materials, West Conshohocken, PA.
- [7] ASTM C496 (2004). Standard Test Method for Splitting Tensile Strength of Cylindrical Concrete Specimens. American Society of Testing and Materials, West Conshohocken, PA.
- [8] ASTM C666 (2008). Standard Test Method for Resistance of Concrete to Rapid Freezing and Thawing. American Society of Testing and Materials, West Conshohocken, PA.
- [9] ASTM C672 (2008). Standard Test Method for Scaling Resistance of Concrete Surfaces Exposed to Deicing Chemicals. American Society of Testing and Materials, West Conshohocken, PA.
- [10] ASTM C1202 (2010). Standard Test Method for Electrical Indication of Concrete's Ability to Resist Chloride Ion Penetration. American Society of Testing and Materials, West Conshohocken, PA.
- [11] ASTM C 1543 (2010). Standard Test Method for Determining the Penetration of Chloride Ion into Concrete by Ponding. American Society of Testing and Materials, West Conshohocken, PA.

- [12] ASTM C1170, (2010), Standard Test Method for Determining Consistency and Density of Roller-Compacted Concrete Using a Vibrating Table, American Society of Testing and Materials, West Conshohocken, PA.
- [13] ASTM C1245, (2012), Standard Test Method for Determining Relative Bond Strength Between Hardened Roller Compacted Concrete Lifts (Point Load Test), American Society of Testing and Materials, West Conshohocken, PA.
- [14] ASTM C1345, (2008), Standard Practice for Molding Roller-Compacted Concrete in Cylinder Molds Using a Vibrating Hammer, American Society of Testing and Materials, West Conshohocken, PA.
- [15] ERMCO, "ERMCO Guide to roller compacted concrete for pavements", ERMCO – European Ready Mixed Concrete Organization, 2013, p. 24
- [16] Pittman, D.W. and G.L. Anderton. 2009. The use of roller-compacted concrete pavements in the United States. Presentation at the Sixth International Conference on Maintenance and Rehabilitation of Pavements and Technological Control (MAIRE PAV 6), Torino, Italy. <http://www.mairepav6.it.uk/>
- [17] Andreasen, A. H. M. and Andersen, J. (1930). Ueber die Beziehung zwischen Kornabstufung und Zwischenraum in Produkten aus losen Körnern (mit einigen Experimenten), Kolloid-Zeitschrift 50: 217 – 228 (in German).
- [18] J.E. Funk, D.R. Dinger, Predictive Process Control of Crowded Particulate Suspensions, Applied to Ceramic Manufacturing, Kluwer Academic Press, Boston, 1994.